Analysis of Response to Climate Change in the Le Sueur River Watershed with Generated Climate Predictions.

A Thesis
SUBMITTED TO THE FACULTY
OF THE
UNIVERSITY OF MINNESOTA
BY

Emily Lynn Steinweg

In partial fulfillment of the requirements for the degree of Master of Science

Dr. Gary R. Sands

March 2020

Acknowledgements

We acknowledge the Minnesota Agricultural Experiment Station for their support of this work.

"We acknowledge the World Climate Research Programme's Working Group on Coupled Modelling, which is responsible for CMIP, and we thank the climate modeling groups (listed in Table 1 of this paper) for producing and making available their model output. For CMIP the U.S. Department of Energy's Program for Climate Model Diagnosis and Intercomparison provides coordinating support and led development of software infrastructure in partnership with the Global Organization for Earth System Science Portals"

Abstract

Climate change may have a variety of impacts on Midwest USA agriculture, including impacts to water quality, soil erosion, and nutrient loss. Existing and future climate scenarios were modeled in the Le Sueur watershed using the Soil & Water Assessment Tool (SWAT) to compare the watershed outflow and nutrient concentration outflows under those scenarios.

The Le Sueur watershed, in south-central Minnesota, USA, is approximately 1,112 square miles, 87% of which is agriculture. The agriculture land is predominantly in corn and soybean rotations. Much work has been done using global climate models to predict the climate impacts from anthropogenic climate changes, resulting in predictions that the Midwest will experience increased temperatures, increased precipitation in the winter months, and decreased precipitation in the summer months. Minnesota has already documented an increase in extreme rainfall events. These events can cause flooding, damage land and property, and impact agricultural production.

This analysis uses six global climate model (GCM) projections from the Coupled Model Intercomparison Project Phase 5 (CMIP5) for the Le Sueur River watershed area. The magnitude of change of five weather inputs; maximum temperature, minimum temperature, relative humidity, solar radiation, and wind speed, was averaged over three future climate time periods (2006-2029, 2030-2059, and 2060-2099) for two emissions scenarios, RCP 4.5 and 8.5. Average changes were applied to local weather in the Weather Input for Nonpoint Data Simulations (WINDS) model to simulate local climate projections. Predictions from WINDS are used in SWAT, to investigate watershed response to climate change in the Le Sueur River watershed.

Table of Contents

List of Tables

List of Figures

Chapter 1 – Downscaling Global Climate Models for Use in SWAT

Introduction

The Le Sueur River watershed is one of twelve major watersheds (HUC-08) in the Minnesota River Basin with outflow to the Minnesota River which subsequently flows into the Mississippi River. The Minnesota River Basin covers 16,770 square miles (10,000,000 acres) (Musser, Kudelka, & Moore, 2009) and is one of Minnesota's most productive agricultural production areas.

The Le Sueur River watershed, and the Minnesota River Basin as a whole, have been the focus of studies relating to the high levels of sediment and nutrients like nitrogen and phosphorus in the Minnesota River and the resulting downstream implications and impacts (Dalzell & Mulla, 2018; Day, Wittkop, Jennings, Gran, & Belmont, 2011; K. B. Gran et al., 2009). The Minnesota River Basin is close to the headwaters of the Mississippi River, which drains to the Gulf of Mexico. Each year, the Gulf of Mexico experiences a hypoxic zone, an area of low (< 2 mg/l) dissolved oxygen, which kills aquatic life and impacts the livelihoods of those who depend on the Gulf for work or sustenance. As an area of intensive agricultural production, water pollution from excess nutrients and sediment is observed, measured and shown to impact the size of the hypoxic zone. The five-year average size of the hypoxic zone between years 2014 – 2019 (excluding 2016) was measured to be approximately 15,000 km^2; higher than the goal of a 5,000 km^2 average over a five-year period set by the Mississippi River Nutrient/Gulf of Mexico Hypoxia Task Force. Size of the hypoxic zone has also been correlated to freshwater flows to the Gulf of Mexico; larger flows to the Gulf of Mexico result in larger hypoxic zones (Rabalais & Turner, 2019). If weather patterns change due to climate change, those changes could potentially have a larger negative impact on the hypoxic zone and others downstream.

Research on the impact of climate change in the Upper Mississippi River Basin (UMRB) has shown that this area is sensitive to predicted climate changes (P. W. Gassman, Reyes, Green, & Arnold, 2007). Investigating the impacts of climate change on the smaller area of the Le Sueur River watershed complements the current research on nutrient outflows, provides more accurate predictions for area response to climate change for local decision makers, and can encourage

actions to reduce negative downstream impacts. As one of Minnesota's two main agricultural regions, it will be important to investigate the effects of climate change to aid producers and land managers in making decisions for the future.

Global climate modeling can be insightful and informative to answer questions of environmental changes due to climate change. Climate models are continually updated by various organizations with the latest technological updates, improved techniques, and new climate scenarios. Climate modeling has progressed over the years and is commonly used by academia, government organizations, and others. Changing climate can have multitudes of environmental impacts including water quality, which is especially dependent on location and land management.

Downscaling global climate models (GCM) is a common practice to get more locational-accurate predictions and to capture the spatial variations of predicted climate on a landscape scale (Jiang et al., 2018; Maurer, Hidalgo, Das, Dettinger, & Cayan, 2010). GCMs are commonly downscaled either using statistical or dynamic methods, to remove any bias the GCM has in representing local conditions and better represent climate at a smaller scale than provided by GCMs (Jang & Kavvas, 2014; Jiang et al., 2018; Mehan, Gitau, & Flanagan, 2018). Dynamic downscaling methods run the large-scale GCMs on a regional climate model, using observational data as boundary conditions. As it is a nesting of two models, it is very computationally demanding. Statistical downscaling establishes relationships between observed weather patterns and applies those patterns to the coarser resolution of a GCM. This method is known to be computationally efficient and used more widely in climate downscaling studies (Fowler, Blenkinsop, & Tebaldi, 2007). The downscaled GCMs are referred to as regional climate models (RCM) and outcomes of RCMs can be informative for scientists and decision makers of that region.

The GCMs used in this analysis are from the Program for Climate Model Diagnosis and Intercomparison's (PCMDI) World Climate Research Programme (WCRP) working. Twenty modeling groups are a part of the fifth phase of the Coupled Model Intercomparison Project (CMIP5) (Taylor, Stouffer, & Meehl, 2012; "WCRP Coupled Model Intercomparison Project - Phase 5 - CMIP 5," 2011). The CMIP provides a common modeling framework, used by many modeling organizations to allow for easier comparisons of existing climate models and future climate modeling. Each phase of the CMIP introduces additions to modeling simulations, works to answer new scientific questions, and contains improvements in modeling calculations (Wayne, 2013).

This study aims to create HUC-08 scale weather inputs for the Soil & Water Assessment Tool (SWAT) model to model and evaluate the Le Sueur River watershed response to two of the most recent carbon emission scenarios, created by the Intergovernmental Panel on Climate Change (IPCC), and modeled by the WCRP. The outcomes of the modeling may provide clarity and insight on the effects of climate change on this HUC-08 watershed in south-central Minnesota. The study area has far reaching water quality impacts, including impacts on the Gulf of Mexico hypoxic zone.

Methods

Global climate models can be used to address various environmental questions. The GCMs are typically downscaled to get improved predictions on smaller scales. This analysis starts with GCM projections for an area in south-central Minnesota, downscales the data using a statistical downscaling method, and uses a weather generation model, to produce more location-representative weather predictions for the area of interest. Those statistical weather predictions are used to evaluate climate change impacts on a HUC-08 watershed in south-central Minnesota, USA.

Location

The Le Sueur River watershed area is approximately 1,112 square miles (710,832 acres), about 7% of the Minnesota River Basin area. Agriculture is the primary land use, accounting for 87% of available acres (Spindler et al., 2012). This watershed sees on average 33.5-inches of precipitation per year, with maximum and minimum temperature averages of 55.1- and 35.5-degrees F, respectively (Department of Natural Resources, 2019). The location of the watershed within the state of Minnesota is displayed in Figure 1.

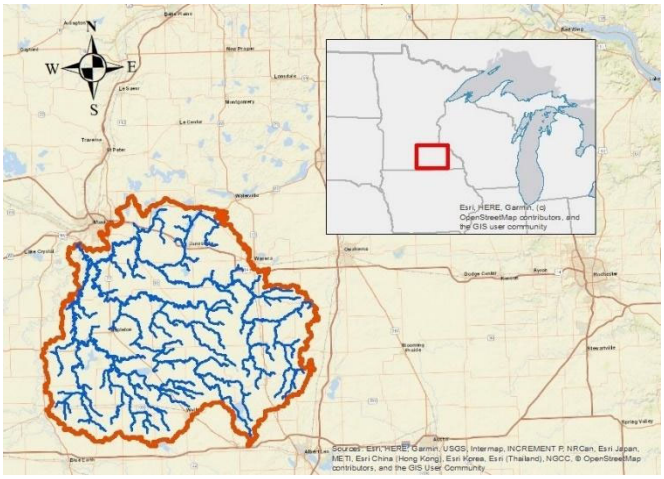

Figure 1: Le Sueur River Watershed

Global Climate Models and Selection

From the modeling organizations using CMIP5 simulations, six GCMs were chosen for this analysis, shown in Table 1 ("WCRP Coupled Model Intercomparison Project - Phase 5 - CMIP 5," 2011). CMIP5 uses four new GHG trajectory scenarios created by the IPCC, called Representative Concentration Pathways (RCP). The four scenarios are RCP 8.5, RCP 6, RCP 4.5, and RCP 2.6. The numbers designating each pathway (8.5, 6, 4.5, and 2.6) represent the level of radiative forcing produced in each pathway that will be seen in the atmosphere by year 2100. Radiative forcing is a measurement of the energy in the earth's atmosphere, recorded as the difference between incoming and outgoing radiation in watts per square meter. A positive number indicates a net gain in energy in the atmosphere. The factors considered by the IPCC to impact energy change include both human-caused (GHG emissions, deforestation, population growth, future energy sources, land use) and natural-caused (solar and volcanic activity) events (IPCC, 2014b; Taylor, Stouffer, & Meehl, 2007; Wayne, 2013).

This study selected two RCP scenarios for in depth analysis: RCP 4.5 and RCP 8.5. RCP 4.5 is described as a stabilization or low emission scenario, with radiative forcing reaching 4.5 watts per square meter (W/m^2) after the year 2100, from pre-industrial conditions with a radiative forcing equal to 0 W/m^2. RCP 8.5 is an uncontrolled, or high emission scenario, with radiative forcing reaching 8.5 W/m^2 after 2100 and continuing to increase.

Figure 2 presents a flow diagram showing the methodology of data processing to create climate change projections.

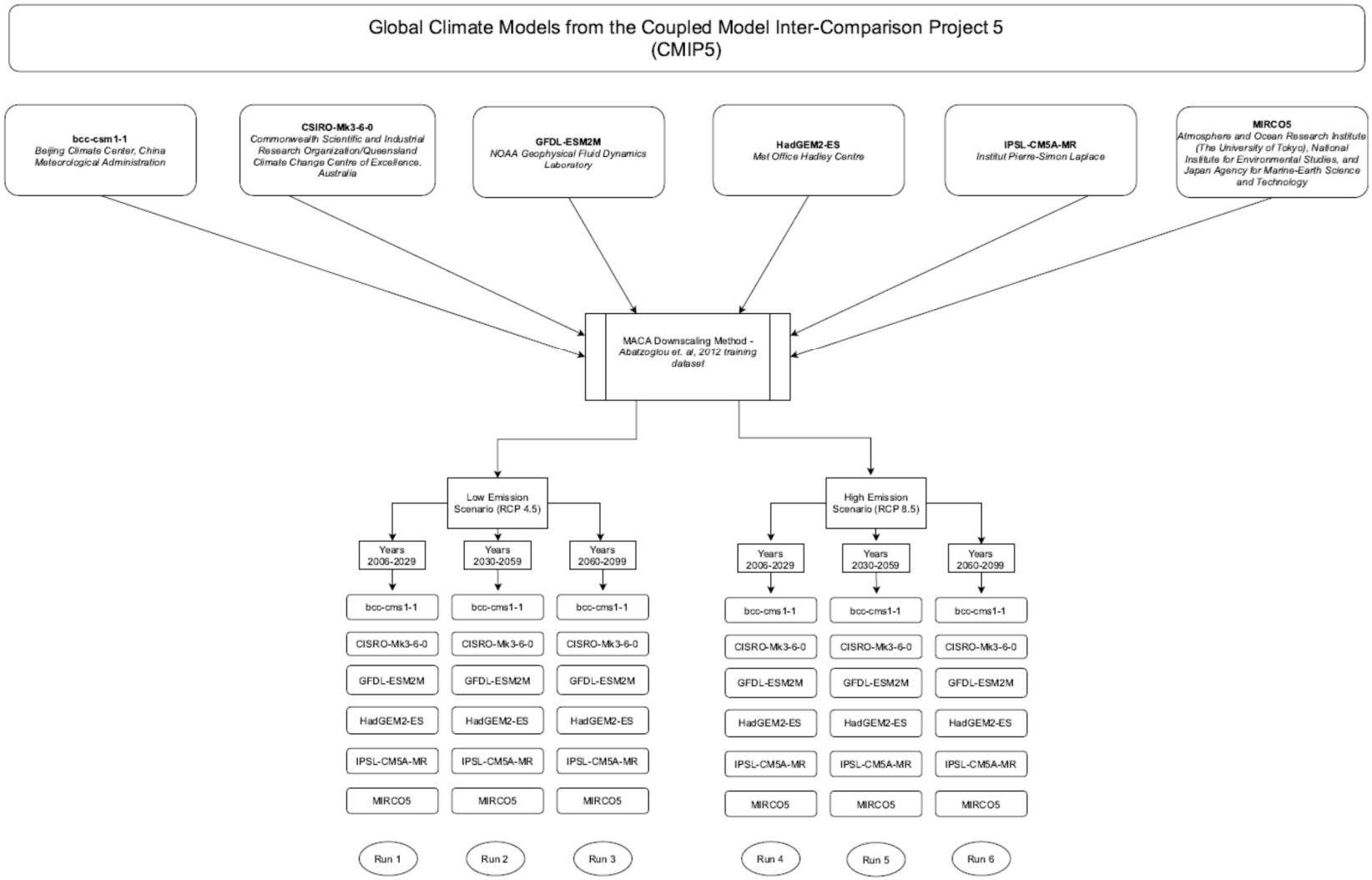

Figure 2: GCM data acquisition process and analysis for climate predictions.

Selection of Multi-Modeling Suite

Due to the variability of the GCMs created by various organizations, it has become standard practice to create a multi-model ensemble, to account for uncertainty amongst climate model predictions. Ensembles consist of structurally different models, built by different organizations. It has been shown that multi-model ensembles lower variability in climate and provide more reliable results, as each model has different strengths and weaknesses in modeling various climate variables(Mote, Brekke, Duffy, & Maurer, 2011; Pierce, Barnett, Santer, & Gleckler, 2009; Sunde, He, Hubbart, & Urban, 2017; Winkler, Guentchev, Liszewska, Perdinan, & Tan, 2011)

Studies have been done on the best method of selecting GCMs, by choosing ones that better represent local climate and therefore are thought to be better predictors of future climate for a specific area (Byun & Hamlet, 2018). Demaria et. al. and K. Byun et al. (2016) looked specifically at GCM performance in the Midwest, performed various statistical analyses and provided recommendations of downscaled GCMs that perform well in the Midwest. Two GCMs were recommended by both studies: GFDL-ESM2M, and MIROC5. Despite no major differences in results for GCM ensemble selection in results, those GCMs were chosen as they have been shown to represent the Midwest well (Demaria, Palmer, & Roundy, 2016). Another study then determined that selecting the GCMs based on performance in a study area versus a random assortment of the same number of GCMs resulted in indistinguishable differences (Pierce et al., 2009). For this reason, the remaining four GCMs chosen for this study (bcc-csm1-1, CSIRO-Mk3-6-0, HadGEM2-ES, and IPSL-CM5A-MR) were chosen to represent the array of organizations that produce global climate models.

Table 1: Global climate models chosen for multi-model ensemble. Source - https://climatenorth westknowledge. net/MACA/GCMs.php

Model Name	Organization	Country of Origin	Atmosphere Resolution (long x lat)
bcc-csm1-1	Beijing Climate Center, China Meteorological Administration	China	2.8° x 2.8°
CSIRO-Mk3-6-0	Commonwealth Scientific and Industrial Research Organization in collaboration with Queensland Climate Change Centre of Excellence	Australia	1.8° x 1.8°
GFDL-ESM2M	NOAA Geophysical Fluid Dynamics Laboratory	United States	2.5° x 2.0°
HadGEM2-ES	Met Office Hadley Centre (additional HadGEM2-ES realization contributed by Instituto Nacional de Pesquisas Espaciais)	United Kingdom	1.88° x 1.25°
IPSL-CM5A-MR	Institut Pierre-Simon Laplace	France	2.5° x 1.25°
MIROC5	Atmosphere and Ocean Research Institute (The University of Tokyo), National Institute for Environmental Studies, and Japan Agency for Marine-Earth Science and Technology	Japan	1.4° x 1.4°

Global Climate Model Downscaling

Because of its computational efficiency (Fowler et al., 2007), statistical downscaling was chosen over dynamical downscaling as the method for this analysis. Statistically downscaled climate data from the CMIP5 suite of climate models were obtained from the University of Idaho-hosted web server for the MACA downscaling method. The process of obtaining and analyzing trends of these GCMs was performed according to Abatzoglou (Abatzoglou, n.d.; Abatzoglou & Brown, 2012) Two training datasets are available and used for downscaled output: METDATA (Abatzoglou, 2013) and Livneh (Livneh et al., 2013). In statistical downscaling, an observational dataset, referred to as a “training dataset”, is used to identify statistical patterns of the historical weather. The weather predictions from the GCMs are then fit to those identified historical statistical patterns and relationships, created a predicted weather dataset that has similar weather patterns to the area of interest. Downscaled outputs are very sensitive to the training datasets

applied. Two different training datasets can result in significantly different outputs (Byun & Hamlet, 2018; Jiang et al., 2018; Kouwen et al., 2005). The Livneh training dataset obtains its historical observations from the National Weather Service Cooperative observer stations as well as the Parameter-Elevation Regressions on Independent Slopes Model (PRISM) (Livneh et al., 2013) and METDATA obtains historical observations from the NASA North American Land Data Assimilation System (NLDAS-2) and the PRISM (Abatzoglou, 2013).

Jiang et al. (2018) compared both METDATA and Livneh training datasets to other downscaling methods in Northwest USA. In comparisons of precipitation and mean annual temperature, their analysis showed the Livneh training dataset resulted in cooler temperatures than the other datasets, by 2-4°C, and mean annual precipitation ranged from 50-80% higher than the other datasets. Although Livneh displays larger differences in variable values from the other dataset, all datasets, including METDATA and the others, showed similar magnitudes of change for annual mean parameters from the reference historical period to future period. Meaning that despite differences in predicted datasets that resulted from the differences in training datasets, the magnitudes of change within each downscaled dataset were similar.

Stochastic Weather Generation

Weather generation models identify relevant statistical relationships between observed weather parameters of an area and use those relationships to generate daily weather. The identified statistical relationships can be used to produce weather data to fill gaps in missing weather observations, predict future weather, and produce long time-series of daily weather. Because of those traits, weather generation models are commonly used in analyses and impact exercises in the environmental and hydrology discipline, also in conjunction with RCMs (Maraun et al., 2010; Wilks & Wilby, 1999).

In the context of predicting climate change and impacts on a local area, it is common to apply the predicted changes of weather from an RCM (often by percent change) to a weather generation model for the area of interest. The outcome is a daily weather series under future climate predictions that match observed patterns and variances.

WINDS is a calibrated, stochastic weather generation model chosen for this analysis (Wilson, Sheshukov, & Pulley, 2006). Statistical relationships from Rochester, Minnesota, a city approximately 75 miles east of the Le Sueur River watershed, are determined based on historically observed weather. A cosine curve is fit to the historical observed data that is then

used in the weather predictions. Figure 3 provides the historical observed maximum temperature for Rochester, MN, and the cosine curve, fitted to the observed records.

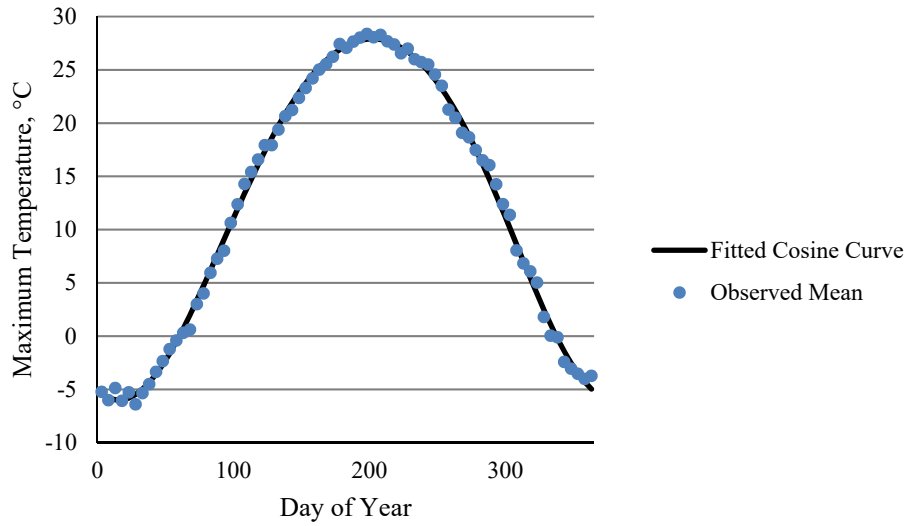

Figure 3: Observed maximum temperature in Rochester, MN with fitted cosine curve.

In predicting weather outcomes, WINDS uses that cosine curve, and applies any climate change parameters, if desired. Figure 4 provides the same fitted cosine curve, but shows the mean maximum temperature by day, for a WINDS prediction simulation of 1000-years. The predicted mean maximum temperature fits the cosine curve, that was developed by historical observed data.

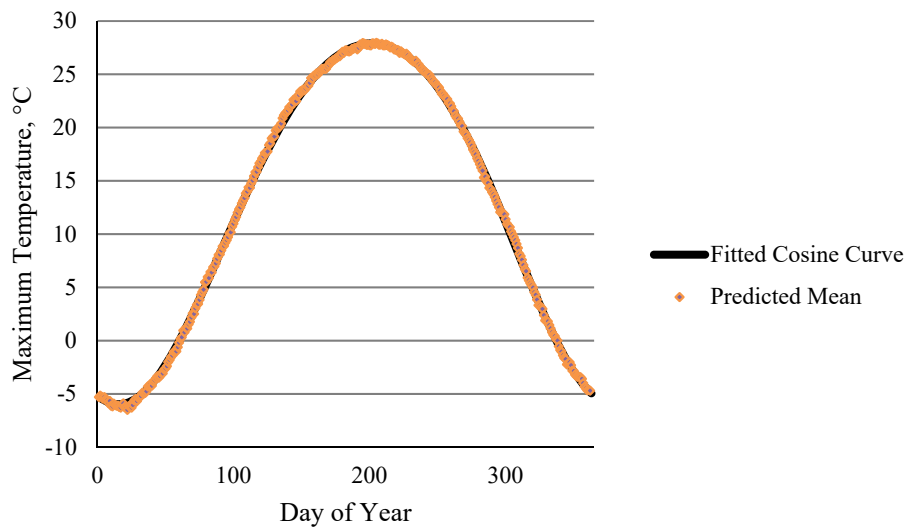

Figure 4: Mean maximum temperature of 1000-years of predicted weather in Rochester, MN with fitted cosine curve.

Cosine relationships, standard deviation relationships, and skew relationships are developed in WINDS for all input parameters. Those relationships are how the statistical parameters of the historical observed weather are used in weather predictions.

Weather is simulated in WINDS as a combination of continuous events and discrete events, as shown in Figure 5. WINDS uses different modeling protocols for each type of event. A continuous variable, like temperature, is simulated as a Markov process, where the outcome of the next day is dependent on the outcome of the previous day. The occurrence of daily precipitation, as a discrete event, is simulated using wet and dry days in a Markov chain. The transitional probabilities of having a dry day when the previous day was either wet or dry and the probability of a wet day when the previous day was either wet or dry are more important to the determination of outcome. Precipitation depth is then estimated using a probability density function (Wilson et al., 2006).

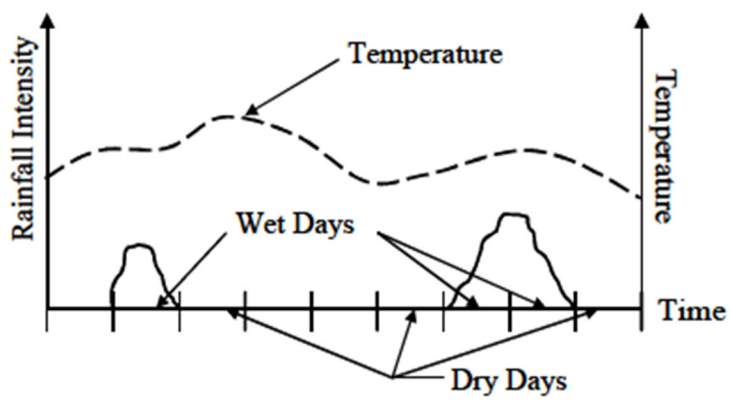

Figure 5: Modeling of continuous (temperature) and discrete (precipitation) variables is done using different modeling protocols (Wilson et al., 2006)

The percent change from the RCMs between historical observed weather predictions (years 1950-2006 from the MACA downscaled data) and the future weather predictions are used as the change factors that are applied to observed weather patterns. The WINDS modeling algorithms used those changes with the statistical weather relationships for the region to produce projected weather under climate change. The change factors from the RCMs are average percent changes from observed weather to predicted weather, averaged in three prediction time ranges: 2006 – 2029, 2030 – 2059, and 2060 – 2099. In doing so, results are presented as three projected years, 2015, 2045, and 2080.

One-thousand potential annual scenarios were generated in WINDS for each RCP scenario, averaged over summary years 2015, 2045, and 2080. Individual years of weather are

produced, with the same climate scenarios. The scenarios developed are not progressions through time, but one-thousand potential annual representations.

WINDS output for maximum and minimum temperature and precipitation are provided in the Results and Discussion section, and the percent changes applied to each weather variable for each RCP scenario and 20-day averages of WINDS output for all weather variables (maximum and minimum temperature, precipitation, solar radiation, wind speed, relative humidity) are in the Appendix, A1.2.

Results and Discussion

Downscaled Stochastic Weather Generation

Temperature

Figure 6 and Figure 7 display the 20-day temperature averages that resulted from the WINDS modeling of each downscaled training dataset, for both RCP 4.5 and RCP 8.5. The averages are from 1000 years of WINDS potential weather scenarios. Monthly minimum and maximum temperature averages and standard deviations from WINDS are provided in Table 2 and Table 3 for both downscaled datasets. Figures and tables present output as Baseline, 2015, 2045, and 2080. Those years represent ranges of years in the modeling, years 1950-2005, 2006-2029, years 2030-2059, and years 2060-2099, as summary years Baseline, 2015, 2045, and 2080, respectively.

METDATA Results

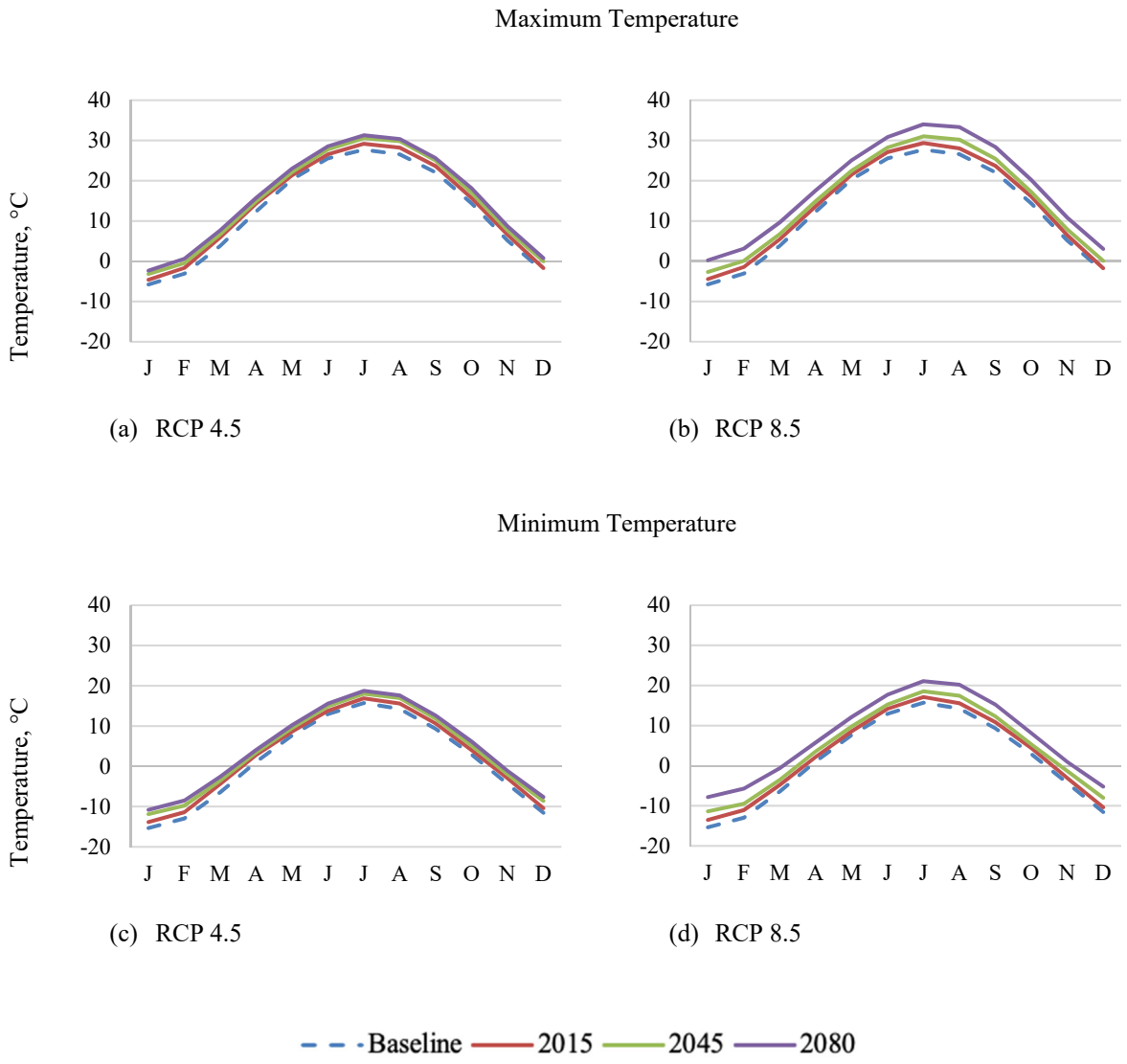

Figure 6: WINDS output of 20-day maximum and minimum temperature averages for METDATA downscaled data for RCP 4.5 and RCP 8.5 scenarios. (a): Maximum Temperature, RCP 4.5; (b): Maximum Temperature, RCP 8.5; (c) Minimum Temperature, RCP 4.5; (d): Minimum Temperature, RCP 8.5

Climate modeling of the Le Sueur watershed using GCMs and WINDS indicate an average annual increase in maximum temperature of 1.4, 2.6, and 3.5°C with standard deviations of 0.4, 0.4, and 0.3 for the METDATA training dataset for RCP 4.5 for summary years 2015, 2045, and 2080. For RCP 8.5, the average annual increase in maximum temperature is 1.4, 2.9, and 5.8°C with standard deviations of 0.3, 0.4, and 0.6.

The average increase in annual minimum temperature for RCP 4.5 is 1.3, 2.6, and 3.4°C with standard deviations of 0.3, 0.5, and 0.6. RCP 8.5 saw annual average increases of 1.4, 2.9, and 5.7°C with standard deviations of 0.3, 0.6, and 1.0, respectively.

Livneh Results

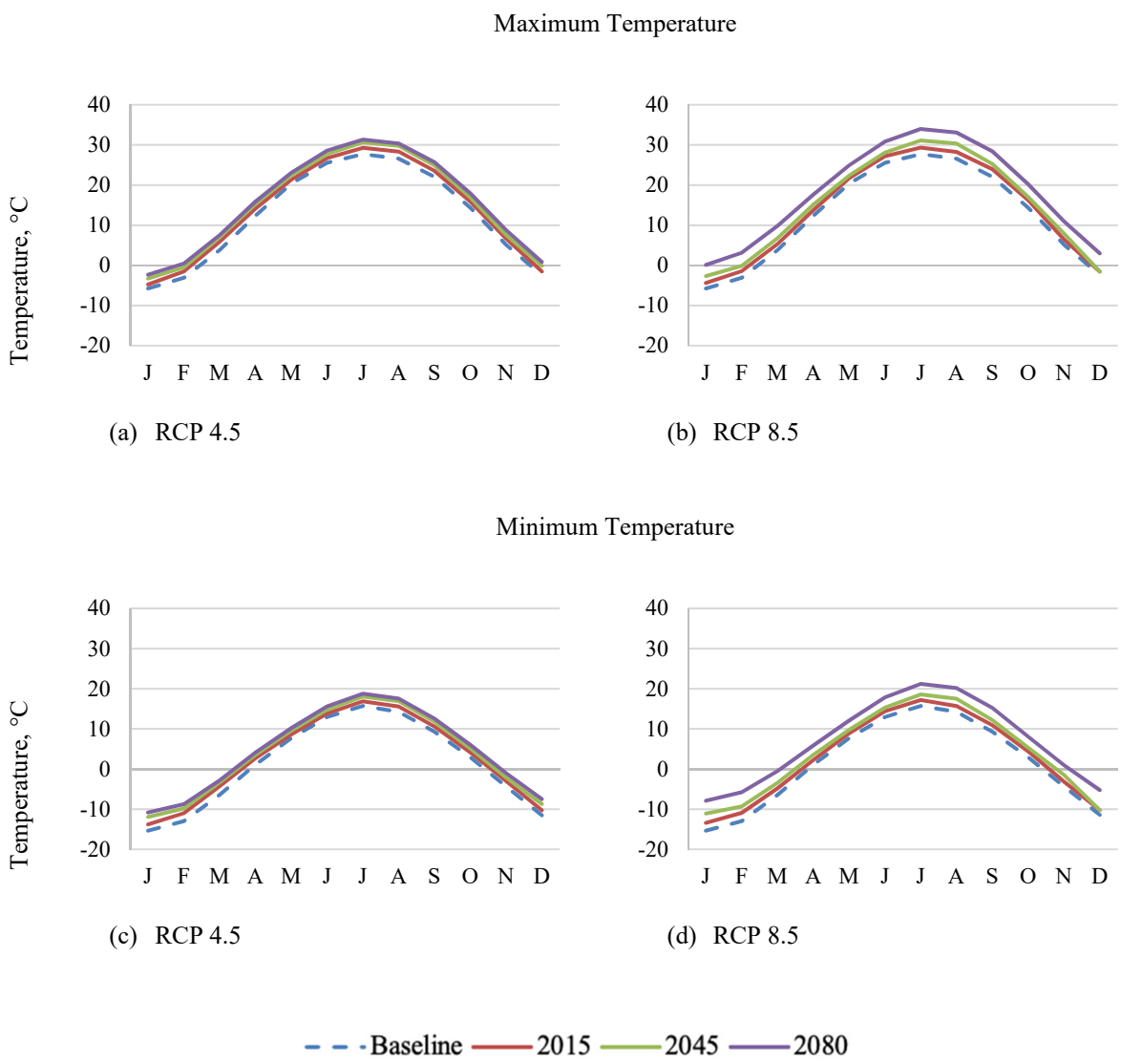

Figure 7: WINDS output of 20-Day Maximum and Minimum Temperature Averages for Livneh downscaled data for RCP 4.5 and RCP 8.5 scenarios. (a): Maximum Temperature, RCP 4.5; (b): Maximum Temperature, RCP 8.5; (c) Minimum Temperature, RCP 4.5; (d): Minimum Temperature, RCP 8.5

Figure 7 shows the WINDS temperature output for the Livneh downscaled dataset. The Livneh training dataset shows increases in annual maximum temperature of 1.4, 2.6, and 3.5°C

with standard deviations of 0.4, 0.4, and 0.3 for representative years 2015, 2045, and 2080 for RCP 4.5 For RCP 8.5, the average increases in annual maximum temperature are 1.5, 2.8, and 5.8°C with standard deviations of 0.3, 0.7, and 0.6. The average increase in annual minimum temperature for RCP 4.5 is 1.4, 2.5, and 3.4°C with standard deviations of 0.4, 0.5, and 0.6, respectively. RCP 8.5 had annual increases of 1.5, 2.8, and 5.7°C with standard deviations of 0.3, 0.8, and 0.9, respectively. An analysis of results of monthly average temperature and standard deviations for both RCP 4.5 and RCP 8.5 are similar between METDATA and Livneh training datasets. Tables of 20-day averages of all variables modeled in WINDS (minimum and maximum temperature, precipitation, wind speed, relative humidity, and solar radiation), are provided in the Appendix as A1.1.

Table 2: Monthly mean maximum and minimum temperatures and standard deviations from WINDS modeling (temperature/standard deviation). RCP 4.5, METDATA and Livneh downscaled datasets.

Month	Maximum Temperature							Minimum Temperature						
	Base line	METDATA			Livneh			Base line	METDATA			Livneh		
		2015	2045	2080	2015	2045	2080		2015	2045	2080	2015	2045	2080
Jan	*-5.76*	-4.59	-3.17	-2.32	-4.76	-3.28	-2.34	*-15.35*	-13.85	-11.87	-10.81	-13.78	-11.94	-10.82
	(0.36)	(0.29)	(0.32)	(0.4)	(0.38)	(0.38)	(0.29)	*(0.48)*	(0.38)	(0.42)	(0.42)	(0.44)	(0.41)	(0.35)
Feb	*-3.1*	-1.66	-0.45	0.64	-1.53	-0.49	0.48	*-12.97*	-11.4	-9.75	-8.51	-11	-9.83	-8.76
	(1.45)	(1.61)	(1.47)	(1.56)	(1.61)	(1.51)	(1.57)	*(1.44)*	(1.49)	(1.28)	(1.35)	(1.48)	(1.31)	(1.3)
March	*3.82*	5.95	6.69	7.73	5.88	7.02	7.55	*-6.44*	-4.4	-3.51	-2.58	-4.31	-3.32	-2.8
	(2.55)	(2.58)	(2.61)	(2.41)	(2.5)	(2.51)	(2.55)	*(2.33)*	(2.34)	(2.25)	(2.03)	(2.18)	(2.12)	(2.13)
April	*12.34*	14.33	14.92	15.76	14.14	15.27	15.87	*1.06*	2.81	3.39	4.04	2.68	3.51	4.1
	(2.38)	(2.33)	(2.27)	(2.15)	(2.19)	(2.33)	(2.16)	*(1.95)*	(1.91)	(1.86)	(1.77)	(1.81)	(1.86)	(1.76)
May	*20.36*	21.32	22.14	23.06	21.31	22.4	23.07	*7.68*	8.61	9.53	10.2	8.6	9.57	10.19
	(1.96)	(1.94)	(2)	(2.08)	(1.88)	(1.91)	(1.83)	*(1.76)*	(1.64)	(1.74)	(1.81)	(1.67)	(1.71)	(1.67)
June	*25.55*	26.56	27.75	28.56	26.7	27.73	28.59	*12.95*	13.79	14.91	15.58	13.83	14.79	15.62
	(1.04)	(1.1)	(1.2)	(1.18)	(1.12)	(1.14)	(1.28)	*(1.25)*	(1.24)	(1.29)	(1.29)	(1.29)	(1.24)	(1.36)
July	*27.71*	29.18	30.58	31.3	29.27	30.64	31.33	*15.72*	16.89	18.02	18.73	16.87	18.05	18.77
	(0.24)	(0.33)	(0.38)	(0.41)	(0.33)	(0.4)	(0.39)	*(0.33)*	(0.38)	(0.39)	(0.45)	(0.41)	(0.47)	(0.44)
Aug	*26.57*	28.22	29.83	30.37	28.32	29.76	30.35	*14.24*	15.58	16.95	17.59	15.59	16.88	17.55
	(0.9)	(0.78)	(0.86)	(0.82)	(0.85)	(0.87)	(0.86)	*(1.12)*	(1.01)	(1.01)	(0.95)	(1.08)	(0.99)	(0.99)
Sept	*22.07*	23.62	24.98	25.59	23.55	24.91	25.68	*9.3*	10.62	11.82	12.6	10.59	11.81	12.57
	(1.79)	(1.76)	(1.87)	(1.77)	(1.91)	(1.93)	(1.85)	*(1.69)*	(1.67)	(1.79)	(1.72)	(1.77)	(1.84)	(1.79)
Oct	*14.37*	15.69	17.02	18.13	15.87	16.93	17.93	*2.92*	3.98	5.11	6.16	4.15	5.11	6
	(2.68)	(2.64)	(2.62)	(2.5)	(2.46)	(2.63)	(2.51)	*(2.05)*	(1.99)	(2.01)	(1.99)	(1.87)	(2.06)	(1.97)
Nov	*5.15*	6.57	7.73	8.72	6.66	7.58	8.78	*-4.35*	-3	-2	-1.12	-2.99	-2.14	-1.04
	(2.59)	(2.67)	(2.55)	(2.69)	(2.58)	(2.61)	(2.58)	*(2.14)*	(2.18)	(1.97)	(2.11)	(2.11)	(2.08)	(1.96)
Dec	*-2.5*	-1.68	0	0.78	-1.5	-0.12	0.86	*-11.54*	-10.41	-8.58	-7.63	-10.27	-8.72	-7.5
	(1.84)	(1.61)	(1.63)	(1.87)	(2.1)	(1.82)	(1.83)	*(1.92)*	(1.64)	(1.51)	(1.67)	(2.1)	(1.66)	(1.64)

Table 3: Monthly mean maximum and minimum temperatures and standard deviations from WINDS modeling (temperature/standard deviation) RCP 8.5, METDATA and Livneh downscaled datasets.

	Maximum Temperature							Minimum Temperature						
Month	**Base line**	**METDATA**			**Livneh**			**Base line**	**METDATA**			**Livneh**		
		2015	**2045**	**2080**	**2015**	**2045**	**2080**		**2015**	**2045**	**2080**	**2015**	**2045**	**2080**
Jan	*-5.76*	-4.45	-2.67	0.23	-4.39	-2.67	0.11	*-15.35*	-13.53	-11.38	-7.83	-13.42	-11.09	-7.9
	(0.36)	(0.31)	(0.26)	(0.35)	(0.43)	(0.39)	(0.32)	*(0.48)*	(0.35)	(0.42)	(0.4)	(0.39)	(0.44)	(0.33)
Feb	*-3.1*	-1.45	0.07	3.14	-1.43	-0.14	3.12	*-12.97*	-11.05	-9.47	-5.72	-10.92	-9.33	-5.8
	(1.45)	(1.46)	(1.5)	(1.45)	(1.53)	(1.42)	(1.54)	*(1.44)*	(1.36)	(1.28)	(1.18)	(1.4)	(1.18)	(1.19)
March	*3.82*	5.45	6.71	9.62	5.33	6.77	9.83	*-6.44*	-4.79	-3.54	-0.63	-4.78	-3.42	-0.5
	(2.55)	(2.25)	(2.41)	(2.19)	(2.41)	(2.4)	(2.16)	*(2.33)*	(2)	(2.15)	(1.71)	(2.11)	(2.05)	(1.64)
April	*12.34*	13.66	14.92	17.58	13.73	15.13	17.62	*1.06*	2.19	3.58	5.78	2.26	3.55	5.87
	(2.38)	(2.26)	(2.26)	(2.17)	(2.45)	(2.24)	(2.19)	*(1.95)*	(1.8)	(1.86)	(1.82)	(1.96)	(1.86)	(1.81)
May	*20.36*	21.53	22.48	25.06	21.71	22.37	24.89	*7.68*	8.58	9.78	12.13	8.89	9.74	12.08
	(1.96)	(2.12)	(2.05)	(2.07)	(2.1)	(1.98)	(2)	*(1.76)*	(1.87)	(1.72)	(1.85)	(1.88)	(1.77)	(1.83)
June	*25.55*	27.13	28.24	30.86	27.2	28.11	30.85	*12.95*	14.19	15.27	17.71	14.4	15.3	17.84
	(1.04)	(1.11)	(1.23)	(1.4)	(1.21)	(1.26)	(1.36)	*(1.25)*	(1.28)	(1.33)	(1.47)	(1.37)	(1.4)	(1.42)
July	*27.71*	29.36	31.02	34.02	29.33	31.1	33.97	*15.72*	17.11	18.55	21.08	17.19	18.58	21.21
	(0.24)	(0.22)	(0.41)	(0.43)	(0.19)	(0.4)	(0.43)	*(0.33)*	(0.34)	(0.5)	(0.46)	(0.24)	(0.44)	(0.48)
Au	*26.57*	28.04	30.2	33.33	28.24	30.36	33.1	*14.24*	15.58	17.46	20.18	15.67	17.51	20.18
	(0.9)	(0.8)	(0.91)	(0.83)	(0.76)	(0.94)	(0.87)	*(1.12)*	(1.05)	(1.1)	(0.96)	(0.99)	(1.06)	(0.97)
Sept	*22.07*	23.69	25.43	28.39	23.95	25.26	28.4	*9.3*	10.83	12.28	15.22	10.88	12.17	15.24
	(1.79)	(1.72)	(1.82)	(1.96)	(1.74)	(1.95)	(1.84)	*(1.69)*	(1.67)	(1.82)	(1.86)	(1.68)	(1.83)	(1.82)
Oct	*14.37*	16.07	17.18	20.2	16.25	17.02	20.22	*2.92*	4.42	5.31	8.1	4.43	5.34	8.08
	(2.68)	(2.61)	(2.75)	(2.79)	(2.69)	(2.73)	(2.72)	*(2.05)*	(1.99)	(2.06)	(2.24)	(2.06)	(2.08)	(2.22)
Nov	*5.15*	6.42	7.93	10.84	6.44	7.93	10.96	*-4.35*	-3.08	-1.37	0.94	-3.15	-1.49	0.96
	(2.59)	(2.78)	(2.42)	(2.56)	(2.7)	(2.45)	(2.67)	*(2.14)*	(2.21)	(1.78)	(1.94)	(2.13)	(1.94)	(1.98)
Dec	*-2.5*	-1.74	0.09	3.05	-1.55	0.36	2.99	*-11.54*	-10.37	-8	-5.19	-10.24	-7.89	-5.25
	(1.84)	(1.7)	(1.79)	(1.76)	(1.72)	(1.83)	(1.77)	*(1.92)*	(1.7)	(1.77)	(1.49)	(1.67)	(1.71)	(1.47)

A seasonal analysis of differences in predicted temperatures from both training datasets is presented in Table 4 and Table 5. Winter season is presented as December - February, Spring season is presented as March - May, Summer season is presented as June - August, and Fall season is presented as September - November. Differences in seasonal average temperature between downscaling methods for each summary year of 2015, 2045, and 2080 in both RCP scenarios are minimal. The largest difference in seasonal average temperature between METDATA and Livneh downscaling methods for RCP 4.5 is 0.2°C in the Spring season of year 2045. The largest difference in RCP 8.5 is 0.6°C in the Winter season of year 2045.

Table 4: Average seasonal temperatures of RCP 4.5 for METDATA and Livneh downscaling methods.

Season	Baseline	METDATA			Livneh		
		2015	2045	2080	2015	2045	2080
Winter	-8.5	-7.3	-5.6	-4.6	-7.1	-5.7	-4.7
Spring	6.5	8.1	8.9	9.7	8.0	9.1	9.7
Summer	20.5	21.7	23.0	23.7	21.8	23.0	23.7
Fall	8.2	9.6	10.8	11.7	9.6	10.7	11.7

Table 5: Average seasonal temperature of RCP 8.5 for METDATA and Livneh downscaling methods.

Season	Baseline	METDATA			Livneh		
		2015	2045	2080	2015	2045	2080
Winter	-8.5	-7.1	-5.2	-2.1	-7.0	-5.8	-2.1
Spring	6.5	7.8	9.0	11.6	7.9	9.0	11.6
Summer	20.5	21.9	23.5	26.2	22.0	23.5	26.2
Fall	8.2	9.7	11.1	14.0	9.8	11.0	14.0

Precipitation

Table 6 displays average (of 1000-years of modeling outcomes) annual depth, maximum depth, minimum depth, and range of precipitation. Yearly precipitation depth averages of 1000-years of modeled data result in increases in average precipitation (mm) from Baseline conditions for the METDATA downscaling method of 14.2, 25.1, and 39 mm for RCP 4.5 and 9.4, 33.9, and 49.6 mm for RCP 8.5. The Livneh downscaling method resulted in increases in precipitation (mm) from Baseline conditions of 13.2, 22.5, and 31.3 mm for RCP 4.5 and 5.5, 36.9, and 43.9 mm for RCP 8.5.

Table 6: 1000-year annual average of precipitation, maximum precipitation depth, minimum precipitation depth, and range of depths, for both METDATA and Livneh downscaling methods for both climate scenarios modeled, RCP 4.5 and RCP 8.5.

METDATA

Variable	Baseline	RCP 4.5			RCP 8.5		
		2015	2045	2080	2015	2045	2080
Average Depth, mm	757.5	771.7	782.6	796.5	766.9	791.4	807.1
Maximum Depth, mm	1236.7	1436.7	1355.9	1297.3	1202.1	1277.6	1283.6
Minimum Depth, mm	438.9	400.6	425.7	412.6	435.6	450.9	452.2
Range	797.8	1036.1	930.2	884.6	766.5	826.7	831.5

Livneh

Variable	Baseline	RCP 4.5			RCP 8.5		
		2015	2045	2080	2015	2045	2080
Average Depth, mm	757.5	770.7	780	788.8	763	794.4	801.4
Maximum Depth, mm	1236.7	1232.3	1267.8	1317.4	1240.9	1293.4	1287.2
Minimum Depth, mm	438.9	426.4	383	421.6	409.3	430.3	447.7
Range	797.8	805.9	884.8	895.8	831.6	863.1	839.5

As WINDS is a stochastic model, the variability and range of output is to be expected and a result of the randomness of a stochastic model. Results indicate average annual precipitation depth increasing in all summary years and RCP scenarios from Baseline conditions.

Table 7 shows the frequency of events that are classified as 1000- to 1-year rain events for both downscaling methods, per the rain event depths from the National Oceanic and Atmospheric Administration (NOAA) Atlas 14 calculations.

Table 7: Number of occurrences in the 1000-year model runs of average daily precipitation that would be considered NOAA Atlas 14-defined design rain events for Le Sueur Watershed, Minnesota. To be considered a certain design event, precipitation depth must be greater than or equal to the Atlas 14 24-hours depth.

Record Year Storm	Atlas 14 - 24-hr depths (in)	Baseline	METDATA						Livneh					
			RCP 4.5			RCP 8.5			RCP 4.5			RCP 8.5		
			2015	2045	2080	2015	2045	2080	2015	2045	2080	2015	2045	2080
1000	11.90	0	0	0	0	0	0	0	0	0	0	0	0	0
500	10.60	0	0	0	0	0	0	0	0	0	0	0	0	0
200	8.89	0	0	0	0	0	0	0	0	0	0	1	0	2
100	7.72	0	2	3	1	1	2	0	2	0	0	2	1	3
50	6.65	3	5	6	4	3	4	4	6	2	1	2	4	7
25	5.66	8	9	11	18	9	13	15	14	7	9	8	9	13
10	4.52	44	36	35	48	32	42	41	53	29	39	42	46	44
5	3.77	107	97	102	111	92	103	103	118	83	99	87	103	95
2	2.98	297	282	291	333	272	299	293	312	252	286	266	279	254
1	2.54	518	524	527	608	475	503	538	550	463	542	501	523	522

A current gap in the weather generation modeling available is the ability of weather generators to reproduce the frequency, intensity, and duration of extreme events (Ailliot, Allard, Monbet, & Naveau, 2015; Maraun et al., 2010). The WINDS model does not show an increase in larger storms in either downscaling method, which would be expected with what has been recently documented with an increase in heavy rain events in Minnesota. The METDATA WINDS results do show a higher frequency of 100-year precipitation events, when compared to the Livneh training dataset results. Livneh results show only three, 200-year rain events, out of a sample size of 1000. With current modeling tools, it is difficult to capture increases in extreme events, in part because the historical observations used in future weather predictions do not yet have a large record of increased heavy precipitation events to be sufficiently captured in statistical relationships. In addition, the modeling tools used in the analysis and method of analysis are not set up to focus on increased heavy precipitation events; those larger events are dampened in monthly and yearly averages

Figure 8 displays WINDS output for cumulative monthly precipitation depth for Baseline, summary years 2015, 2045, and 2080 of the METDATA and Livneh downscaled datasets. April and May see the largest increases in monthly precipitation.

The METDATA dataset sees increases in April and May from Baseline to summary year 2080 of 7 and 11 mm for RCP 4.5 and 11 and 15 mm for RCP 8.5. The Livenh dataset sees increases in April and May from Baseline to summary year 2080 of 6 and 10 mm for RCP 4.5 and 15 and 11 mm for RCP 8.5.

The METDATA dataset sees the largest decreases in the months of July and August. For RCP 4.5, those decreases, largest in summary year 2045, are 5 and 9 mm, respectively. RCP 8.5 has largest decreases in July and August of summary year 2080, and are 15 and 8 mm, respectively. The Livneh dataset sees its largest decreases in July in August, from Baseline to summary year 2045, for RCP 4.5 of 8 and 9 mm, respectively. Largest decreases for RCP 8.5 from Baseline to summary year 2080 are 14 and 9 mm, for July and August, respectively.

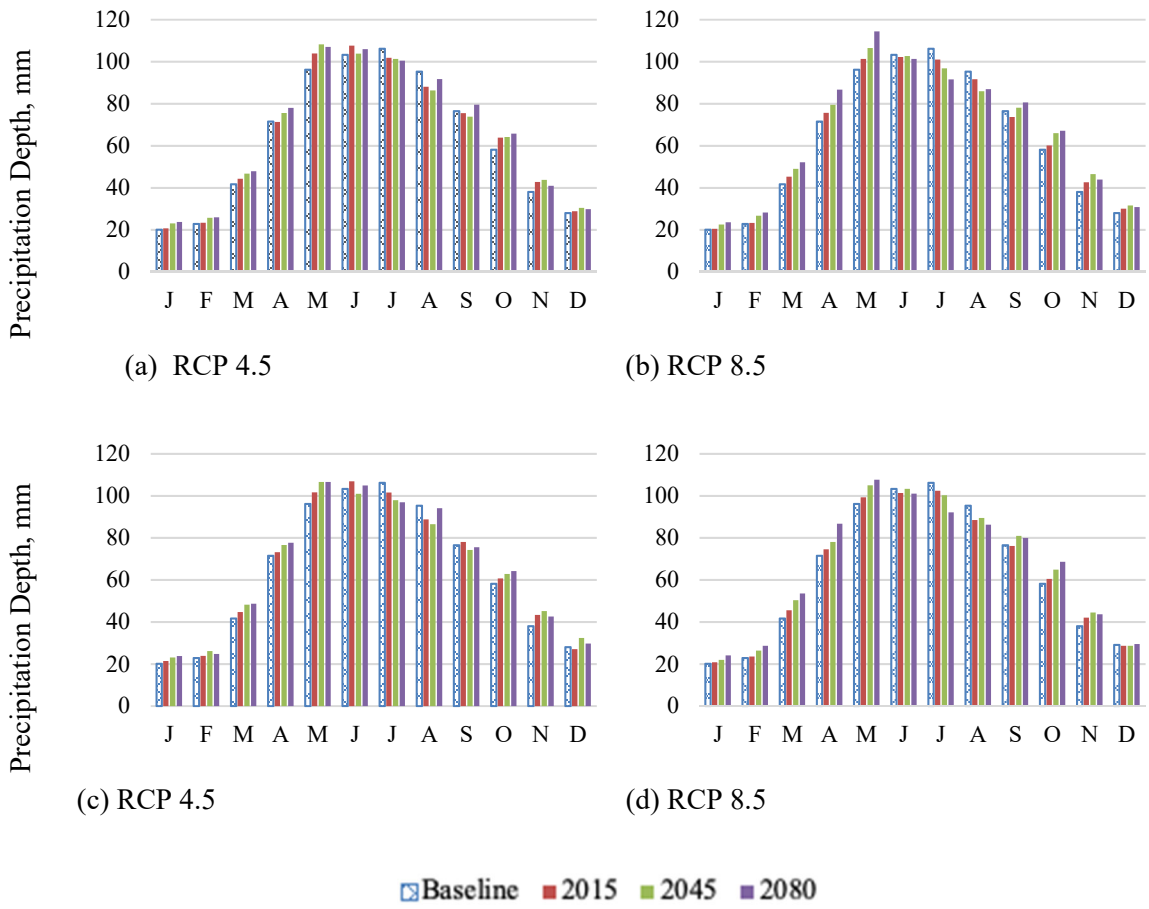

Figure 8: WINDS output for monthly precipitation totals for METDATA and Livneh downscaled datasets, for both RCP 4.5 and RCP 8.5. (a) METDATA downscaling, RCP 4.5; (b) METDATA downscaling, RCP 8.5; (c) Livneh downscaling, RCP 4.5; (d) Livneh downscaling, RCP 8.5.

Relative Humidity

Across the state, relative humidity ranges from approximately 50% to 75%. Similar monthly and yearly relative humidity values from WINDS modeling are shown in Figure 9 and Figure 10.

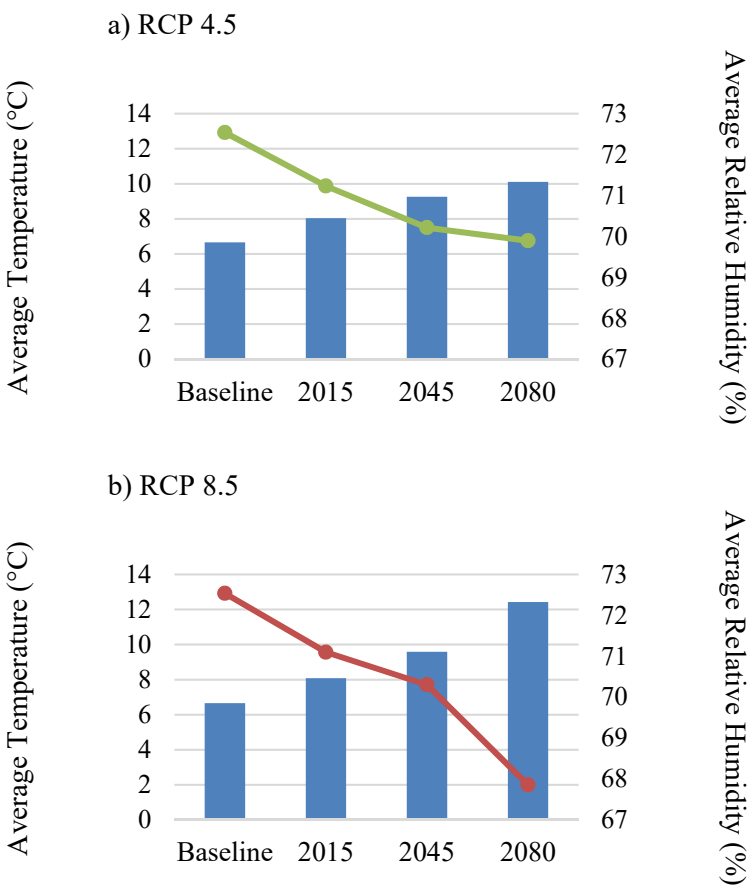

Figure 9: WINDS output for average temperature and average relative humidity for METDATA downscaling, summary years Baseline, 2015, 2045, and 2080, for a) RCP 4.5 modeling scenario and b) RCP 8.5 modeling scenarios

As annual average temperature increases, average relative humidity decreases. This is clearly seen in the annual trends, Figure 9. In RCP 4.5, annual average relative humidity for Baseline, 2015, 2045, and 2080 are 72.5, 71.2, 70.2, and 69.9%, respectively. RCP 8.5 relative humidity values for Baseline, 2015, 2045, and 2080 are 72.5, 71.1, 70.3, and 67.9%, respectively. A larger difference is seen from Baseline to year 2080 in RCP 8.5. This reflects a known relationship between temperature, relative humidity, and water vapor. As temperature increases and water vapor stays the same, relative humidity decreases (Hardwick Jones, Westra, & Sharma, 2010).

Month by month, average relative humidity decreases from Baseline to summary years 2015, 2045, and 2080 for both RCP 4.5 and RCP 8.5, seen in Figure 10. Research on relative humidity output from GCMs show a decrease in relative humidity in the mid-latitudes

(encompassing south-central Minnesota), which also corresponds to cloud cover trends (Sherwood et al., 2010), fitting with the WINDS output of this analysis.

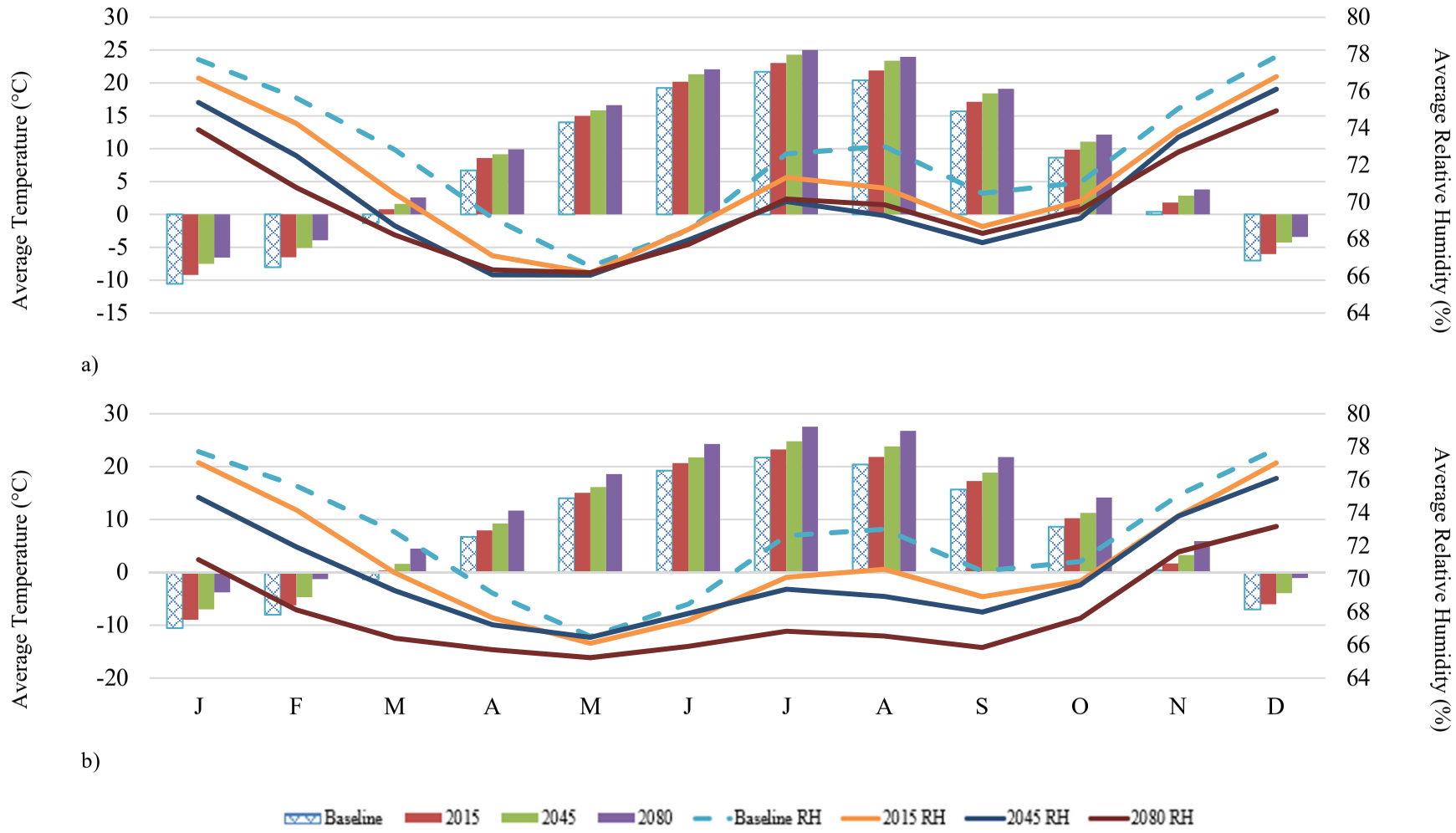

Figure 10: Average monthly temperature and average relative humidity, for METDATA downscaling method, for a) RCP 4.5 and b) RCP 8.5 modeling scenarios.

Summary

Uncertainty surrounds future weather and potential impacts from climate change. GCMs are frequently updated to reflect improvements in modeling capabilities and updated scenario predictions, to better represent likely predicted world conditions. This analysis attempted to downscale GCMs that use the latest climate change scenarios (RCP 4.5 and RCP 8.5) at a HUC-8 level, to create projected weather inputs to assess potential impacts due to climate change. Weather variables obtained and downscaled included minimum and maximum temperature, precipitation, wind speed, relative humidity, and solar radiation. Two training datasets, downscaled using the MACA method, were assessed for developing climate datasets. Percent changes from Baseline conditions to summary years 2015, 2045, and 2080 were used in a weather generation model, calibrated for the area of interest. The climate change scenarios produced from this exercise will be used in a calibrated watershed model to investigate the watershed response to climate change.

Many have undertaken the work to apply global climate data to an area of interest. The methods chosen for this analysis are commonly used in climate modeling. Global climate models were obtained from the WCRP CMIP5, for both RCP 4.5 and 8.5. The predictions were downscaled using the MACA method, using two training datasets, METDATA and Livneh. One thousand years of the potential weather per climate scenario was modeled using WINDS, a stochastic weather generator.

Conclusions

Temperature

For both downscaling methods and both RCP scenarios, ranges in maximum temperature projections are greater than the ranges in minimum temperature projections. All models show an increase in mean minimum and maximum temperatures. Increases are larger for the RCP 8.5 scenario in the summary year 2080. All scenarios showed smaller increase in early spring (April, May, June) when compared to other months. The increases in temperatures and scales between each summary year was expected, based on previous climate modeling and resulting studies.

Precipitation

Yearly precipitation increases from RCP 4.5 to 8.5, as well as from 2015 to 2080 for both RCP scenarios. An increase in precipitation has the potential to impact growing success and transport of nutrients and sediment downstream, impacting water quality.

Both downscaling methods predict that the summer months will experience decreased precipitation depths compared to Baseline conditions. The largest increase in daily average precipitation depth was in May, output for the months of July and August resulted in the largest decreases.

Relative Humidity

Model results indicate increasing heat in the atmosphere due to temperature and water vapor. Intuitively, one would expect with increasing temperature and precipitation, the atmosphere is able to hold more moisture, increasing relative humidity. If temperature rises and relative humidity decreases, that indicates a stable amount of water vapor in the atmosphere. Despite increasing precipitation in future scenarios, relative humidity will decrease because higher temperatures will increase the air capacity to contain more water vapor.

Implications for Watershed Modeling

These data will be used as weather input for SWAT, to analyze watershed response to climate change conditions. Watershed models rely on weather data in a variety of ways that can be impacted by climate change. Not only that, but as found with downscaled data sets of climate predictions, it is not difficult to use potentially inaccurate or unlikely climate predictions of said weather variables. The quality of model output is dependent on the quality of model inputs, and it needs to be remembered that models are only tools to be used to ask and answers questions, not always fact. While most results reported here relate to temperature and precipitation, because of the large impact on runoff, the other weather variables are still important to watershed modeling. Solar radiation and wind speed projections are two variables that were also obtained for the study time period, but not analyzed in this text. Those two variables, as well as relative humidity, do play important roles in other environmental processes, including evapotranspiration.

Uncertainties and Future Research

This research is limited by the available modeling procedures and technologies, which improve over time. Thus, climate modeling and downscaling methodologies may change and may result in different predicted outcomes for the Le Sueur River basin. The work done in this analysis uses common modeling procedures that are available for public use. As predictions of future climate, modeling technologies and procedures improve, further research for this study area is recommended.

This research was done with six selected GCMs, for two of four available RCP scenarios. The six models chosen in this analysis were chosen in part because they proved to be good representations of climate in the Midwest as well as from a variety of organizations, to represent the different organizations participating in the CMIP5 project. Results may differ with a different set of GCMs, as each model produces different results (Cherie, 2013). Further research can be done with a different suite of GCMs, as well as other RCPs available, to get a broader understand of changes due to climate change.

Climate change may have impacts to watershed water balances and water quality and will be impactful on human and animal health, producers, land use managers, and those downstream. Each year the Gulf of Mexico measures a hypoxic zone, which is in part caused by excess nutrients entering the Gulf of Mexico from upstream sources. This work of preparing predicted climate for the Le Sueur River watershed will be used in SWAT modeling, to investigate the potential impacts to the watershed and downstream water quality due to climate change. The 1000-years of potential future weather generated using WINDS will become input to SWAT, to run 1000-year model runs with predicted weather conditions. Output will hopefully guide those involved in land management and water quality in what may be seen and experienced in the future.

Chapter 2 - Modeling Watershed Response to Climate Change in the Le Sueur River Basin using SWAT

Introduction

Climate change is resulting in varying impacts across the United States. Sea level rise will be seen along all coastal areas, impacting infrastructure and human life. The Northeast is expected to experience heat waves and heavier downpours, impacting fisheries. Extreme heat will impact the Southeast and Southwest, with increased drought specifically in the Southwest. The North-and Southwest will see a change in insect outbreaks and tree diseases. The Midwest will also see extreme heat, changes in rainfall patterns leading to frequent flooding (USGCRP, 2018). A range of potential impacts and changes will be seen across the United States, and even within regions, experiences will vary. Understanding of potential impacts at a local scale will be critical for the planning and health of those regional populations.

Global climate models (GCM) have the ability to predict changes in climate on a large-resolution, but the large scale resolution does not always accurately represent regional conditions (Maurer et al., 2010; Zhang, Xu, & Fu, 2014). Downscaled climate data provides a more accurate picture of local conditions and is a well-established practice for climate impact assessment on a smaller scale (Byun & Hamlet, 2018; Ficklin, Luo, Luedeling, & Zhang, 2009; Mehan, Kanan, Neupane, McDaniel, & Kumar, 2016).

The ease of obtaining climate data, downscaling the data to a smaller area, and improvements in modeling technology and speed have resulted in numerous studies assessing the impacts of climate change on watersheds located in the upper Midwest (Byun & Hamlet, 2018; Chien, Yeh, & Knouft, 2013a; Jha, Arnold, Gassman, Giorgi, & Gu, 2006; Thomson et al., 2014; Winkler, Arritt, & Pryor, 2012). Downscaled climate data can be a valuable resource to producers, land use mangers, academia, and public and private sectors, for planning and understanding regional climate projections.

The Upper Mississippi River Basin (UMRB) has been noted to be especially sensitive to climate change because of the three air mass regions, Gulf of Mexico, Arctic, and Pacific, that control climate (USGS, 1999). Jha et al., 2006 used the Soil & Water Assessment Tool (SWAT)

to study potential climate changes on the UMRB and found that when the only change in the model was a doubling of atmospheric carbon dioxide, streamflow increased 36%. Scenarios with only precipitation changes of -20, -10, 10, and 20% resulted in average annual stream flow changes of -49, -26, 28, and 58%. Within the study high seasonal variability was also observed (Jha et al., 2006).

Other climate modeling exercises on watersheds in the UMRB also revealed a range of results (Jha, Gassman, Secchi, Gu, & Arnold, 2004; Rosenberg, Brown, Izaurralde, & Thomson, 2003). A study on four predominantly agricultural watersheds in the UMRB, ranging in size from 30-90,000 km2, found that under the SRES climate change scenarios, annual flows were projected to decrease between 44.6% to 61.3% in the 2086-2095 prediction timeframe. The four watersheds were spread throughout the UMRB (Wisconsin, Illinois, and Indiana), and results revealed a spatial variability of streamflow, supporting the conclusion that response to climate change can be different from region to region (Chien, Yeh, & Knouft, 2013b).

Thus far, most of the currently published modeling of climate change in the Midwest use previous phases of the Coupled Model Intercomparison Project (CMIP) emissions scenarios (SRES scenarios), associated with earlier versions of the Intergovernmental Panel on Climate Change (IPCC) Assessment Reports. The latest report and updated emissions scenarios (CMIP5) were published in 2014 (IPCC, 2014a), suggesting a new round of modeling is due to predict local responses to these updated climate predictions.

Climate modeling in conjunction with watershed modeling can provide information on watershed outputs, in predicted scenarios. Nitrogen, phosphorus, and total suspended solids (TSS), are outflows from agricultural watersheds and impact water quality. Approximately 160 million pounds of total nitrogen (TN) enter the Mississippi River from Minnesota watersheds each year. The Le Sueur River watershed is the fourth highest contributor of TN to the Minnesota River basin, which drains to the Mississippi River, at 5.7% of the total amount, or approximately 20 pounds per acre per year (Minnesota, 2013). The Lower Minnesota, Blue Earth, Le Sueur and Watonwan watersheds combined contribute approximately 75% of the total nitrate N load from the Minnesota River Basin to the Mississippi River (Randall & Mulla, 2001).

On average, the state of Minnesota's total phosphorus (TP) contributions to surface waters are 31% from point sources and 69% non-point sources. Phosphorus loading in the Minnesota River Basin consists of 25% point source and 75% non-point source, during average flow conditions (Barr Engineering, 2004). Higher levels of TP in runoff and surface waters lead

to eutrophication and low dissolved oxygen in the water. Phosphorus amounts in water is one factor that impacts the size of the hypoxic zone in the Gulf of Mexico.

Lake Pepin, in Minnesota, is an impoundment on the Mississippi River where sediment contributions from Minnesota watersheds is measured. Gauge records have indicated that 74% of the sediment delivered to Lake Pepin comes from the Minnesota River Basin. The Blue Earth River and Le Sueur River watersheds are the highest contributors of TSS to the Minnesota River. For only making up one-fifth of the Minnesota River drainage area, it is estimated that the two watersheds contribute half the sediment to the Minnesota River (Wilcock, 2009). This area, and the Minnesota River Basin as a whole, has been the focus of multiple studies relating to the high levels of sediment in the Minnesota River and the resulting downstream implications and impacts (Dalzell & Mulla, 2018; Day et al., 2011; K. B. Gran et al., 2009; Kelley & Nater, 2000; Wilcock, 2009). The Le Sueur River watershed has geologic conditions that are especially susceptible to erosion, as a large portion of the watershed is made of glacial till soil with steep riverbanks. In higher precipitation events, bluffs and streambanks are the largest places for erosion and the source of TSS pollution (K. Gran et al., 2011).

The Minnesota Pollution Control Agency has set goals for the state to reduce nitrogen and phosphorus in surface water, through the Minnesota Nutrient Reduction Strategy. The strategy was created because it was recognized that nutrients in the water can cause problems for both humans and aquatic life within the state. In addition, as described above, Minnesota's contribution to the Gulf of Mexico hypoxic zone is also significant, making another goal of the Nutrient Reduction Strategy to decrease the state's impact on the hypoxic zone. The study determined that to minimize impact to the Gulf of Mexico hypoxic zone, Minnesota will need a 45% reduction in nitrogen and phosphorus to the Mississippi River, compared to amounts prior to 2000. Other goals set by the state include a 20% nitrate load reduction by 2025, a 45% nitrate load reduction by 2040, a 45% phosphorus reduction in nearly 500 impaired lakes, approximately a 40% reduction in phosphorus for Minnesota rivers, and reducing nitrates to meet drinking water standards (MPCA, 2014).

Improved and updated research of the Le Sueur River watershed's response to climate change will be especially impactful for both local and downstream water quality and is needed to see how nutrient discharges change due to climate change conditions. Understanding the potential response of this highly agricultural watershed will be helpful to the state in its measurements to meet the goals of the Nutrient Reduction Strategy.

The aim of this study is to use the latest climate predictions and emissions scenarios from the Coupled Model Intercomparison Project 5 (CMIP5) (IPCC, 2014a) to model projected climate scenarios in the Le Sueur River watershed and analyze how the watershed responds, both with hydrology and water quality. It is anticipated that the watershed will experience changes in hydrological patterns and pollutant discharges, making the modeling a tool to prepare land managers for potential changes due to climate change in this agricultural area.

Methods

The Le Sueur River watershed is the study area for investigating watershed responses to climate change. Downscaled weather data from the CMIP5 experiments associated with the most recent IPCC report was used as inputs to Weather Input for Nonpoint Data Simulations (WINDS), a weather generation model, to create a 1000-year time series for SWAT modeling of multiple climate change scenarios. Output from SWAT is analyzed for hydrology and pollutant response.

Project Area

The Minnesota River Basin is divided into twelve major watersheds (HUC 08): Blue Earth River, Chippewa River, Cottonwood River, Lac Qui Parle River, Le Sueur River, Lower Minnesota River, Minnesota River (Mankato), Pomme de Terre River, Redwood River, Minnesota River (Headwaters), Watonwan River, and Minnesota River (Yellow Medicine River) watersheds, shown in Figure 11. The Minnesota River Basin drains approximately 20% of Minnesota, as well as areas in North and South Dakota and Iowa (Musser et al., 2009). Pre-settlement, the area was mostly described as containing prairie land, wetlands, and forested areas (Musser et al., 2009). Today, agriculture is the major land use in the basin. Early settlers drained the wetlands upon arrival to farm the nutrient rich land (Musser et al., 2009). The area is characterized with steep slopes and incised valleys along the Minnesota River by the melting of glacial Lake Agassiz. The large volume of melt water cut through the glacial sediment and bedrock, making the valley larger than what would have been created by only the Minnesota River, with steeper and larger bluffs. Those steep bluffs and incision points are a source of sediment to the Minnesota River (Wilcock, 2009).

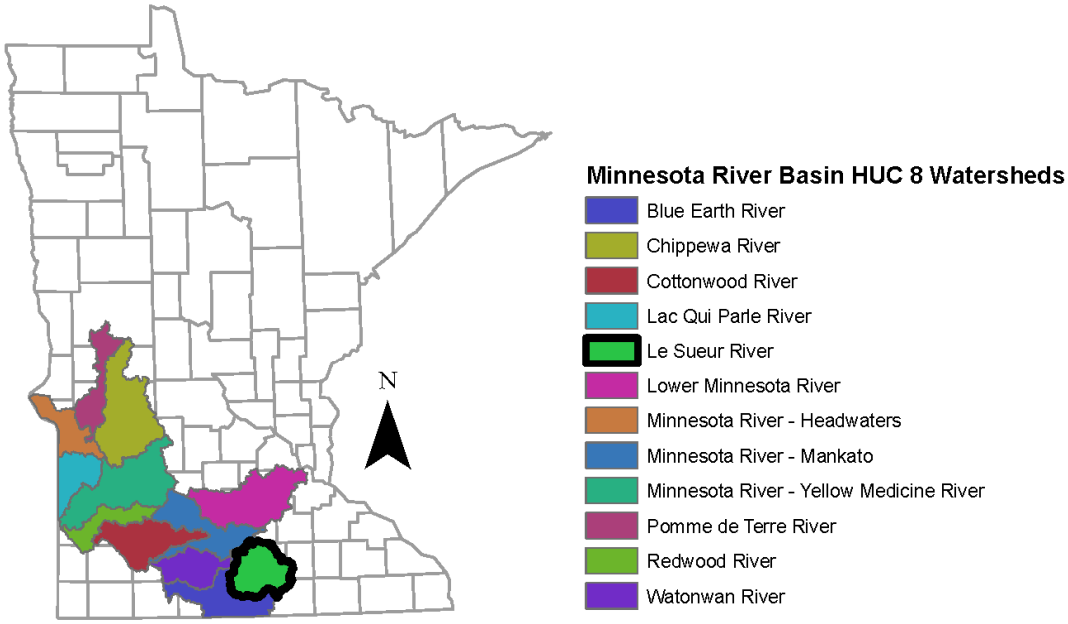

Service Layer Credits: DNR Watersheds - DNR Level 04 - HUC08 - Majors, Originator: Minnesota DNR - Division of Waters - Watershed Delineation Project, Publication Date: 4/7/2009

Figure 11: Minnesota River Basin HUC 8 Watersheds

The Le Sueur River watershed (Figure 12) is approximately 710,832 acres, 7.4% of the total Minnesota River Basin area. Agriculture is the primary land use, at 87% of the watershed. Other land covers are forest (1.5%), wetland (3.5%), open water (2.0%), and urban (6.4%) (Spindler et al., 2012). Estimated population in the Le Sueur River watershed from the 2010 Census was approximately 37,000 (Campbell et al., 2015).

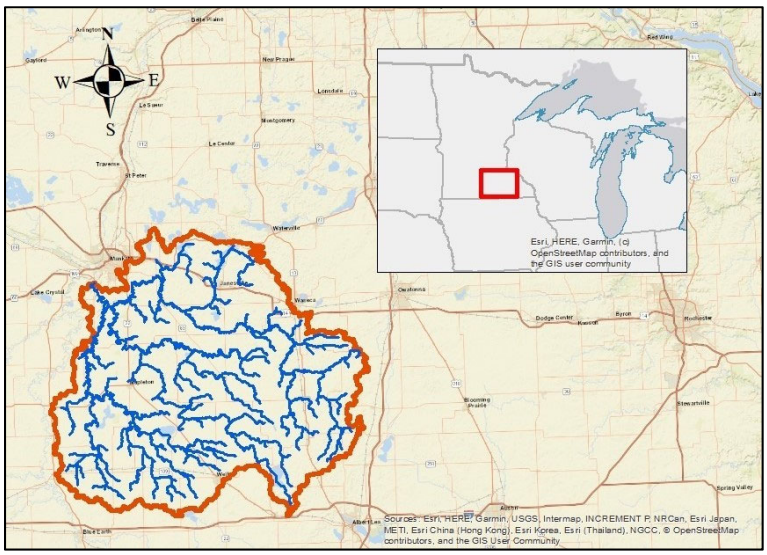

Figure 12: Le Sueur River Watershed, located in southern Minnesota

SWAT Hydrologic Model

The Soil & Water Assessment Tool (SWAT) is a river-basin scale hydrologic model. SWAT integrates soil, land use, topographic, and climate data in watershed modeling and is a popular tool for modeling water resources, nonpoint source pollution, and responses to climate change (P. W. Gassman et al., 2007; Philip W. Gassman, Sadeghi, & Srinivasan, 2014; Ouyang et al., 2015; Sunde et al., 2017; Zeiger & Hubbart, 2016). The model is often used by water resource managers to analyze water supplies and nonpoint source pollution under different management scenarios (Arnold, Srinivasan, Muttiah, & Williams, 1998).

In this study, a calibrated SWAT model of the Le Sueur River watershed is used to model climate change scenarios and examine watershed response. Response to climate change is evaluated by predicted changes in hydrology and pollutant loading from the watershed.

Modeling the Le Sueur River Watershed

The model used in this work is a calibrated SWAT model of the Le Sueur River watershed was built with support of the Minnesota Department of Agriculture (Finlay, Dalzell, Dolph, Baker, & Rorer, 2019). The model was created with historical weather data from years 2002-2013. Precipitation data was created based on the NEXRAD synthetic network of gauges. Temperature, wind speed, relative humidity, and solar radiation values were obtained from the Global Weather Generator Data for SWAT (https://globalweather.tamu.edu/), based on the Climate Forecast System Reanalysis (CFSR) (Fuka et al., 2013) dataset. The model was calibrated and validated with data from 2004 to 2013. Calibration parameters included streamflow, sediment, total phosphorus, and total nitrogen.

Climate Inputs

For modeling the Le Sueur watershed, the only changes made to the calibrated model were the weather inputs (maximum and minimum temperature, precipitation, solar radiation, wind speed and relative humidity).

Climate change parameters from GCMs were obtained and downscaled using the Multivariate Adaptive Constructed Analogs (MACA) datasets and methods. Table 8 displays a list of GCMs chosen in this analysis ("WCRP Coupled Model Intercomparison Project - Phase 5 - CMIP 5," 2011).

Table 8: Global climate model names, organization, and resolution of climate models chosen for analysis.

Model Name	Organization	Country of Origin	Atmosphere Resolution (long x lat)
bcc-csm1-1	Beijing Climate Center, China Meteorological Administration	China	2.8° x 2.8°
CSIRO-Mk3-6-0	Commonwealth Scientific and Industrial Research Organization in collaboration with Queensland Climate Change Centre of Excellence	Australia	1.8° x 1.8°
GFDL-ESM2M	NOAA Geophysical Fluid Dynamics Laboratory	United States	2.5° x 2.0°
HadGEM2-ES	Met Office Hadley Centre (additional HadGEM2-ES realizations contributed by Instituto Nacional de Pesquisas Espaciais)	United Kingdom	1.88° x 1.25°
IPSL-CM5A-MR	Institut Pierre-Simon Laplace	France	2.5° x 1.25°
MIROC5	Atmosphere and Ocean Research Institute (The University of Tokyo), National Institute for Environmental Studies, and Japan Agency for Marine-Earth Science and Technology	Japan	1.4° x 1.4°

The GCMs in Table 8 were chosen to reflect the wide array of organizations doing climate modeling work to create a multi-model ensemble. It has become standard practice to use a multi-model ensemble to reduce the amount of uncertainty that can be found in only one model (Lambert & Boer, 2001; Mote et al., 2011; Palmer, Doblas-Reyes, Hagedorn, & Weisheimer, 2005).

The latest report from the IPCC produced four new Representative Concentration Pathways (RCP) for use by climate modeling groups to aid in model comparisons, reduce duplication of work, and better understand uncertainties in climate projections (Wayne, 2013). The four scenarios are RCP 8.5, RCP 6, RCP 4.5, and RCP 2.6. RCPs represent the potential radiative forcing, or energy in the atmosphere causing warming, based on distinct scenarios to look at the impacts of human-caused climate change. Levels of radiative forcing are based on multiple factors, including population growth and size, economic factors, energy sources, land

use changes, and individual lifestyle choices and updated in parallel with climate projections, as opposed to a sequential development process (Wayne, 2013).

RCP 8.5 results in the highest level of radiative forcing by year 2100 and RCP 2.6 represents the lowest level of radiative forcing by year 2100. Two RCPs were chosen for this analysis: RCP 4.5 and RCP 8.5. RCP 4.5 is described as a stabilization or low emission scenario, with radiative forcing reaching 4.5 watts per square meter (W/m^2) by year 2100. RCP 8.5 is an uncontrolled, or high emission scenario, with radiative forcing reaching 8.5 W/m^2 by 2100 and continues to increase (IPCC, 2014b; Taylor et al., 2007; Wayne, 2013). These RCPs indicate positive warming in the atmosphere (4.5 and 8.5 W/m^2) by 2100.

The direct output from each GCM RCP is at a large resolution and is commonly downscaled to the area of interest. The MACA method was chosen as the downscaling method, as statistically downscaling data is a more computationally efficient method that dynamic downscaling (Fowler et al., 2007), as well as this method's ease in creating SWAT inputs. In statistical downscaling, an observational dataset, referred to as a "training dataset", is used to identify statistical patterns of the historical weather. The weather predictions from the GCMs are then fit to those identified historical statistical patterns and relationships, created a predicted weather dataset that has similar weather patterns to the area of interest. Two training datasets were used for downscaled output: METDATA (Abatzoglou, 2013) and Livneh (Livneh et al., 2013). Choice of training dataset is very impactful on outputs, meaning two different training datasets can result in significantly different outputs (Byun & Hamlet, 2018; Jiang et al., 2018; Kouwen et al., 2005).

The changes between the historical and predicted weather from the downscaled MACA data for each RCP scenario were used for input to WINDS, a weather generation model. WINDS is a stochastic weather generator that uses statistics of daily weather patterns and variability to simulate weather with the same characteristics as observed weather (Wilson et al., 2006). The magnitude of changes from the MACA weather output (from historical to predicted) were applied as input into the WINDS algorithm to predict weather. The potential weather outcomes from WINDS can be described as predicted weather with the same statistical characteristics as the local weather. WINDS was used to produce a time-series of 1000-years of potential climate scenarios that are statistically representative of the historical weather patterns of the watershed.

WINDS output was averaged into three time-range scenarios, 2006 – 2029, 2030 – 2059, and 2060 – 2099, for RCPs 4.5 and 8.5. Those averages (represented as summary years 2015, 2045, and 2080) were input into the calibrated SWAT model. Final analysis is between the back-

predicted historical data (Baseline) and the predicted year scenarios (2015, 2045, 2080), to determine magnitude of watershed response and changes. The historical data are from years 1950 – 2006. Although this analysis does not use observed or predicted weather data from the GCMs, it is assumed that the applied magnitudes of change applied to the WINDS model accurately represents the local conditions, and the calibrated SWAT model is representative of the watershed response.

A detailed description of climate change parameters and outcomes can be found in Chapter 1: Downscaling Global Climate Models for Use in SWAT.

SWAT Sensitivity Analysis

Weather Gauge Site Sensitivity

To understand the spatial resolution of the GCMs and spatial capacity of SWAT, a sensitivity analysis of model output with varying numbers of weather gauges was performed. The purpose was to compare the output of SWAT with multiple gauge locations and the output with one and determine if the number of gauges in the area of interest had a significant impact on model results. The calibrated model that is used for climate change modeling has eight-gauge locations for temperature, wind speed, relative humidity, and solar radiation, and fifty-one precipitation gauge locations.

Using the historical weather data in the calibrated model, weather averages over all gauge locations for each day were calculated, resulting in average weather for the watershed. Those averages were input at each of the existing latitude and longitude stations in the calibrated model, meaning each sub-area in the model used the watershed average for each weather variable.

To compare the impact of each weather variable on watershed output, five separate scenarios were run, with each weather variable average applied in the center of the watershed and modeled with the remaining calibrated weather inputs with the original number of unique weather gauges. For example, in one run, the relative humidity file was replaced with the averaged relative humidity file, while wind speed, temperature, precipitation and solar radiation all remained the same weather inputs as what is in the calibrated model. A sixth scenario was run with all five weather files replaced with the watershed average file, one record for the entire watershed.

Outlet flow, total nitrogen, total phosphorus, and nitrate concentrations were compared between all sensitivity analysis runs and summarized in Table 9.

Table 9: Results of sensitivity analysis to determine number of gauges needed in simulation.

Results are percent differences from the calibrated model (with 51 precipitation gauges and 8 gauges for temperature, solar radiation, wind speed, and relative humidity) to replacing one weather input at a time with one gauge.

Weather Input Replaced	Outflow	Total Nitrogen	Total Phosphorus	Nitrate Concentration
Existing				
Humidity	0%	0%	0%	0%
Wind Speed	0%	0%	0%	0%
Temperature	2%	13%	4%	15%
Precipitation	-3%	-3%	-11%	-2%
Solar Radiation	0%	0%	0%	0%
All replaced	-2%	0%	-5%	3%

Temperature and precipitation changes resulted in the largest percent difference in outputs from calibrated model results, which makes sense given the importance of those two weather variables in this modeling study. When looking at changes in runoff conditions and water quality, and other hydrological outputs, temperature and precipitation play a major role in exports (Bronstert, Kolokotronis, Schwandt, & Straub, 2007; Maraun et al., 2010).

Due to the small percent differences between replacement of the equivalent of one weather gauge with either 8 or 51, depending on the variable, compared to the size of the Le Sueur River watershed, it was determined that one gauge location will be used when collecting climate projections from the global climate models. The weather information from one gauge location will be applied to the entire watershed for the climate change analysis.

A second sensitivity analysis was done to look at the importance of number of years of simulation in SWAT. This would answer the question of how many runs does one need to come to a stable average of SWAT output. In this analysis, ten, 100-year simulations were run, with the 1000 years of weather data generated as described in Chapter 1. Outputs of all 10 model runs of evapotranspiration, surface flow, tile flow, groundwater, and water yield were compared to find the variable with the most variability. In the Baseline condition analysis, surface flow was seen to have the largest variability between 100-year model runs (labeled Yr 1 through Yr 10), displayed in Figure 13.

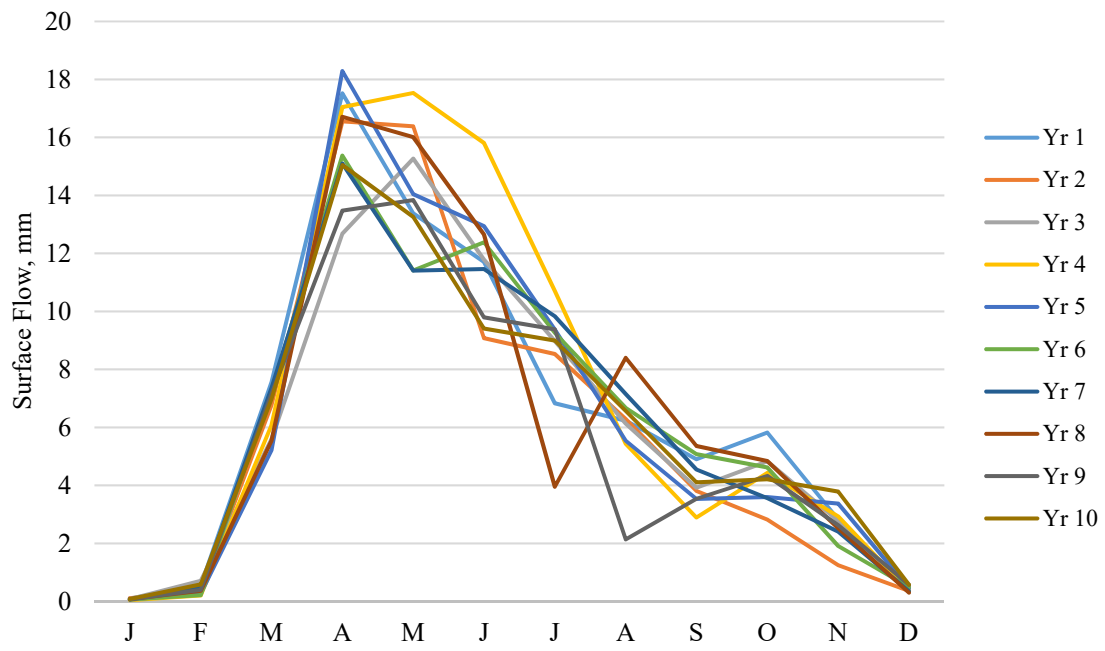

Figure 13: Average of surface flow for Baseline conditions. Each year in the legend represents monthly average of a 100-year SWAT model

Confidence intervals were calculated on the monthly output to determine if one, 100-year run would suffice to represent the range of potential SWAT outcomes, or if two, 100-year runs would suffice, or three, or all ten, 100-year scenarios should be run to represent the variability of SWAT modeling.

Two confidence intervals, 95% and 99% were calculated for each month, to see how increasing the number of years would change the confidence intervals in number of runs. Intervals for May-October are summarized in Table 10. Graphical presentation is provided in Appendix as A2.1.

Table 10: Confidence interval testing of number of years of simulated data required in SWAT to get stable output. Two confidence intervals calculated, 95% and 99%. Values show are limits of surface flow in mm.

Month	No. of 100-Yr runs	95%			99%		
		Upper	Lower	Range	Upper	Lower	Range
May	1	17.08	9.67	7.41	18.25	8.51	9.74
	2	18.17	11.59	6.58	19.20	10.56	8.65
	3	17.60	12.42	5.17	18.41	11.61	6.80
	4	17.88	13.40	4.48	18.58	12.70	5.89
	5	17.27	13.37	3.91	17.89	12.75	5.13
	10	15.53	12.98	2.55	15.93	12.58	3.35
June	1	15.40	8.01	7.39	16.56	6.85	9.71
	2	13.02	7.76	5.26	13.85	6.94	6.91
	3	12.87	8.84	4.03	13.51	8.21	5.30
	4	14.02	10.17	3.85	14.63	9.56	5.06
	5	14.03	10.50	3.52	14.58	9.95	4.63
	10	12.90	10.50	2.40	13.28	10.12	3.15
July	1	9.83	3.83	5.99	10.77	2.89	7.88
	2	9.89	5.47	4.42	10.58	4.77	5.81
	3	10.01	6.22	3.79	10.60	5.62	4.98
	4	10.44	7.08	3.35	10.96	6.56	4.40
	5	10.39	7.37	3.02	10.87	6.90	3.97
	10	9.57	7.59	1.98	9.88	7.28	2.60
August	1	8.94	3.52	5.42	9.79	2.67	7.13
	2	8.12	4.39	3.74	8.71	3.80	4.91
	3	7.65	4.78	2.87	8.10	4.33	3.78
	4	7.20	4.84	2.36	7.57	4.47	3.10
	5	6.99	4.86	2.13	7.32	4.53	2.80
	10	6.82	5.29	1.53	7.06	5.05	2.02
September	1	6.78	3.03	3.75	7.37	2.44	4.93
	2	5.60	3.10	2.50	5.99	2.71	3.28
	3	5.19	3.23	1.96	5.50	2.92	2.58
	4	4.65	3.10	1.55	4.90	2.86	2.04
	5	4.51	3.10	1.41	4.74	2.88	1.85
	10	4.74	3.60	1.14	4.92	3.42	1.50
October	1	8.21	3.44	4.78	8.96	2.69	6.28
	2	5.67	2.97	2.70	6.10	2.55	3.55
	3	5.59	3.39	2.20	5.94	3.04	2.89
	4	5.42	3.53	1.89	5.72	3.24	2.48
	5	5.11	3.49	1.63	5.37	3.23	2.14
	10	4.89	3.72	1.16	5.07	3.54	1.53

For the months shown, the confidence intervals show that running ten, 100-year model runs results in the best, or smallest, confidence interval for the variability of the data. Because of the variance of input data, and the variability of observed watershed outputs, it is to be expected that there will be variability in 1000-years of model simulations. To have more confidence in the watershed outputs for each modeled scenario, all 1000-years of weather data generated in Chapter 1 were run.

As mentioned, this variability is to be expected, when comparing SWAT outputs to the calibrated model outputs. Table 11 displays the mean, standard deviation, and percent difference between means between the output from the calibrated model and the Baseline SWAT output, for precipitation, surface flow, ET, and water yield. The data are presented as Calibrated Model / Baseline Model. There is a large difference in the number of years of calibrated data and simulated data, but this supports the large range and variance of the model output seen in the simulated output.

Table 11: Comparison of calibrated model output and Baseline simulated model output for water outputs. Differences in mean and standard deviation indicate a range of outputs is to be expected from SWAT. Table is presented as Calibrated Model / Baseline Model.

Parameter	Precipitation (mm)	Surface Flow (mm)	ET (mm)	Water Yield (mm)
Mean	827.34 / 748.73	134.43 / 74.17	541.51 / 522.71	250.9 / 202.1
% Diff. of Mean	-10%	-45%	-3%	-19%
St. Dev.	155.97 / 27.74	59.66 / 5.1	42.34 / 21.06	87.2 / 10.27
Count	12 / 980			

Discussed in Chapter 1, 1000-years of simulated weather, generated by WINDS, provides the inputs to SWAT. With confidence in the weather inputs, the variability of the simulated SWAT scenarios can be compared to the variability of the calibrated model. Although a large difference in the number of scenarios available for comparison between the calibrated / simulated model runs, the comparisons show an interesting perspective of SWAT output. As more simulations are done, the standard deviation of the yearly output decreases, indicating a higher level of confidence in locational representative results.

Statistical Analyses

A statistical analysis for significance of monthly and yearly averages for water yield, ET and outflow was performed at the 95% confidence level, based on the large sample sizes of the

analyzed outputs (Neideen & Brasel, 2007; Wilson, n.d.). The standard calculation protocol for a two tailed T-test analysis of paired means was used in Microsoft Excel. Analyses were performed for summary years compared to Baseline conditions: Baseline to 2015, Baseline to 2045, and Baseline to 2080, for both RCP 4.5 and RCP 8.5. The large sample size supports the assumption that the sample means of the data are normally distributed, due to the central limit theorem. But since the variances of the data are unknown, a T-test for significance is used. This t-test tests the null hypothesis that the two-sample means are equal. A larger t-value indicates a larger difference between the two sample means.

A unique feature of this modeling exercise is the large sample size that was modeled in SWAT. With so many sample years, all with weather inputs of the same statistical parameters as historical weather, the range, or variance, of potential outcomes is worth investigating. Microsoft Excel procedures for an F-test were performed to determine if the variance of the outputs, is statistically different in each summary year, compared to Baseline conditions.

Results and Discussion

Two forms of model output and results are presented in the following section: watershed scale results and field scale results. Watershed scale refers to output at the outlet of the watershed. Field scale in this analysis is model output at the hydrologic response unit (HRU) level, representing a smaller, uniform part of the watershed. HRUs are sections of the watershed with similar slopes, land uses, and soil types (Neitsch, Arnold, Kiniry, & Williams, 2011). The watershed scale analysis includes hydrologic analysis including precipitation, water yield, evapotranspiration (ET), outflow, and a nitrate loss assessment. Water yield is the contribution to stream flow that is conveyed out of the HRU, calculated in SWAT as a sum of surface flow, lateral flow, groundwater flow, tile flow, less transmission losses from tributary channels (Neitsch et al., 2011). Nitrogen, phosphorus, and sediment are analyzed at the field scale. Phosphorus and sediment are only analyzed at the field scale due to complexities in modeling these constituents in the Minnesota River Basin. This area experiences frequent bank sloughing along the riverbanks, adding sediment and phosphorus to the main channels. Additional calculations and modeling outside the SWAT interface are needed to accurately represent phosphorus and sediment at the watershed outlet, but SWAT can predict phosphorus and sediment processes at the field scale without having to account for bank and near-bank processes.

Watershed Scale Hydrologic Analysis

A review of precipitation, water yield, evapotranspiration (ET), and outflow at the watershed outlet is described in the following sections. Precipitation and temperature are major drivers in watershed modeling. Figure 14 and Table 12 summarize the predicted (and modeled) annual changes in precipitation and temperature that are input into SWAT, for both RCP scenarios.

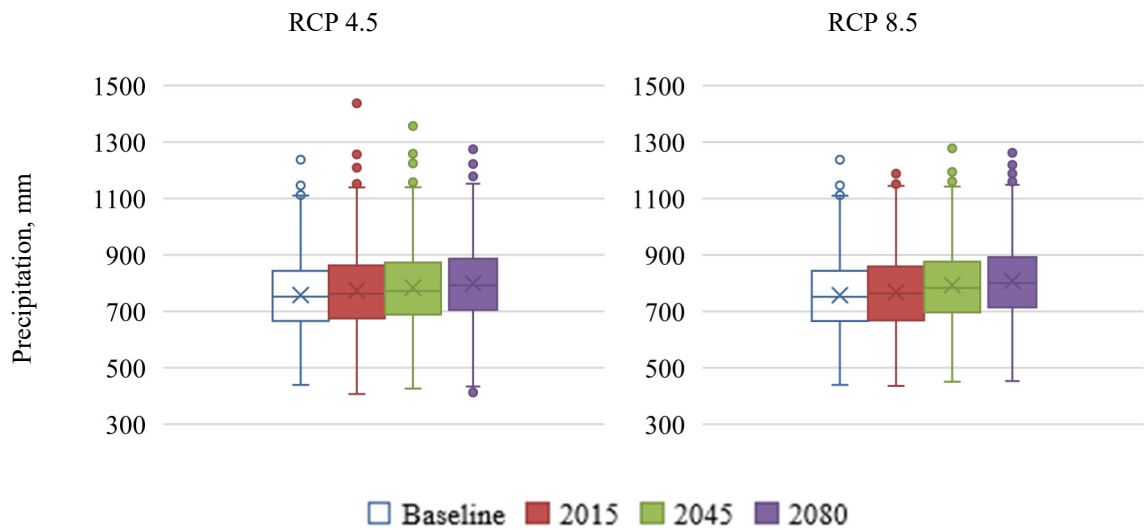

Figure 14: Box plots of average annual precipitation, mm, for METDATA downscaling method and RCP 4.5 and RCP 8.5.

Table 12: Changes in average annual maximum temperature (°C) from Baseline conditions for RCP 4.5 and RCP 8.5.

Summary	RCP 4.5	RCP 8.5
Year	Δ°C	Δ°C
2015	1.4	1.4
2045	2.6	2.9
2080	3.5	5.8

Timing of precipitation can impact crop growth and flooding conditions. With the predicted increases in temperature, it would be expected to see more precipitation as rain in the winter months, potentially causing more flood events, specifically if the soil is frozen but air temperature warm enough for precipitation as rain. Average annual precipitation amounts for Baseline, 2015, 2045, and 2080 for RCP 4.5 and RCP 8.5 are 758, 774, 784, and 798 mm and 758, 768, 793, and 807 mm, respectively. Temperature also increases over time, seen in Table 12,

for both RCP scenarios. Temperature can impact the crop growth season and even the frequency and use of pesticides and fertilizers.

A more detailed analysis of predicted changes in weather inputs is presented in Chapter 1. Table 13 provides the average maximum monthly temperature over time in the METDATA downscaling method for RCP 4.5 and RCP 8.5 from that research. These values are the downscaled values, predicted by the GCMs.

Table 13: Monthly average temperatures (°C) for Baseline conditions and years 2015, 2045, and 2080 for RCPs 4.5 and 8.5.

Month	Baseline	RCP 4.5			RCP 8.5		
		2015	2045	2080	2015	2045	2080
January	-10.6	-9.2	-7.5	-6.6	-9.0	-7.0	-3.8
February	-8.0	-6.5	-5.1	-3.9	-6.3	-4.7	-1.3
March	-1.3	0.8	1.6	2.6	0.3	1.6	4.5
April	6.7	8.6	9.2	9.9	7.9	9.2	11.7
May	14.0	15.0	15.8	16.6	15.1	16.1	18.6
June	19.2	20.2	21.3	22.1	20.7	21.8	24.3
July	21.7	23.0	24.3	25.0	23.2	24.8	27.6
August	20.4	21.9	23.4	24.0	21.8	23.8	26.8
September	15.7	17.1	18.4	19.1	17.3	18.9	21.8
October	8.6	9.8	11.1	12.1	10.2	11.2	14.2
November	0.4	1.8	2.9	3.8	1.7	3.3	5.9
December	-7.0	-6.0	-4.3	-3.4	-6.1	-4.0	-1.1
Ave. Annual Temperature	6.7	8.0	9.3	10.1	8.1	9.6	12.4

Figure 15 shows SWAT output of monthly averages for precipitation, water yield, ET, and outflow for the METDATA downscaling method, for both RCP scenarios.

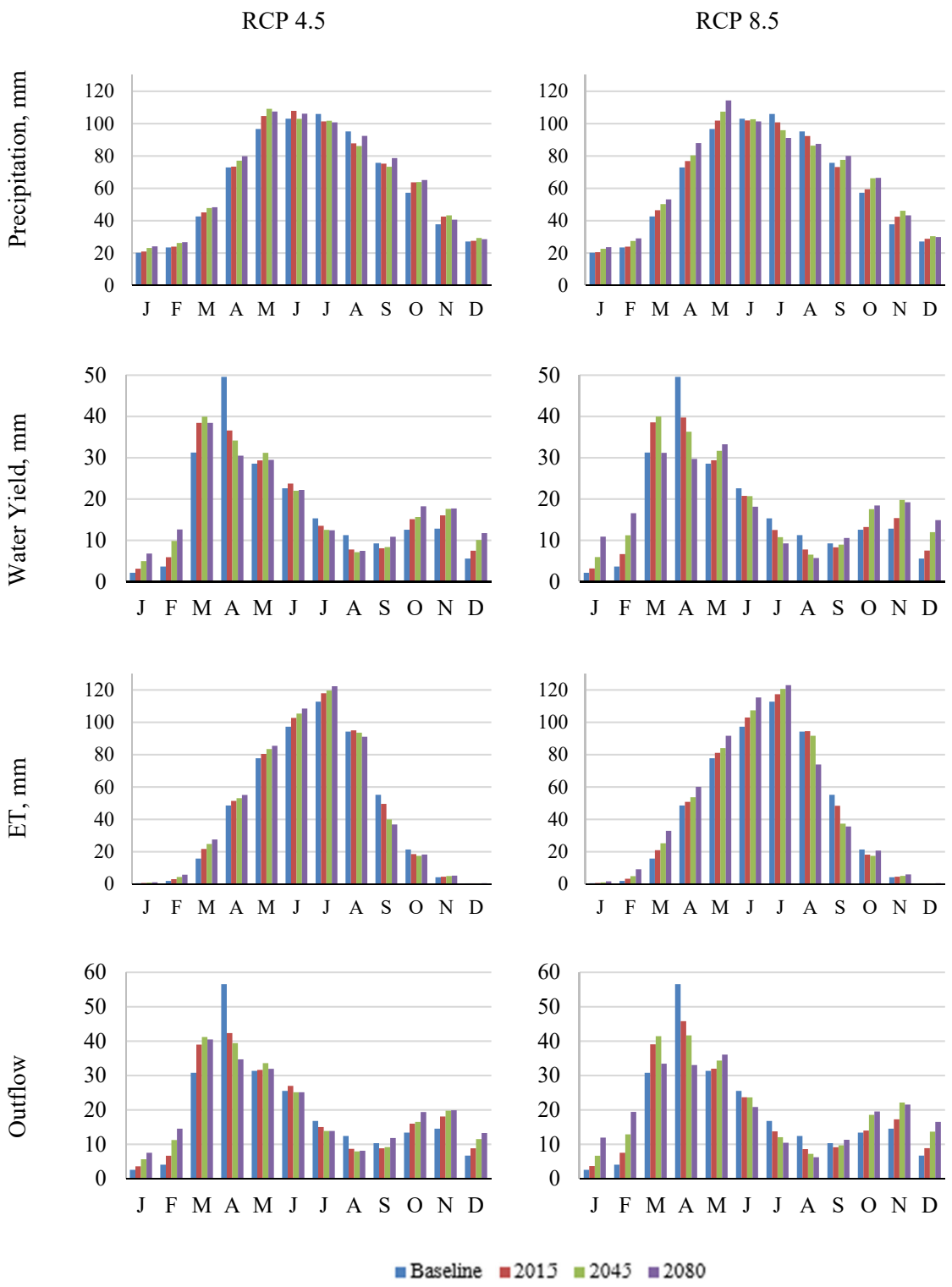

Figure 15: SWAT monthly output for precipitation, water yield, ET, and outflow for METDATA downscaling method for RCP 4.5 and RCP 8.5.

Both RCP 4.5 and RCP 8.5 show the largest increase in precipitation depth from Baseline conditions in May, for summary year 2080. Increases in depth were 11 and 18 mm, respectively. December through May show increasing precipitation for both RCP scenarios over time. RCP 4.5 precipitation depth increases in year 2080 for December, January, February, March, April, May are 4, 3, 6, 7, and 11 mm, respectively. RCP 8.5 precipitation depth increases in year 2080 for December, January, February, March, April, May are 4, 6, 11, 15, and 18 mm, respectively. The results reveal the largest decrease in monthly precipitation in July, and August, when compared to Baseline conditions. The decreasing precipitation depths for RCP 4.5 and RCP 8.5, from Baseline to year 2080 for July and August are 5 and 3 mm, and 15 and 8 mm, respectively.

In RCP 4.5, ET has the highest percent increase from Baseline conditions in January, February, and March, of 53%, 66%, and 43%, respectively, for year 2080. RCP 8.5 has the largest percent increases in the same months of year 2080, of 71%, 79%, and 52%, respectively. RCP 8.5 has an apparent trend of decreases in ET from Baseline conditions in August and September, with decreases from Baseline to year 2080 of 28% and 55%, respectively.

Both trends of decreasing and increasing ET with increasing precipitation have been documented in research. It has been noted that water availability impacts ET; increases in ET occur in areas with high water availability and decreases in ET occur in areas with low water availability (Yang, Zhang, & Hao, 2016). Research in the Mississippi River Basin have supported the hypothesis of increases in ET with increases in precipitation, indicating that climate variables and location are major factors in ET (Milly & Dunne, 2001; Walter, Wilks, Parlange, & Schneider, 2004).

Water yield generally follows similar trends between model scenarios, except for the month of April, where Baseline water yield is higher than the RCP scenario outputs. Increases in water yield follow increases in precipitation in the winter months and decreases in the summer months. RCP 4.5 has the largest increase in percent change of water yield from Baseline conditions to year 2080 of 53%, 69%, and 71% for December, January, and February, respectively. RCP 8.5 also has the highest percent increase from Baseline to year 2080 for the same months, with increases of 63%, 80%, and 78%, respectively. June, July and August report consistently decreasing water yield for both RCP 4.5 and RCP 8.5. Percent decreases for those months for RCP 4.5 are 2%, 24%, and 51%, respectively, and decreases for RCP 8.5 are 25%, 66%, and 97%, respectively. Increased water yield in the late fall and winter months has potential to convey sediments, nitrogen and phosphorus downstream during non-growing seasons, impacting effectiveness of management practices and downstream water quality.

April results in the highest outflow, of 57 m^3/s in the Baseline condition. April also has the largest decrease in outflow, for both RCP 4.5 and RCP 8.5, of 22% and 24%, respectively. Like water yield, outflow decreases in the spring and early summer months and increases in winter months. Percent increase in outflow from Baseline conditions are largest in December and January, with increases of 50% and 66% for RCP 4.5 and 59% and 78% for RCP 8.5. Increased outflow during non-growing seasons can result in higher export of sediment and nutrients, if BMPs are not in place to prevent the loss.

The hydrologic trends seen fit with what has been predicted for climate change in this part of the Midwest. Large changes are seen in water flows in spring and fall/winter, both having different impacts on agriculture. Wetter winters and springs can impact planting and management practices, and drier summers, even pushing towards drought conditions, make agriculture production challenging, even with irrigation. Most of the largest differences from Baseline conditions are seen in year 2080 for both RCP 4.5 and RCP 8.5, fitting with that year being the longest amount of time with climate change, where more significant changes would be expected to be seen.

See Table 14 and Table 15 for numerical values from Figure 15 for changes from Baseline conditions for precipitation, water yield, ET, and outflow, and percent increases and decreases from Baseline conditions.

4.5 Results

Table 14: Changes from Baseline conditions for RCP 4.5 for precipitation, water yield, ET, and outflow.

Darker blue indicates a larger negative change, light blue/white cells indicate a larger positive change from Baseline. Right column: percent change of difference from Baseline conditions. Red cells indicate a larger negative change, green cells indicate a larger positive change from Baseline conditions.

Precipitation Change in Depth from Baseline, mm				Precipitation Percent Change from Baseline			
	2015	2045	2080		2015	2045	2080
J	0.8	2.9	3.9	J	3.9%	12.7%	16.3%
F	0.5	2.7	3.2	F	2.0%	10.5%	12.2%
M	2.4	5.2	5.6	M	5.4%	10.8%	11.7%
A	0.4	4.2	6.9	A	0.6%	5.4%	8.6%
M	8.0	12.4	10.8	M	7.7%	11.4%	10.0%
J	4.8	-0.1	3.1	J	4.5%	-0.1%	2.9%
J	-4.6	-4.2	-5.2	J	-4.5%	-4.1%	-5.1%
A	-7.4	-9.1	-2.8	A	-8.4%	-10.5%	-3.0%
S	-0.5	-2.5	2.9	S	-0.7%	-3.4%	3.7%
O	6.5	6.6	7.9	O	10.2%	10.4%	12.1%
N	4.8	5.6	2.9	N	11.3%	12.8%	7.1%
D	0.4	2.2	1.4	D	1.6%	7.5%	5.0%
Total, mm	773.84	783.63	798.25				

Water Yield Change in Depth from Baseline, mm				Water Yield Percent Change from Baseline			
	2015	2045	2080		2015	2045	2080
J	1.0*	2.8*	4.7*	J	31.7%	57.0%	68.6%
F	2.2*	6.2*	9.0*	F	38.0%	62.9%	71.1%
M	7.2*	8.7*	7.2*	M	18.7%	21.7%	18.7%
A	-13.0*	-15.4*	-19.1*	A	-35.6%	-45.2%	-62.6%
M	0.8	2.6*	0.9	M	2.7%	8.4%	3.1%
J	1.2	-0.6	-0.4	J	4.9%	-2.6%	-1.8%
J	-1.8*	-2.8*	-2.9*	J	-13.4%	-22.3%	-23.5%
A	-3.5*	-4.1*	-3.8*	A	-44.6%	-58.1%	-50.9%
S	-1.2*	-0.9	1.6*	S	-14.7%	-10.4%	14.8%
O	2.6*	3.1*	5.7*	O	16.9%	19.6%	31.1%
N	3.2*	4.8*	4.9*	N	20.0%	27.2%	27.7%
D	1.9*	4.5*	6.2*	D	25.4%	44.7%	52.5%

ET Change in Depth from Baseline, mm

	2015	2045	2080
J	0.2*	0.4*	0.5*
F	1.0*	2.4*	3.8*
M	6.0*	9.1*	11.8*
A	2.8*	4.5*	6.5*
M	2.7*	5.6*	7.6*
J	5.5*	8.2*	11.3*
J	5.2*	6.9*	9.6*
A	0.7	-0.7	-3.1*
S	-5.7*	-15.3*	-18.4*
O	-2.8*	-3.9*	-3.0*
N	0.3*	0.7*	1.0*
D	0.0*	0.1*	0.1*

ET Percent Change from Baseline

	2015	2045	2080
J	25.0%	44.1%	53.2%
F	34.5%	55.5%	66.2%
M	27.5%	36.6%	43.0%
A	5.5%	8.4%	11.9%
M	3.3%	6.8%	8.9%
J	5.3%	7.8%	10.4%
J	4.4%	5.8%	7.8%
A	0.8%	-0.7%	-3.5%
S	-11.4%	-38.3%	-50.0%
O	-15.0%	-22.6%	-16.6%
N	7.7%	15.2%	19.2%
D	7.3%	13.4%	17.4%

Outflow Change from Baseline, m^3/s

	2015	2045	2080
J	1.0*	3.1*	5.0*
F	2.6*	7.2*	10.5*
M	8.2*	10.4*	9.7*
A	-14.2*	-17.1*	-21.9*
M	0.3	2.2	0.6
J	1.4	-0.4	-0.4
J	-1.8*	-2.9*	-2.9*
A	-3.7*	-4.5*	-4.3*
S	-1.5*	-1.1	1.5
O	2.6*	3.1*	6.0*
N	3.6*	5.2*	5.4*
D	2.1*	4.8*	6.6*
Total (m^3/s)	225.6	235.0	240.8

Outflow Percent Change from Baseline

	2015	2045	2080
J	28.9%	54.5%	65.8%
F	38.9%	63.6%	71.9%
M	21.0%	25.3%	23.9%
A	-33.6%	-43.5%	-63.1%
M	0.9%	6.6%	1.8%
J	5.3%	-1.6%	-1.6%
J	-11.9%	-20.9%	-20.8%
A	-43.0%	-56.8%	-52.4%
S	-17.3%	-12.4%	12.5%
O	16.3%	18.9%	30.9%
N	19.6%	26.5%	26.9%
D	24.0%	41.8%	49.6%

* Statistically significant from Baseline values using t-test at 5% level

8.5 Results

Table 15: Changes from Baseline conditions for RCP 8.5 for precipitation, water yield, ET, and outflow.

Darker blue indicates a larger negative change, light blue/white cells indicate a larger positive change from Baseline. Right column: percent change of difference from Baseline conditions. Red cells indicate a larger negative change, green cells indicate a larger positive change from Baseline conditions.

Precipitation Change in Depth from Baseline, mm

	2015	2045	2080
J	0.3	2.4	3.5
F	0.5	4.0	5.6
M	3.8	7.6	10.5
A	3.9	7.4	15.0
M	5.2	10.7	17.6
J	-1.1	-0.4	-1.7
J	-5.2	-10.0	-14.8
A	-2.9	-8.8	-7.7
S	-2.6	1.8	4.2
O	2.1	9.0	9.2
N	4.7	8.4	5.5
D	1.7	3.3	2.8
Total, mm	768.16	792.98	807.39

Precipitation Percent Change from Baseline

	2015	2045	2080
J	1.6%	10.8%	14.7%
F	1.9%	14.5%	19.3%
M	8.3%	15.1%	19.8%
A	5.1%	9.2%	17.1%
M	5.1%	10.0%	15.4%
J	-1.0%	-0.4%	-1.6%
J	-5.1%	-10.5%	-16.2%
A	-3.1%	-10.2%	-8.8%
S	-3.5%	2.3%	5.3%
O	3.6%	13.5%	13.8%
N	11.1%	18.2%	12.7%
D	5.8%	10.9%	9.3%

Water Yield Change in Depth from Baseline, mm

	2015	2045	2080
J	1.0*	3.8*	8.7*
F	3.0*	7.6*	12.9*
M	7.3*	8.7*	-0.1
A	-9.8*	-13.3*	-19.9*
M	0.8	3.1*	4.7*
J	-1.8*	-1.9*	-4.5*
J	-2.8*	-4.6*	-6.1*
A	-3.5*	-4.7*	-5.5*
S	-1.0*	-0.3	1.3*
O	0.7	5.0*	5.9*
N	2.6*	7.0*	6.4*
D	1.9*	6.4*	9.3*

Water Yield Percent Change from Baseline

	2015	2045	2080
J	32.7%	64.1%	80.4%
F	45.2%	67.5%	78.0%
M	18.9%	21.8%	-0.2%
A	-24.8%	-36.6%	-66.9%
M	2.8%	9.8%	14.1%
J	-8.9%	-9.1%	-24.7%
J	-22.7%	-42.3%	-66.0%
A	-44.9%	-72.7%	-97.2%
S	-11.5%	-3.0%	12.6%
O	5.0%	28.3%	31.8%
N	16.7%	35.3%	33.3%
D	25.8%	53.4%	62.6%

ET Change in Depth from Baseline, mm	2015	2045	2080
J	0.2*	0.5*	1.1*
F	1.3*	2.9*	7.2*
M	5.2*	9.4*	17.2*
A	2.2*	5.0*	11.5*
M	3.3*	6.2*	13.9*
J	5.7*	10.2*	18.1*
J	4.6*	7.9*	10.2*
A	0.2	-2.6*	-20.4*
S	-6.8*	-17.8*	-19.6*
O	-3.2*	-3.9*	-0.6*
N	0.3*	0.8*	1.7*
D	0.0*	0.1*	0.1*

ET Percent Change from Baseline	2015	2045	2080
J	29.1%	49.8%	70.6%
F	40.0%	59.9%	78.7%
M	24.8%	37.5%	52.3%
A	4.4%	9.4%	19.2%
M	4.1%	7.4%	15.1%
J	5.6%	9.5%	15.7%
J	3.9%	6.5%	8.3%
A	0.2%	-2.8%	-27.6%
S	-14.2%	-47.8%	-55.2%
O	-17.4%	-22.3%	-3.1%
N	7.5%	16.1%	28.9%
D	7.7%	14.3%	26.9%

Outflow Change from Baseline, m3/s	2015	2045	2080
J	1.1*	4.1*	9.4*
F	3.4*	8.8*	15.3*
M	8.3*	10.6*	2.7*
A	-10.7*	-14.9*	-23.5*
M	0.6	3.0*	4.7*
J	-1.9	-1.9	-4.7*
J	-3.0*	-4.7*	-6.3*
A	-3.8*	-5.2*	-6.2*
S	-1.2	-0.7	1.0
O	0.6	5.2*	6.2*
N	2.7*	7.6*	7.0*
D	2.2*	7.0*	9.8*
Total, m3/s	223.3	244.0	240.4

Outflow Percent Change from Baseline	2015	2045	2080
J	29.9%	61.4%	78.4%
F	45.7%	68.3%	78.9%
M	21.2%	25.7%	8.0%
A	-23.5%	-35.7%	-71.2%
M	1.9%	8.7%	13.1%
J	-7.9%	-8.0%	-22.3%
J	-21.9%	-39.3%	-60.7%
A	-44.7%	-72.1%	-99.2%
S	-12.9%	-6.8%	8.7%
O	4.2%	27.8%	31.5%
N	15.9%	34.4%	32.6%
D	24.4%	51.0%	59.4%

* Statistically significant from Baseline values using t-test at 5% level

A summary of the monthly results, Table 16 displays yearly averages for all hydrologic parameters for all scenarios.

Table 16: Simulated SWAT output for METDATA downscaling method, RCP 4.5 and RCP 8.5, for Baseline, 2015, 2045, and 2080. Mean yearly values of precipitation, water yield, ET, and outflow.

Output	Baseline	RCP 4.5			RCP 8.5		
		2015	2045	2080	2015	2045	2080
Precipitation, mm	757.6	773.8	783.6	798.3	768.2	793.0	807.4
Water Yield, mm	204.5	205.1	213.3	218.3*	202.8	221.3*	217.7*
ET, mm	529.5	545.5*	547.5*	557.2*	542.7*	548.2*	569.9*
Outflow, m3/s	18.8	18.8	19.6*	20.0*	18.6	20.3*	20.0*

* Statistically significant from Baseline values using t-test at 5% level

Statistical analysis of difference of monthly mean values from Baseline conditions to each summary year was performed. T-values for water yield, ET, and outflow, when compared to Baseline conditions, are provided in Table 17 through

Table 19. Across the analysis, RCP 8.5 scenario has more statistically significant results, indicated by the bolded values in the tables. RCP 8.5 has larger changes in weather inputs, so larger changes from Baseline conditions are to be expected.

Water Yield

Table 17: T-test significance for water yield at watershed outlet, for RCP 4.5 and RCP 8.5.

Month	RCP 4.5			RCP 8.5		
	2015	2015	2045	2015	2045	2080
January	***t < 0.05***	***t < 0.05***	***t < 0.05***	***t < 0.05***	***t < 0.05***	***t < 0.05***
February	***t < 0.05***	***t < 0.05***	***t < 0.05***	***t < 0.05***	***t < 0.05***	***t < 0.05***
March	***t < 0.05***	***t < 0.05***	***t < 0.05***	***t < 0.05***	***t < 0.05***	9.48E-01
April	***t < 0.05***	***t < 0.05***	***t < 0.05***	***t < 0.05***	***t < 0.05***	***t < 0.05***
May	3.12E-01	***t < 0.05***	2.15E-01	2.92E-01	***t < 0.05***	***t < 0.05***
June	1.28E-01	4.10E-01	5.85E-01	***t < 0.05***	***t < 0.05***	***t < 0.05***
July	***t < 0.05***	***t < 0.05***	***t < 0.05***	***t < 0.05***	***t < 0.05***	***t < 0.05***
August	***t < 0.05***	***t < 0.05***	***t < 0.05***	***t < 0.05***	***t < 0.05***	***t < 0.05***
September	***t < 0.05***	6.39E-02	***t < 0.05***	***t < 0.05***	5.51E-01	***t < 0.05***
October	***t < 0.05***	***t < 0.05***	***t < 0.05***	2.24E-01	***t < 0.05***	***t < 0.05***
November	***t < 0.05***	***t < 0.05***	***t < 0.05***	***t < 0.05***	***t < 0.05***	***t < 0.05***
December	***t < 0.05***	***t < 0.05***	***t < 0.05***	***t < 0.05***	***t < 0.05***	***t < 0.05***

Bold and italicized values are statistically significant.

ET

Table 18: T-test significance average watershed ET, for RCP 4.5 and RCP 8.5.

Month	RCP 4.5			RCP 8.5		
	2015	**2045**	**2080**	**2015**	**2045**	**2080**
January	***t < 0.05***	***t < 0.05***	***t < 0.05***	***t < 0.05***	***t < 0.05***	***t < 0.05***
February	***t < 0.05***	***t < 0.05***	***t < 0.05***	***t < 0.05***	***t < 0.05***	***t < 0.05***
March	***t < 0.05***	***t < 0.05***	***t < 0.05***	***t < 0.05***	***t < 0.05***	***t < 0.05***
April	***t < 0.05***	***t < 0.05***	***t < 0.05***	***t < 0.05***	***t < 0.05***	***t < 0.05***
May	***t < 0.05***	***t < 0.05***	***t < 0.05***	***t < 0.05***	***t < 0.05***	***t < 0.05***
June	***t < 0.05***	***t < 0.05***	***t < 0.05***	***t < 0.05***	***t < 0.05***	***t < 0.05***
July	***t < 0.05***	***t < 0.05***	***t < 0.05***	***t < 0.05***	***t < 0.05***	***t < 0.05***
August	8.49E-02	1.41E-01	***t < 0.05***	6.04E-01	***t < 0.05***	***t < 0.05***
September	***t < 0.05***	***t < 0.05***	***t < 0.05***	***t < 0.05***	***t < 0.05***	***t < 0.05***
October	***t < 0.05***	***t < 0.05***	***t < 0.05***	***t < 0.05***	***t < 0.05***	***t < 0.05***
November	***t < 0.05***	***t < 0.05***	***t < 0.05***	***t < 0.05***	***t < 0.05***	***t < 0.05***
December	***t < 0.05***	***t < 0.05***	***t < 0.05***	***t < 0.05***	***t < 0.05***	***t < 0.05***

Bold and italicized values are statistically significant.

Outflow

Table 19: T-test significance for outflow at watershed outlet, for RCP 4.5 and RCP 8.

Month	RCP 4.5			RCP 8.5		
	2015	**2045**	**2080**	**2015**	**2045**	**2080**
January	***t < 0.05***	***t < 0.05***	***t < 0.05***	***t < 0.05***	***t < 0.05***	***t < 0.05***
February	***t < 0.05***	***t < 0.05***	***t < 0.05***	***t < 0.05***	***t < 0.05***	***t < 0.05***
March	***t < 0.05***	***t < 0.05***	***t < 0.05***	***t < 0.05***	***t < 0.05***	***t < 0.05***
April	***t < 0.05***	***t < 0.05***	***t < 0.05***	***t < 0.05***	***t < 0.05***	***t < 0.05***
May	8.35E-01	9.58E-02	6.71E-01	6.47E-01	***t < 0.05***	***t < 0.05***
June	2.77E-01	7.56E-01	7.74E-01	1.30E-01	1.32E-01	***t < 0.05***
July	***t < 0.05***	***t < 0.05***	***t < 0.05***	***t < 0.05***	***t < 0.05***	***t < 0.05***
August	***t < 0.05***	***t < 0.05***	***t < 0.05***	***t < 0.05***	***t < 0.05***	***t < 0.05***
September	***t < 0.05***	9.96E-02	5.03E-02	9.20E-02	3.57E-01	1.84E-01
October	***t < 0.05***	***t < 0.05***	***t < 0.05***	4.70E-01	***t < 0.05***	***t < 0.05***
November	***t < 0.05***	***t < 0.05***	***t < 0.05***	***t < 0.05***	***t < 0.05***	***t < 0.05***
December	***t < 0.05***	***t < 0.05***	***t < 0.05***	***t < 0.05***	***t < 0.05***	***t < 0.05***

Bold and italicized values are statistically significant.

Watershed Scale Nitrate Analysis

Nitrate can negatively impact water quality downstream and contributes to the hypoxic zone in the Gulf of Mexico (MPCA, 2014). According to Minnesota's Nutrient Reduction

Strategy (MPCA, 2014), Minnesota has a goal to reduce nitrogen and phosphorus losses 45% by year 2040. Knowing how nutrient loading is affected by climate change will affect this goal and the timeline to reach the goal. Nitrate was analyzed at the watershed scale, as it is well represented in the SWAT model.

Table 20 displays monthly averages of nitrate export in kg/ha/mo.

Table 20: Monthly averages (and year total) of nitrate export at watershed outlet, for RCP 4.5 and RCP 8.5, METDATA downscaling method.

Month	**Baseline**	**RCP 4.5**			**RCP 8.5**		
		2015	**2045**	**2080**	**2015**	**2045**	**2080**
January	0.2	0.3	0.7	1.0	0.3	0.8	1.9
February	0.6	1.1	1.8	2.5	1.2	2.2	3.6
March	8.2	8.6	8.8	8.6	8.4	9.0	7.2
April	11.9	7.0	6.0	5.3	7.4	6.4	5.1
May	5.7	5.5	6.0	5.9	5.5	5.9	6.9
June	4.8	4.7	4.2	4.2	4.1	3.8	3.3
July	1.7	1.1	0.8	0.8	1.0	0.6	0.4
August	0.4	0.2	0.2	0.1	0.2	0.1	0.1
September	0.3	0.2	0.1	0.2	0.2	0.2	0.4
October	0.6	0.5	0.5	0.7	0.5	0.7	1.1
November	1.2	1.2	1.3	1.4	1.1	1.6	2.0
December	0.7	0.8	1.1	1.3	0.8	1.4	2.1
Total	**36.2**	**31.2**	**31.6**	**32.1**	**30.7**	**32.7**	**34.1**

Graphs of monthly nitrate export and outflow, for comparison, are in the Appendix, A2.2. The largest decreases from Baseline conditions for RCP 4.5 were seen in April, June, and July, with export decreases in year 2080 of 6.6, 0.6, and 0.9 kg/ha. The largest decrease in export from Baseline conditions for RCP 8.5 were seen in April, June, and July, with decreases of 6.8, 1.5, and 1.3 kg/ha from Baseline conditions.

Generally, results reveal increasing nitrate export from October to February from the watershed in predicted years, compared to Baseline conditions for both RCP scenarios. Increases for RCP 4.5 for October through February are 0.2, 0.2, 0.6, 0.7, and 1.9 kg/ha, respectively. Increases for RCP 8.5 for October through February are 0.6, 0.8, 1.4, 1.7, and 2.9, respectively. Both RCP scenarios resulted in the largest increase in February. As can be expected based on described trends of increasing precipitation and outflow in the non-growing season months, it is fitting to see increased nutrient flows in those months.

There is an initial decrease in nitrate export from Baseline to 2015, 2045, and 2080 in both RCP 4.5 and RCP 8.5. This could be a result of the shifts in water yield (which includes surface flow) and tile flow (Table 21), both sources of nitrate export. Seen in Table 14 and Table 15, water yield decreases in most summer months for all summary years.

Table 21: Changes in average monthly tile flow (mm) from Baseline conditions, for years 2015, 2045, and 2080 for RCP 4.5 and RCP 8.5.

Month	**RCP 4.5**			**RCP 8.5**		
	2015	**2045**	**2080**	**2015**	**2045**	**2080**
January	0.73	2.25	3.80	0.83	3.02	7.50
February	1.89	5.23	7.76	2.59	6.42	11.05
March	5.71	6.83	5.24	5.66	6.24	-2.18
April	-11.74	-14.59	-17.35	-9.59	-13.59	-19.08
May	0.04	0.94	0.78	0.17	0.85	1.95
June	0.26	-0.63	-0.32	-0.81	-1.16	-2.30
July	-1.23	-1.55	-1.67	-1.51	-2.38	-2.95
August	-1.75	-1.95	-1.95	-1.55	-2.22	-2.39
September	-0.54	-0.28	1.21	-0.41	0.01	1.62
October	1.77	2.26	4.29	0.91	3.83	4.99
November	2.11	3.66	3.78	1.91	5.21	5.25
December	1.36	3.60	5.04	1.46	4.86	7.81
Total Yearly Tile Flow	**118.4**	**125.5**	**130.4**	**119.4**	**130.8**	**131.0**

The trend indicates yearly tile flow increasing, but the timing is changing from Baseline conditions. Tiles flow decreases in summer months, a possible explanation in the initial decrease in nitrate export. Decreases seen in RCP 4.5 are seen in April, with a decrease of 17 mm from Baseline in year 2080. June, July and August see smaller decreases, of 0.3, 1.7, and 2.0 mm for year 2080, RCP 4.5. RCP 8.5 sees the largest decrease in April as well, of 19 mm, and the months of June, July, and August have decreases of 2.3, 3.0, and 2.4 mm, respectively. More interesting are the larger increases in tile flow from Baseline conditions in November, December, and January. RCP 4.5 sees increases in year 2080 of 3.8, 5.0, and 7.8 mm and RCP 8.5 sees increases in year 2080 of 5.3, 7.8, and 11.0 mm, for November, December, and January. Warming temperatures and increasing tile flow and water yield in the winter months may then contribute to increasing nitrate export from years 2015, 2045, and 2080.

The change in precipitation patterns has potential to impact nitrate export as well. Local observations have noted increased heavy precipitation events in Minnesota ("Historic Mega-Rain Events in Minnesota," n.d.), and that in combination with the climate models predicting more

precipitation in the winter and less in the summer, plays a role in changing nitrate export patterns related to precipitation. As this is model output with predicted weather, there is uncertainty in the values, but trends can be enlightening. Multiple factors must be considered with nitrate export, a few as described above are temperature, precipitation, surface flow, and tile flow.

Since the model produced an initial decrease in nitrate export from Baseline to 2015 before an increase, the change in export from years 2015-2045 and 2045-2080 is compared to see how nitrate export changes over time. Yearly averages of nitrate export reveal increasing nitrate export from 2015 to 2080. In RCP 4.5, from year 2015 to 2045, model results show nitrate export increase 1.1%, and increasing 1.8% from year 2045 to 2080. For RCP 8.5, nitrate increases 6.5% from year 2015 to 2045 and 4.3 % from year 2045 to 2080 (Table 22). Under the same land management practices, nitrate export is not decreasing under climate change scenarios.

Table 22: Changes in nitrate export between summary years 2015 to 2045 and years 2045 to 2080 for RCP 4.5 and RCP 8.5.

Scenario	2015-2045	2045-2080
RCP 4.5	1.1%	1.8%
RCP 8.5	6.5%	4.3%

As nitrate exports follow an increasing trend over time in both RCP 4.5 and RCP 8.5, it may be beneficial for producers to evaluate and install BMPs in the non-growing season, to prevent nitrate export when precipitation, tile flow, and surface flow follow increasing trends. Examples may include cover crops, no-till practices, smart application of fertilizers, and winter drainage controls.

Statistical Analysis

A standard t-test was performed on the nitrate amounts outflowing from the watershed per month. Values for both RCP 4.5 and RCP 8.5 are summarized in Table 23.

Table 23: T-test significance for nitrate at watershed outlet, for RCP 4.5 and RCP 8.5.

Month	RCP 4.5			RCP 8.5		
	2015	**2045**	**2080**	**2015**	**2045**	**2080**
January	***t < 0.05***	***t < 0.05***	***t < 0.05***	***t < 0.05***	***t < 0.05***	***t < 0.05***
February	***t < 0.05***	***t < 0.05***	***t < 0.05***	***t < 0.05***	***t < 0.05***	***t < 0.05***
March	1.56E-01	***t < 0.05***	1.49E-01	4.52E-01	***t < 0.05***	***t < 0.05***
April	***t < 0.05***	***t < 0.05***	***t < 0.05***	***t < 0.05***	***t < 0.05***	***t < 0.05***
May	6.24E-01	1.98E-01	3.93E-01	5.71E-01	3.35E-01	***t < 0.05***
June	8.17E-01	***t < 0.05***	***t < 0.05***	***t < 0.05***	***t < 0.05***	***t < 0.05***
July	***t < 0.05***	***t < 0.05***	***t < 0.05***	***t < 0.05***	***t < 0.05***	***t < 0.05***
August	***t < 0.05***	***t < 0.05***	***t < 0.05***	***t < 0.05***	***t < 0.05***	***t < 0.05***
September	***t < 0.05***	***t < 0.05***	***t < 0.05***	***t < 0.05***	***t < 0.05***	***t < 0.05***
October	7.43E-02	4.00E-01	***t < 0.05***	***t < 0.05***	***t < 0.05***	***t < 0.05***
November	8.09E-01	1.13E-01	***t < 0.05***	2.56E-01	***t < 0.05***	***t < 0.05***
December	1.96E-01	***t < 0.05***	***t < 0.05***	6.87E-02	***t < 0.05***	***t < 0.05***

Bold and italicized values are statistically significant.

Most of the nitrate export statistical analysis show significance when compared to Baseline conditions. This is not surprising, based on the interested initial decrease in nitrate from Baseline conditions and following increase in years 2015, 2045, and 2080.

Field Scale Nutrient and Sediment Analysis

The following HRUs (referred to as Fields) were chosen for a field scale analysis. All Fields are agricultural land cover. These fields are in the center of the watershed and consist of two different soil types. Both soil types are poorly drained and commonly associated with lacustrine areas.

Table 24: HRU (Fields) used in analysis of nitrogen, phosphorus, and sediment export.

Field ID	Area (acres)	Soil Type	Slope
1108	2164.89	Marna (HSG - type C)	Flat
1109	350.47	Marna (HSG - type C)	Steep
1111	2814.60	Guckeen (HSG - type C)	Flat
1112	448.37	Guckeen (HSG - type C)	Steep

These soil types were chosen for the analysis as there are both flat (0-3%) and sloped (3-5%) soils for each soil type, for comparison purposes. The Marna and Guckeen soils also represent a combined total of 7.9% of the watershed (Marna – 5.2.%, Guckeen – 2.7% of watershed. The Minnesota River Basin is predominately fine glacial till and lake bed deposits,

which are commonly made up of clayey soils that are poorly drained (Moncrief, Evans, & Randall, 1997). Both Marna and Guckeen are characterized as poorly drained soils with clay particles, found in lacustrine environments, making these soils and fields good representations of the characteristics of the Le Sueur River watershed.

Nitrogen

Nitrogen export at the field scale is reported as a sum of surface flow nitrogen, lateral flow nitrogen, groundwater nitrate, and tile nitrate, reported in kg/ha. Monthly plots are in the Appendix, A2.3. Box and whisker plots showing mean, quartiles, and spread for yearly results are in the Appendix, A2.4.

Monthly Analysis

Similar broad trends as seen in the yearly analysis of nitrate at the watershed scale are seen in nitrogen at the field scale. Larger differences in nitrogen export from Baseline conditions are seen in RCP 8.5. The non-growing season months (September through February) show increases in nitrogen export, when comparing years 2015 to 2080. The flat fields (1108 and 1111) showed the largest decrease in nitrogen export from Baseline conditions in March and April in RCP 8.5, with average reductions at 3.5 and 4.9 kg/ha and 4.2 and 4.6 kg/ha for March and April for Fields 1108 and 1111. The largest increases in nitrogen export for those fields were also seen in RCP 8.5, with increases in December and January. Field 1108 saw increases for December and January of 1.2 and 1.5 kg/ha and Field 1111 saw increases for December and January of 1.6 and 1.9 kg/ha for RCP 8.5.

Steep fields (1109 and 1112) show similar results. The greatest decreases, seen in RCP 8.5, are in months June and July. For Field 1109, those decreases from Baseline conditions are 0.6 and 0.5 kg/ha for June and July; Field 1112 has decreases of 0.7 and 0.6 kg/ha for June and July. The greatest increases in nitrogen export, again seen in RCP 8.5, are in January and February. Field 1109 indicates increases of 0.3 and 0.3 kg/ha and Field 1112 indicates increases of 0.4 and 0.4 kg/ha for those months. Tables and charts with nitrogen export for all fields analyzed and both RCP scenarios are in the Appendix, A2.3. In the comparison of flat versus steep slopes, under same management practices, it would be expected that steeper slope fields have more nutrient and sediment loss in surface water flow, as water would flow at a higher velocity and dislodge particles from the surface, which is seen in the results.

Nitrogen and Tile Flow

Like what was seen on the watershed scale, tile flow increases in the field scale analysis for both RCP scenarios, as precipitation increases. The field scale tile flow and tile nitrate analyses were only performed for Fields 1108 and 1111, as they are flat fields and have tile drainage. Continual increases of tile flow over time are seen in the colder months (October through February) for both fields in both RCP 4.5 and RCP 8.5. For Field 1108, the largest percent increase in tile flow is seen in January, with increases by year 2080 of 400% and 745% for RCP 4.5 and RCP 8.5, respectively. Field 1111 also has the largest percent increase in tile flow in January, at 340% and 620% increases for RCP 4.5 and RCP 8.5, respectively. With increases in tile flow come increase in tile nitrate. Results for Field 1108 show increases in January nitrate export of 0.8 and 1.5 kg/ha for RCP 4.5 and RCP 8.5. Field 1111 indicates increases in January nitrate export of 1.0 and 1.9 kg/ha for RCP 4.5 and RCP 8.5. Graphs for nitrate export and tile flow for all months for Fields 1108 and 1111 are in the Appendix, A2.5.

Yearly Analysis

Table 25 provides yearly average nitrogen export for Fields 1108, 1109, 1111, and 1112 from the 1000-year model runs.

Table 25: Average yearly nitrogen export (kg/ha) for Fields 1108, 1109, 1111, and 1112.

Soil	Field	Baseline	RCP 4.5			RCP 8.5		
			2015	2045	2080	2015	2045	2080
Marna	1108	40.70	34.06*	34.66*	34.96*	33.5*7	35.46*	36.89*
	1109	7.36	6.52*	6.66*	6.51*	6.50*	6.77*	6.57*
Guckeen	1111	46.40	39.83*	40.82*	41.44*	39.27*	41.82*	44.56
	1112	8.53	7.72*	7.94*	7.77*	7.67*	8.03*	7.90*

* Statistically significant from Baseline values using t-test at 5% level

Results shows higher nitrogen export on the flat fields, for both soil types. The main reason for those differences is the nitrogen that gets transported through tile flow, and the flat fields have tile drainage.

A t-test of significance was performed to compare mean yearly export for each field. For individual field analysis, all fields and scenarios, except Field 1111 for year 2080 in RCP 8.5 showed statistically different average nitrogen export from Baseline conditions. All other comparisons to Baseline conditions resulted in means that are considered equal. T-values are

reported in Table 26. This indicates that predicted conditions will see a large change from Baseline conditions in the amount of yearly nitrogen exported at the field scale.

Table 26: T-test significance for each field within respective RCP (comparison of Field 1108 for Baseline to 2015, Baseline to 2045, and Baseline to 2080, etcetera).

Field	**RCP 4.5**			**RCP 8.5**		
	2015	**2045**	**2080**	**2015**	**2045**	**2080**
1108	***t < 0.05***	***t < 0.05***	***t < 0.05***	***t < 0.05***	***t < 0.05***	***t < 0.05***
1109	***t < 0.05***	***t < 0.05***	***t < 0.05***	***t < 0.05***	***t < 0.05***	***t < 0.05***
1111	***t < 0.05***	***t < 0.05***	***t < 0.05***	***t < 0.05***	***t < 0.05***	0.069
1112	***t < 0.05***	***t < 0.05***	***t < 0.05***	***t < 0.05***	***t < 0.05***	***t < 0.05***

Bold and italicized values are statistically significant.

Again, all scenarios showed statistically different mean exports when comparing field types (flat versus sloped). This would be expected, as the flat fields have tile drainage, increasing nitrogen export. T-values for this analysis are in Table 27.

Table 27: T-values for comparison of nitrogen export between fields of the same soil type but different slopes, within RCPs 4.5 and 8.5.

Field	**Baseline**	**RCP 4.5**			**RCP 8.5**		
		2015	**2045**	**2080**	**2015**	**2045**	**2080**
1108-1109	***t < 0.05***	***t < 0.05***	***t < 0.05***	***t < 0.05***	***t < 0.05***	***t < 0.05***	***t < 0.05***
1111-1112	***t < 0.05***	***t < 0.05***	***t < 0.05***	***t < 0.05***	***t < 0.05***	***t < 0.05***	***t < 0.05***

Bold and italicized values are statistically significant.

Analysis of Variance

Table 28 provides output for an F-test, to determine if the variance of the models runs, or range in outputs, is statistically different in each summary year, compared to Baseline conditions. The analysis showed that all yearly average nitrogen export had a statistically different variance of data. A ratio of 1 indicates the variances of the two datasets are equal, and if the ratio is greater than the F-value of 1.1109, the variances are statistically significantly different.

Table 28: F-test values for analysis of variance of nitrogen export. Comparison is within each field, comparing each summary year to Baseline conditions.

Field	RCP 4.5			RCP 8.5		
	2015	**2045**	**2080**	**2015**	**2045**	**2080**
1108	***1.193***	***1.136***	***1.198***	***1.163***	***1.250***	***1.567***
1109	***1.148***	***1.117***	***1.371***	***1.169***	***1.190***	***1.500***
1111	***1.194***	***1.135***	***1.204***	***1.176***	***1.245***	***1.537***
1112	***1.153***	***1.122***	***1.334***	***1.170***	***1.225***	***1.545***

Bold and italicized values are statistically significant.

The box and whisker plots in the Appendix, A2.4, show the wide range of nitrogen outputs that come with the large sample size used in the study. For nitrogen export, all summary years (2015, 2045, and 2080) had smaller ranges of output, increasing confidence in output predictions.

Phosphorus

Phosphorus export at the field scale is reported as a sum of organic phosphorus, sediment phosphorus, and soil phosphorus, reported in kg/ha. Monthly plots are in the Appendix, A2.6. Box and whisker plots showing mean, quartiles, and spread of yearly results are in the Appendix, A2.7.

Monthly Analysis

April, May, and June see the highest phosphorus export at the field scale. The largest increases in export are in May, in RCP 8.5, for all fields analyzed. For Fields 1108, 1109, 1111, and 1112, the increase in phosphorus export in May is 0.02, 0.20, 0.01, and 0.19 kg/ha, respectively. That corresponds to percent increases in May export of 70%, 53%, 64%, and 50%, for Fields 1108, 1109, 1111, and 1112. RCP 4.5 does not show the same increasing trend in April, May, and June. Phosphorus export is predicted to decrease over time in RCP 8.5. Continual decreases are seen in June, July, and August.

Higher export totals are seen on the sloped fields. Phosphorus travels with water and sediment, which also are more mobile on steep landscapes. Tables and charts with phosphorus export for all fields analyzed and both RCP scenarios are in the Appendix, A2.6.

Yearly Analysis

Table 29 displays phosphorus export for Fields 1108, 1109, 1111, and 1112. Export values are averages of the 1000-year model runs.

Table 29: Average yearly phosphorus export (kg/ha) for Fields 1108, 1109, 1111, and 1112

Soil	Field	Baseline	RCP 4.5			RCP 8.5		
			2015	2045	2080	2015	2045	2080
Marna	1108	0.09	0.09	0.09	0.09	0.09	0.10	0.10*
	1109	1.44	1.42	1.48	1.48	1.36	1.58*	1.63*
Guckeen	1111	0.09	0.09	0.09	0.08	0.08	0.09	0.09
	1112	1.53	1.49	1.54	1.52	1.42	1.64	1.66

* Statistically significant from Baseline values using t-test at 5% level

For individual field analysis, only Fields 1108 and 1109 showed any significance at the 5% level. In Field 1108, the comparison of means from Baseline to year 2080 for RCP 8.5 showed significance that the mean phosphorus export total is not equal to the Baseline export. Field 1109 showed that mean exports are not equal for comparisons of Baseline to year 2045 and year 2080, for RCP 8.5. All other comparisons to Baseline conditions resulted in means that are considered equal. T-values are reported in Table 30.

Table 30: T-test significance for each field within respective RCP (comparison of Field 1108 for Baseline to 2015, Baseline to 2045, and Baseline to 2080, etcetera).

Field	RCP 4.5			RCP 8.5		
	2015	2045	2080	2015	2045	2080
1108	0.344	0.468	0.703	0.550	0.141	***t < 0.05***
1109	0.764	0.493	0.590	0.169	***t < 0.05***	***t < 0.05***
1111	0.492	0.834	0.895	0.343	0.289	0.315
1112	0.541	0.886	0.930	0.094	0.109	0.055

Bold and italicized values are statistically significant.

Lastly, a t-test of significance of phosphorus export comparing flat to steep slopes within a soil type was performed. Comparisons included Fields 1108 to 1109 and Fields 1111 to 1112, within each RCP scenario. The t-testing showed significant differences in mean export between flat and sloped fields, within the same soil types. Statistical values are in Table 31. The significance is not surprising, as sloped fields are more likely to have faster surface runoff, which can dislodge sediment and therefore phosphorus, when compared to flat slopes.

Table 31: T values for comparison of phosphorus export between fields of the same soil type but different slopes, within RCPs 4.5 and 8.5

Field	Baseline	RCP 4.5			RCP 8.5		
		2015	2045	2080	2015	2045	2080
1108-1109	***t < 0.05***	***t < 0.05***	***t < 0.05***	***t < 0.05***	***t < 0.05***	***t < 0.05***	***t < 0.05***
1111-1112	***t < 0.05***	***t < 0.05***	***t < 0.05***	***t < 0.05***	***t < 0.05***	***t < 0.05***	***t < 0.05***

Bold and italicized values are statistically significant.

Analysis of Variance

The low number of significant comparisons is not surprising, given the small area of analysis. An F-test of differences of variances was performed to see if other patterns are within the datasets. A ratio of 1 indicates the variances of the two datasets are equal, and if the ratio is greater than the F-value of 1.1109, the variances are statistically significantly different.

Table 32: F-test values for analysis of variance of phosphorus export. Comparison is by field, comparing each summary year to Baseline conditions.

Field	RCP 4.5			RCP 8.5		
	2015	2045	2080	2015	2045	2080
1108	***1.604***	1.065	***1.176***	***1.230***	***1.334***	***1.521***
1109	1.087	1.019	***1.207***	***1.173***	***1.176***	***1.356***
1111	***1.601***	1.000	***1.111***	***1.332***	***1.315***	***1.411***
1112	1.091	1.018	***1.174***	***1.171***	***1.165***	***1.550***

Bold and italicized values are statistically significant.

All variances in RCP 8.5 and summary year 2080 in RCP 4.5 are statistically significant from Baseline conditions. In those scenarios, the range of phosphorus export, also seen in the box and whiskers plots in the Appendix, A2.7, are larger than the range seen in Baseline conditions. More variability in the modeling and uncertainty in the output is seen for those climate scenarios. Most of the mean values of phosphorus export did not show significance in difference from Baseline conditions. The analysis of variance shows another side to the export, that in the predicted outputs, there may be a wider range of export values year to year.

Sediment

Sediment export at the field scale is reported as a total of sediment yield, reported in metric tons/ha. Monthly plots of sediment export are in the Appendix, A2.8. Box and whisker plots showing mean, quartiles, and spread of yearly results are in the Appendix, A2.9.

Monthly Analysis

Sediment loss at the field scale follows the same trends as changing precipitation: precipitation is predicted to decrease in June, July and August and sediment loss also is shown to decrease in June, July, and August. Precipitation increases in September, October, and November, and sediment export also increases in September, October, and November. This shows a relationship between sediment export and precipitation. Again, larger losses are seen in RCP 8.5, which is fitting as RCP 8.5 has more precipitation than RCP 4.5. Export ranges from 30-50% less than Baseline conditions for all fields analyzed in RCP 8.5. In September, October, and November, increases in sediment export for RCP 8.5 range from 30-70% more than Baseline conditions for flat fields and 30-100% more than Baseline conditions for steep fields.

Yearly Analysis

Table 33 provides average yearly sediment export for Fields 1108, 1109, 1111, and 1112. Export values are averages of the 1000-year model runs.

Table 33: Average yearly sediment export (metric tons/ha) for Fields 1108, 1109, 1111, and 1112.

Soil	Field	Baseline	RCP 4.5			RCP 8.5		
			2015	2045	2080	2015	2045	2080
Marna	1108	0.06	0.07	0.07	0.07	0.06	0.07	0.07
	1109	1.87	1.95	2.03*	2.00	1.87	2.15*	2.17*
Guckeen	1111	0.06	0.06	0.06	0.06	0.06	0.07	0.07
	1112	2.16	2.21	2.29	2.25	2.13	2.42*	2.40*

* Statistically significant from Baseline values using t-test at 5% level

For individual field analysis, Fields 1109 and 1112 (both sloped fields) showed significance in differences in export from Baseline conditions at the 5% level. In Field 1109, the comparison of means from Baseline to year 2015 for RCP 8.5 and Baseline to year 2045 and 2080 for RCP 8.5 showed significance that the mean values are not equal. Field 1112 showed significance that the mean values are not equal for years 2045 and 2080 for RCP 8.5, when compared to Baseline. All other comparisons to baseline conditions resulted in means that are considered equal. T-values are provided in Table 34.

Table 34: T-test significance for each field within respective RCP (comparison of Field 1108 for Baseline to 2015, Baseline to 2045, and Baseline to 2080, etcetera) of sediment export.

Field	RCP 4.5			RCP 8.5		
	2015	**2045**	**2080**	**2015**	**2045**	**2080**
1108	0.523	0.706	0.814	0.979	0.165	0.218
1109	0.306	***t < 0.05***	0.080	0.910	***t < 0.05***	***t < 0.05***
1111	0.823	0.846	0.742	0.713	0.336	0.812
1112	0.522	0.120	0.303	0.698	***t < 0.05***	***t < 0.05***

Bold and italicized values are statistically significant.

Lastly, a t-test of significance of sediment export between flat and steel slopes within a soil type was performed. Comparisons included Fields 1108 to 1109 and 1111 to 1112, within each RCP scenario. The t-testing showed significant differences in mean export between flat and sloped fields, with the same soil types. Statistical T-values are in Table 35. The significance is not surprising, as sloped fields are more likely to have faster surface runoff, which can dislodge sediment, when compared to flat slopes.

Table 35: T values for comparison of sediment export between fields of the same soil type but different slopes, within RCPs 4.5 and 8.5.

Field	Baseline	RCP 4.5			RCP 8.5		
		2015	**2045**	**2080**	**2015**	**2045**	**2080**
1108-1109	***t < 0.05***	***t < 0.05***	***t < 0.05***	***t < 0.05***	***t < 0.05***	***t < 0.05***	***t < 0.05***
1111-1112	***t < 0.05***	***t < 0.05***	***t < 0.05***	***t < 0.05***	***t < 0.05***	***t < 0.05***	***t < 0.05***

Bold and italicized values are statistically significant.

Analysis of Variance

As described above, an F-test was performed to test the differences in variances. A ratio of 1 indicates the variances of the two datasets are equal, and if the ratio is greater than the F-value of 1.1109, the variances are statistically significantly different.

Table 36: F-test values for analysis of variance of sediment export. Comparison is within each field, comparing each summary year to Baseline conditions.

Field	RCP 4.5			RCP 8.5		
	2015	**2045**	**2080**	**2015**	**2045**	**2080**
1108	1.099	1.015	1.103	1.065	***1.219***	***1.291***
1109	***1.139***	1.102	***1.250***	1.038	***1.264***	***1.372***
1111	1.049	1.088	1.030	***1.181***	***1.168***	***1.185***
1112	***1.155***	***1.114***	***1.225***	1.056	***1.263***	***1.344***

Bold and italicized values are statistically significant.

All variances in RCP 8.5, summary years 2045 and 2080 are statistically significant from Baseline conditions. In those scenarios, the range of sediment export, also seen in the box and whiskers plots in the Appendix, A2.9, are larger. More variability in the modeling and uncertainty in the output is seen in those modeled scenarios. Most of the mean values of sediment export did not show significance in difference from Baseline conditions. The analysis of variance shows another side to the export, that in the predicted outputs, there may be a wider range of export values year to year.

Annual RCP Impacts

Some significant results are seen in the comparisons of summary years to Baseline conditions, within each RCP. Another analysis performed was the difference in watershed outputs between year 2015 in RCP 4.5 and year 2015 in RCP 8.5. A t-test of nitrogen, phosphorus, and sediment export was performed, comparing the same year across RCP scenarios.

Nitrogen

Only year 2080 shows nitrogen export as statistically different for Fields 1108 and 1111, the flat fields, shown in Table 37. In all other model scenarios, comparison of nitrogen export of the same year in difference RCP scenarios are predicted to be similar.

Table 37: T-values for comparison of fields between RCP scenarios. An example of a comparison is the 2015 average nitrogen export for Field 1108 in RCP 4.5 to the average nitrogen export of Field 1108 in RCP 8.5.

Soil	Field	2015	2045	2080
Marna	1108	0.571	0.344	***t < 0.05***
	1109	0.865	0.509	0.735
Guckeen	1111	0.537	0.261	***t < 0.05***
	1112	0.806	0.629	0.470

Bold and italicized values are statistically significant.

Phosphorus

In comparisons of each field's phosphorus export in RCP 4.5 and RCP 8.5, only Field 1109 in year 2080 showed a statistically significant difference in average phosphorus export between RCPs 4.5 and 8.5 (see Table 38). All other phosphorus export comparisons by year in each RCP scenarios indicate similar export amounts.

Table 38: T-values for comparison of fields between RCP scenarios. An example of a comparison is the 2015 average phosphorus export for Field 1108 in RCP 4.5 to the average phosphorus export of Field 1108 in RCP 8.5.

Soil	Field	2015	2045	2080
Marna	1108	0.129	0.456	0.114
	1109	0.297	0.123	***t < 0.05***
Guckeen	1111	0.122	0.396	0.293
	1112	0.320	0.136	0.059

Bold and italicized values are statistically significant.

Sediment

In comparisons of sediment export of each field over RCP 4.5 and RCP 8.5, only Field 1109 in year 2080 showed a statistically significant difference in average export between RCPs 4.5 and 8.5 (see Table 39). All other sediment export comparison of year between RCP scenarios indicated similar sediment export.

Table 39: T-values for comparison of fields between RCP scenarios for sediment export. An example of a comparison is the 2015 average sediment export for Field 1108 in RCP 4.5 to the average sediment export of Field 1108 in RCP 8.5.

Soil	Field	2015	2045	2080
Marna	1108	0.498	0.321	0.341
	1109	0.246	0.107	***t < 0.05***
Guckeen	1111	0.553	0.254	0.598
	1112	0.299	0.125	0.100

Bold and italicized values are statistically significant.

Conclusions

Research has shown varying impacts to the Midwest as a result of climate change (IPCC, 2014b; USGCRP, 2018; USGS, 1999). The exact impacts and environmental changes are unknown and are dependent on many factors including population growth, energy sources and use, deforestation, and economic statistics.

This research evaluated a watershed scale hydrologic response and nitrate loss assessment and field scale nitrogen, phosphorus, and sediment loss assessment due to climate change in the Le Sueur River watershed, a predominately agricultural watershed in south–central Minnesota. One-thousand years of four representative scenarios, Baseline, 2015, 2045, and 2080, were modeled under two climate change scenarios, RCP 4.5 and RCP 8.5. The goal of this work was to assess watershed response and water quality impacts and changes due to climate change.

Hydrologic Analysis

The hydrologic components analyzed in this work; precipitation, water yield, ET, and outflow, indicated many years of significant changes from Baseline conditions in mean values, both on monthly and annual time scales. As summarized in Chapter 1, temperature and precipitation increases in RCP 4.5 and RCP 8.5, and both continue to increase over time, from Baseline year to 2080. The timing of precipitation also changes in both RCP scenarios, with increasing precipitation amounts in the winter months (November through April) and decreasing in the summer months (June through August).

Those trends and impacts are seen in the watershed modeling of the Le Sueur River watershed. Model outputs show increasing precipitation and ET. Research has shown both that increasing temperature leads to increases in ET (Abtew & Melesse, 2013) as well as decreases in ET from increases in humidity and carbon dioxide (Snyder et al., 2011). In these modeling scenarios, ET and precipitation increase together, supporting research that ET will increase under climate change scenarios in this part of the United States. ET is also impacted by wind, humidity, and water availability, making a clearer relationship harder to define.

Changing temperature may be the stronger driving factor in these modeling results, as yearly precipitation does not have extremely large increases over the RCP scenarios (a 50 mm increase, for the most extreme scenario, RCP 8.5 in year 2080). Water yield and outflow closely follow the trends shown in precipitation increases in the fall and winter months, decreases in the spring and summer months. Increasing surface flow can lead to larger sediment and nutrient loss if soil protection measures are not in place, as well as cause more flooding.

In both RCP 4.5 and RCP 8.5, increasing yearly values in water yield, ET, and outflow showed significance at the 5% level, meaning the model output is statistically different from Baseline conditions for those summary years. Model results for year 2015 are significant in some scenarios, meaning changes in watershed output may be seen very soon from the model's current day. These results suggest that climate changes may not be noticeable from day to day but changes may be seen in the near future.

Nitrate Losses

Nitrate loading to surface waters can decrease water quality, promote algae growth, decrease the amount of dissolved oxygen in the water, and in severe cases, cause or contribute to hypoxic zones. For nitrate that is applied to the surface through agriculture, increased surface

runoff, like what is predicted by this watershed model, has the potential to increase the amount of nitrates entering the streams and channels, to be transported downstream.

The watershed modeling shows significant changes in the amount of nitrate in watershed outflow. Most significance is seen in December through February and June through September. As nitrate moves in the dissolved phase, these results make sense, with increasing surface flows in the winter months. In the summer months, as surface flow decreases, the nitrates may be carried more with tile flow.

The analysis of tile flow and tile nitrate show increasing nitrate export during non-growing months. This is significant, as typically tile flow is minimal during non-growing months, if present at all, and dependent on weather conditions. If nitrate export continues to increase over time, land management practices should be revisited to decrease export and increase downstream water quality and help the state meet the goals outlined in the Nutrient Reduction Strategy.

Field Scale Nitrogen, Phosphorus, and Sediment Losses

At the field scale, nitrogen export increases over time in both RCP scenarios, but has an initial decrease from Baseline conditions. Flat fields showed higher nitrogen export amounts, likey the result of tile flow in the agricultural land. Month by month, nitrogen export is increasing from September through February. Of those months with increasing nitrogen export, the largest increases in export were seen in December and January. Results indicate that with increasing precipitation, overall, total nitrogen export will increase, under existing land cover and management practices.

Phosphorus can attach to soil particles, and travels with runoff. This is exhibited in the model results, as the higher precipitation months of April, May, and June have the highest percent increases of phosphorus export. Annually on the sloped fields, phosphorus exports are increasing over time, more so in the RCP 8.5 scenario. Sloped fields show higher phosphorus exports compared to flat, likely as a result of higher velocity of runoff over the steeper slopes.

Sediment follows similar patterns to phosphorus. Larger exports are recorded on the steep fields, for both soil types analyzed. Larger differences from Baseline conditions were commonly seen in summary year 2080.

An analysis indicated minimal differences in a year to year comparison across RCP scenarios, as in model export for year 2045 is statistically similar for both RCP 4.5 and RCP 8.5 climate scenarios. This indicates that the climate changes predicted, especially precipitation, by

the currently GCMs are not very different enough between RCP sceneries to result in differing model outputs.

Future Research

Clear, certain predictions are not guaranteed in the practice of climate modeling. Therefore, it is important to look at big pictures and trends and relate model outputs to knowledge of the environmental system, rather than take outputs as fact. This is clearly seen as an appropriate practice of climate modeling analysis in the nitrate export of this modeling exercise.

This work has set up a framework for taking global climate model predictions and applying them locally, with locational representative weather patterns. As further study and improvements are made in the global climate modeling field, with improvements in modeling techniques, predictions, and updates in future scenarios that inform the creation of RCPs, this exercise can be redone to produce more updated and applicable results. In addition to updating the model with new climate projections, as land management practices change in the Le Sueur River watershed, those changes can be applied to the model. This research can also be repeated with the other currently available RCP scenarios, to get a broader understanding of climate projections for the Le Sueur River watershed. Global climate models are uncertain, so more modeling may give more certainty or understanding of the range of results.

This work also does not highlight the increase in heavy precipitation events that have been seen and recorded in Minnesota. That analysis was not done in this work as the modeling tools used do not yet recognize and factor in the increase in events. Heavy, intense precipitation events can carry large quantities of sediment and nutrients downstream, which currently is not identified in the model. Further research to investigate the impacts on the Le Sueur River watershed due to these heavier precipitation events may provide useful information for land managers.

Next steps for climate change modeling of phosphorus and sediment export in the Le Sueur River watershed will be to analyze export at the watershed scale. As stated, additional modeling effort must be undertaken to accurately represent the export of phosphorus and sediment export in the watershed from the steep banks along the river, caused by glacial melt. That work will give a valuable estimate of the total export of phosphorus and sediment from the Le Sueur River watershed due to climate change.

This tool can also be used to test various land use and management changes, to see how best management practices and landscape changes may impact the hydrology of the watershed

and water quality under climate change predictions. It is possible that changes in climate will encourage land managers to modify their practices, or development of new crops and/or crop markets will cause changes in crops grown or land cover. This research did not apply any land management changes, meaning results may not represent what would occur under climate change conditions. This modeling exercise did not go to that level but changing land management practices in conjunction with climate changes is an area for further research.

Lastly, as agricultural areas are large exporters of sediments and nutrients, that can impact downstream water quality, this analysis can be performed for other watersheds in the area and region, to see the magnitude of impacts from the entire Midwest agricultural area on nutrient and sediment export. All watersheds play a role in downstream water quality and it will be a benefit to have more information regarding future environmental conditions.

Bibliography

Abatzoglou, J. T. (n.d.). Analysis Tips. Retrieved August 6, 2019, from https://climate.northwestknowledge.net/MACA/MACAanalysis.php

Abatzoglou, J. T. (2013). Development of gridded surface meteorological data for ecological applications and modelling. *International Journal of Climatology*, *33*, 121–131. https://doi.org/10.1002/joc.3413

Abatzoglou, J. T., & Brown, T. J. (2012). A comparison of statistical downscaling methods suited for wildfire applications. *International Journal of Climatology*, *32*, 772–780. https://doi.org/10.1002/joc.2312

Abtew, W., & Melesse, A. (2013). *Evaporation and Evapotranspiration: Measurements and Estimations*.

Ailliot, P., Allard, D., Monbet, V., & Naveau, P. (2015). Stochastic weather generators: an overview of weather type models. *Journal de La Société Française de Statistique*, *156*(1), 101–113. Retrieved from http://www.sfds.asso.fr/journal

Arnold, J. G., Srinivasan, R., Muttiah, R. S., & Williams, J. (1998). Large area hydrologic modeling and assessment part I: model development. *Journal of the American Water Resources Association*, *34*(1), 73–89. https://doi.org/10.1016/S0899-9007(00)00483-4

Bronstert, A., Kolokotronis, V., Schwandt, D., & Straub, H. (2007). Comparison and evaluation of regional climate scenarios for hydrological impact analysis: General scheme and application example Axel. *International Journal of Climatology*, *27*, 1579–1594. https://doi.org/10.1002/joc.1612

Byun, K., & Hamlet, A. F. (2018). Projected changes in future climate over the Midwest and Great Lakes region using downscaled CMIP5 ensembles. *International Journal of Climatology*, *38*, e531–e553. https://doi.org/10.1002/joc.5388

Campbell, S.-E., Baskfield, P., Maclean, S., Ganske, L., Drewitz, B. S.-M., Hughes, C., … Bateman, B. (2015). Le Sueur River WRAPS Report, (August).

Cherie, N. (2013). Downscaling and modeling the effects of climate change on hydrology and water resources in the Upper Blue Nile River Basin, Ethiopia. https://doi.org/10.5675/ICWRER

Chien, H., Yeh, P. J. F., & Knouft, J. H. (2013a). Modeling the potential impacts of climate change on streamflow in agricultural watersheds of the Midwestern United States. *Journal of Hydrology*, *491*(1), 73–88. https://doi.org/10.1016/j.jhydrol.2013.03.026

Chien, H., Yeh, P. J. F., & Knouft, J. H. (2013b). Modeling the potential impacts of climate change on streamflow in agricultural watersheds of the Midwestern United States. *Journal of Hydrology*, *491*(1), 73–88. https://doi.org/10.1016/j.jhydrol.2013.03.026

Dalzell, B. J., & Mulla, D. J. (2018). Perennial vegetation impacts on stream discharge and channel sources of sediment in the Minnesota River Basin. *Journal of Soil and Water Conservation*, *73*(2), 120–132. https://doi.org/10.2489/jswc.73.2.120

Day, S. S., Wittkop, C., Jennings, C. E., Gran, K., & Belmont, P. (2011). Holocene landscape evolution and erosional processes in the Le Sueur River, central Minnesota. *Geological Society of America*, *24*, 439–455. https://doi.org/10.1130/2011.0024(21)

Demaria, E. M. C., Palmer, R. N., & Roundy, J. K. (2016). Regional climate change projections of streamflow characteristics in the Northeast and Midwest U.S. *Journal of Hydrology: Regional Studies*, *5*, 309–323. https://doi.org/10.1016/j.ejrh.2015.11.007

Department of Natural Resources, M. (2019). *Climate Summary for Watersheds*.

Engineering, B. (2004). *Detailed Assessment of Phosphorus Sources to Minnesota Watersheds*.

Ficklin, D. L., Luo, Y., Luedeling, E., & Zhang, M. (2009). Climate change sensitivity assessment of a highly agricultural watershed using SWAT. *Journal of Hydrology*, *374*, 16–29. https://doi.org/10.1016/j.jhydrol.2009.05.016

Finlay, J., Dalzell, B., Dolph, C., Baker, A., & Rorer, M. (2019). *Measuring and modeling watershed phosphorus loss and transport for improved management of agricultural landscapes*. *Minnesota Department of Agriculture*.

Fowler, H. J., Blenkinsop, S., & Tebaldi, C. (2007). Linking climate change modelling to impacts studies: recent advances in downscaling techniques for hydrological modelling. *International Journal of Climatology*, *27*(12), 1547–1578. https://doi.org/10.1002/joc.1556

Fuka, D. R., Walter, M. T., Macalister, C., Degaetano, A. T., Steenhuis, T. S., & Easton, Z. M. (2013). Using the Climate Forecast System Reanalysis as weather input data for watershed models. *Hydrological Processes*. https://doi.org/10.1002/hyp.10073

Gassman, P. W., Reyes, M. R., Green, C. H., & Arnold, J. G. (2007). THE SOIL AND WATER ASSESSMENT TOOL: HISTORICAL DEVELOPMENT, APPLICATIONS, AND FUTURE RESEARCH DIRECTIONS. *TransactAmerican Society of Agricultural and Biological Engineers*, *50*(4), 1211–1250. Retrieved from http://www.card.iastate.edu/research/resource-and-environmental/items/asabe_swat.pdf

Gassman, Philip W., Sadeghi, A. M., & Srinivasan, R. (2014). Applications of the SWAT Model Special Section: Overview and Insights. *Journal of Environment Quality*, *43*(1), 1.

https://doi.org/10.2134/jeq2013.11.0466

Gran, K. B., Belmont, P., Day, S. S., Jennings, C., Johnson, A., Perg, L., & Wilcock, P. R. (2009). Geomorphic evolution of the Le Sueur River, Minnesota, USA, and implications for current sediment loading. *Geological Society of America*, *451*, 119–130. https://doi.org/10.1130/2009.2451(08).

Gran, K., Belmont, P., Day, S., Jennings, C., Lauer, J. W., Viparelli, E., … Parker, G. (2011). *An integrated sediment budget for the Le Sueur River Basin*.

Hardwick Jones, R., Westra, S., & Sharma, A. (2010). Observed relationships between extreme sub-daily precipitation, surface temperature and relative humidity. *Geophysical Research Letters*, *37*(L22805), 1–5. https://doi.org/10.1029/2010GL045081

Historic Mega-Rain Events in Minnesota. (n.d.). Retrieved May 11, 2019, from https://www.dnr.state.mn.us/climate/summaries_and_publications/mega_rain_events.html

IPCC. (2014a). Climate Change 2014: Synthesis Report. Contribution of Working Groups I, II and III to the Fifth Assessment Report of the Intergovernmental Panel on Climate Change. *Journal of Paediatrics and Child Health*, 1–151. https://doi.org/10.1111/jpc.14569

IPCC. (2014b). Climate Change 2014 Synthesis Report Summary Chapter for Policymakers. *IPCC Synthesis Report*, 31. https://doi.org/10.1017/CBO9781107415324

Jang, S., & Kavvas, M. L. (2014). Statistical Downscaling versus Dynamic Downscaling: An Assessment Based upon a Sample Study. *World Environmental and Water Resources Congress 2014: Water Without Borders*, 591–595. https://doi.org/10.1061/9780784413548.062

Jha, M., Arnold, J. G., Gassman, P. W., Giorgi, F., & Gu, R. R. (2006). Climate change sensitivity assessment on Upper Mississippi River Basin streamflows using SWAT. *Journal of the American Water Resources Association*, *42*(4), 997–1016. https://doi.org/10.1111/j.1752-1688.2006.tb04510.x

Jha, M., Gassman, P. W., Secchi, S., Gu, R., & Arnold, J. (2004). Effect of watershed subdivision on swat flow, sediment, and nutrient predictions. *Journal of the American Water Resources Association*, *40*(3), 811–825. https://doi.org/10.1111/j.1752-1688.2004.tb04460.x

Jiang, Y., Kim, J. B., Still, C. J., Kerns, B. K., Kline, J. D., & Cunningham, P. G. (2018). Inter-comparison of multiple statistically downscaled climate datasets for the Pacific Northwest, USA. *Scientific Data*, *5*(February 2018). https://doi.org/10.1038/sdata.2018.16

Kelley, D. W., & Nater, E. A. (2000). Historical Sediment Flux from Three Watersheds into Lake Pepin, Minnesota, USA. *Journal of Environmental Quality*, *29*(4), 1369–1369.

https://doi.org/10.2134/jeq2000.00472425002900040051x

Kouwen, N., Asce, M., Danard, M., Bingeman, A., Luo, W., Seglenieks, F. R., & Soulis, E. D. (2005). Case Study : Watershed Modeling with Distributed Weather Model Data. *Journal of Hydrologic Engineering*, *10*(1), 23–38. https://doi.org/10.1061/(ASCE)1084-0699(2005)10

Lambert, S. J., & Boer, G. J. (2001). CMIP1 evaluation and intercomparison of coupled climate models. *Climate Dynamics*, *17*, 83–106. https://doi.org/10.1007/PL00013736

Livneh, B., Lin, C., Maurer, E. P., Andreadis, K. M., Rosenberg, E. A., Lettenmaier, D. P., … Mishra, V. (2013). A Long-Term Hydrologically Based Dataset of Land Surface Fluxes and States for the Conterminous United States: Update and Extensions. *Journal of Climate*, *26*, 9384–9392. https://doi.org/10.1175/jcli-d-12-00508.1

Maraun, D., Brienen, S., Rust, H. W., Sauter, T., Themeßl, M., Venema, V. K. C., & Chun, K. P. (2010). Precipitation Downscaling under Climate Change: Recent Developments to Bridge the Gap Between Dynamical Models and the End User. *Review of Geophysics*, *48*(3), 1–34. https://doi.org/10.1029/2009RG000314

Maurer, E. P., Hidalgo, H. G., Das, T., Dettinger, M. D., & Cayan, D. R. (2010). The utility of daily large-scale climate data in the assessment of climate change impacts on daily streamflow in California. *Hydrology and Earth System Sciences*, *14*(6), 1125–1138. https://doi.org/10.5194/hess-14-1125-2010

Mehan, S., Gitau, M. W., & Flanagan, D. C. (2018). Development of reliable future climatic projections to assess hydro-meteorological implications in the Western Lake Erie Basin. *Hydrology and Earth System Sciences*, 1–36. https://doi.org/10.5194/hess-2018-204

Mehan, S., Kanan, N., Neupane, R., McDaniel, R., & Kumar, S. (2016). Climate Change Impacts on the Hydrological Processes of a Small Agricultural Watershed. *Climate*, *4*(4), 56. https://doi.org/10.3390/cli4040056

Milly, P. C. D., & Dunne, K. A. (2001). Trends in Evaporation and Surface Cooling in the Mississippi River Basin. *Geophysical Research Letters*, *28*(7), 1219–1222. https://doi.org/10.1029/2000GL012321

Minnesota, P. C. A. (2013). *Nitrogen in Minnesota Surface waters*.

Moncrief, J. F., Evans, S. D., & Randall, G. W. (1997). Description of the Minnesota River Basin and Residue Management Systems Sediment Control Importance of Soil Texture and, 1–8.

Mote, P. W., Brekke, L., Duffy, P. B., & Maurer, E. (2011). Guidelines for constructing climate scenarios. *Eos*, *92*(31), 257–264. https://doi.org/10.1029/2011EO310001

MPCA. (2014). The Minnesota Nutrient Reduction Strategy. *Minnesota Pollution Control*

Agency. https://doi.org/10.13031/aim.20162492032

Musser, K., Kudelka, S., & Moore, R. (2009). *Minnesota River Basin Trends*. *Water Resources Center, Minnesota State University, Mankato* (Vol. 1). Retrieved from http://mrbdc.mnsu.edu/sites/mrbdc.mnsu.edu/files/public/mnbasin/trends/pdfs/trends_full.pdf

Neideen, T., & Brasel, K. (2007). Understanding Statistical Tests. *Journal of Surgical Education*, *64*(2), 93–96. https://doi.org/10.1016/j.jsurg.2007.02.001

Neitsch, S. L., Arnold, J. G., Kiniry, J. R., & Williams, J. R. (2011). *Soil and Water Assessment Tool Theoretical Documentation Version 2009*.

Ouyang, F., Zhu, Y., Fu, G., Lü, H., Zhang, A., Yu, Z., & Chen, X. (2015). Impacts of climate change under CMIP5 RCP scenarios on streamflow in the Huangnizhuang catchment. *Stochastic Environmental Research and Risk Assessment*, *29*(7), 1781–1795. https://doi.org/10.1007/s00477-014-1018-9

Palmer, T. N., Doblas-Reyes, F. J., Hagedorn, R., & Weisheimer, A. (2005). Probabilistic prediction of climate using multi-model ensembles: From basics to applications. *Philosophical Transactions of the Royal Society*, *360*, 1991–1998. https://doi.org/10.1098/rstb.2005.1750

Pierce, D. W., Barnett, T. P., Santer, B. D., & Gleckler, P. J. (2009). Selecting global climate models for regional climate change studies. *Proceedings of the National Academy of Sciences*, *106*(21), 8441–8446. https://doi.org/10.1073/pnas.0900094106

Rabalais, N. N., & Turner, R. E. (2019). Gulf of Mexico Hypoxia: Past, Present, and Future. *Limnology and Oceanography Bulletin*, 117–124. https://doi.org/10.1002/lob.10351

Randall, G. W., & Mulla, D. J. (2001). Nitrate Nitrogen in Surface Waters as Influenced by Climatic Conditions and Agricultural Practices. *Journal of Environmental Quality*, *30*, 337–344. https://doi.org/10.2134/jeq2001.302337x

Rosenberg, N. J., Brown, R. A., Izaurralde, R. C., & Thomson, A. M. (2003). Integrated assessment of Hadley Centre (HadCM2) climate change projections on agricultural productivity and irrigation water supply in the conterminous United States I. Climate change scenarios and impacts on irrigation water supply simulated with the HUM. *Agricultural and Forest Meteorology*, *117*(1–2), 73–96. https://doi.org/10.1016/S0168-1923(03)00025-X

Sherwood, S. C., Ingram, W., Tsushima, Y., Satoh, M., Roberts, M., Vidale, P. L., & O'Gorman, P. A. (2010). Relative humidity changes in a warmer climate. *Journal of Geophysical Research*, *115*(D09104), 1–11. https://doi.org/10.1029/2009JD012585

Snyder, R. L., Moratiel, R., Song, Z., Swelam, A., Jomaa, I., & Shapland, T. (2011). Evapotranspiration Response to Climate Change. *Acta Horticulturae*, *922*, 91–98. https://doi.org/10.17660/ActaHortic.2011.922.11

Spindler, B., Baskfield, P., O'Hara, K., Helwig, D., Hotka, L., Thompson, S., … Parson, K. (2012). *LeSueur River Watershed Monitoring and Assessment Report*. Retrieved from http://www.pca.state.mn.us/index.php/view-document.html?gid=17986

Sunde, M. G., He, H. S., Hubbart, J. A., & Urban, M. A. (2017). Integrating downscaled CMIP5 data with a physically based hydrologic model to estimate potential climate change impacts on streamflow processes in a mixed-use watershed. *Hydrological Processes*, *31*, 1790–1803. https://doi.org/10.1002/hyp.11150

Taylor, K. E., Stouffer, R. J., & Meehl, G. A. (2012). An overview of CMIP5 and the experiment design. *Bulletin of the American Meteorological Society*. https://doi.org/10.1175/BAMS-D-11-00094.1

Taylor, K. E., Stouffer, R. J., & Meehl, G. a. (2007). A Summary of the CMIP5 Experiment Design. *World*, *4*(January 2011), 1–33. https://doi.org/10.1175/BAMS-D-11-00094.1

Thomson, A. M., Kyle, G. P., Zhang, X., Bandaru, V., West, T. O., Wise, M. A., … Calvin, K. V. (2014). The contribution of future agricultural trends in the US Midwest to global climate change mitigation. *Global Environmental Change*, *24*(1), 143–154. https://doi.org/10.1016/j.gloenvcha.2013.11.019

USGCRP. (2018). Impacts, Risks, and Adaptation in the United States: Fourth National Climate Assessment, Volume II. *U.S. Global Change Research Program*, *II*, 1–1515. https://doi.org/10.7930/NCA4.2018

USGS. (1999). Evidence of Climate Change over the Last 10,000 Years from the Sediments of Lakes in the Upper Mississippi Basin. *US Geological Service Fact Sheet FS-059-99*, 1–3. Retrieved from http://pubs.usgs.gov/fs/fs-0059-99/

Walter, M. T., Wilks, D. S., Parlange, J. Y., & Schneider, R. L. (2004). Increasing Evapotranspiration from the Conterminous United States. *Journal of Hydrometeorology*, *5*(3), 405–408. https://doi.org/10.1175/1525-7541(2004)005<0405:IEFTCU>2.0.CO;2

Wayne, G. P. (2013). The Beginner's Guide to Representative Concentration Pathways. *Skeptical Sciece*, *1.0*, 1–24.

WCRP Coupled Model Intercomparison Project - Phase 5 - CMIP 5. (2011). *CLIVAR Exchanges*, *16*(56). Retrieved from www.wcrp-climate.org/conference2011

Wilcock, P. (2009). *Identifying Sediment Sources in the Minnesota River Basin*. *Minnesota River*

Sediment Colloquium.

Wilks, D. S., & Wilby, R. L. (1999). The weather generation game: a review of stochastic weather models. *Progress in Physical Geography*, *23*(3), 329–357. https://doi.org/10.1191/030913399666525256

Wilson, B. N. (n.d.). *Chapter Two: Overview of Statistical Concepts*. *Parameter Estimation*.

Wilson, B. N., Sheshukov, A., & Pulley, R. (2006). *Erosion Risk Assessment Tool For Construction Sites*. Retrieved from http://www.dot.state.mn.us/environment/erosion/pdf/erosionriskassesmenttoolforconstsites.pdf

Winkler, J. A., Arritt, R. W., & Pryor, S. C. (2012). *Climate Projections for the Midwest: Availability, Interpretation and Synthesis*. *US National Climate Assessment Midwest Technical Input Report*. https://doi.org/9781610915113

Winkler, J. A., Guentchev, G. S., Liszewska, M., Perdinan, & Tan, P.-N. (2011). Climate Scenario Development and Applications for Local/Regional Climate Change Impact Assessments: An Overview for the Non-Climate Scientist: Part II: Considerations When Using Climate Change Scenarios. *Geography Compass*, *5/6*, 301–328. https://doi.org/10.1111/j.1749-8198.2011.00426.x

Yang, Z., Zhang, Q., & Hao, X. (2016). Evapotranspiration Trend and Its Relationship with Precipitation over the Loess Plateau during the Last Three Decades. *Advances in Meteorology*, *2016*. https://doi.org/10.1155/2016/6809749

Zeiger, S. J., & Hubbart, J. A. (2016). A SWAT model validation of nested-scale contemporaneous stream flow, suspended sediment and nutrients from a multiple-land-use watershed of the central USA. *Science of the Total Environment*, *572*, 232–243. https://doi.org/10.1016/j.scitotenv.2016.07.178

Zhang, X., Xu, Y. P., & Fu, G. (2014). Uncertainties in SWAT extreme flow simulation under climate change. *Journal of Hydrology*, *515*. https://doi.org/10.1016/j.jhydrol.2014.04.064

Appendix

A1.1 - WINDS 20-Day Weather Outputs for RCP 4.5 (METDATA downscaling method). Results are averages of outputs for respective day ranges

Baseline						
Days	Maximum Temperature °C	Minimum Temperature °C	Precipitation mm	Wind Speed m/s	Solar Radiation MJ/m^2	Relative Humidity %
1-20	-5.77	-15.26	0.65	6.19	5.99	77.98
21-40	-5.34	-15.16	0.68	6.18	7.77	76.83
41-60	-2.18	-12.05	0.87	6.21	10.21	75.26
61-80	2.56	-7.60	1.27	6.29	12.72	73.36
81-100	8.16	-2.46	1.80	6.34	15.21	70.88
101-120	13.73	2.20	2.55	6.30	17.28	68.66
121-140	19.23	6.65	2.99	6.09	19.42	66.63
141-160	23.22	10.38	3.39	5.68	21.42	66.59
161-180	26.06	13.55	3.44	5.24	22.52	69.06
181-200	27.58	15.54	3.35	4.87	22.43	71.97
201-220	27.77	15.79	3.49	4.67	21.08	73.70
221-240	26.39	14.01	2.98	4.72	19.00	72.87
241-260	23.63	10.82	2.69	4.98	16.10	71.03
261-280	19.46	6.94	2.31	5.36	12.91	69.82
281-300	13.96	2.62	1.82	5.72	9.75	71.18
301-320	7.87	-2.12	1.46	5.97	7.19	74.03
321-340	1.98	-7.07	1.07	6.13	5.60	76.25
341-366	-3.13	-12.19	0.84	6.16	5.12	78.05

2015						
Days	Maximum Temperature °C	Minimum Temperature °C	Precipitation mm	Wind Speed m/s	Solar Radiation MJ/m^2	Relative Humidity %
1-20	-4.61	-13.75	0.66	6.15	5.93	76.97
21-40	-4.02	-13.56	0.71	6.13	7.68	75.85
41-60	-0.73	-10.53	0.89	6.15	10.11	73.65
61-80	4.65	-5.55	1.34	6.25	12.69	71.13
81-100	10.29	-0.58	1.84	6.35	15.11	68.53
101-120	15.69	3.95	2.54	6.29	17.30	66.60
121-140	20.12	7.58	3.24	6.02	19.46	65.98
141-160	24.26	11.28	3.64	5.61	21.57	66.90
161-180	27.10	14.37	3.55	5.15	22.82	68.99
181-200	29.01	16.67	3.32	4.80	22.74	70.99
201-220	29.27	16.99	3.12	4.64	21.53	71.69
221-240	28.09	15.39	2.80	4.72	19.33	70.63
241-260	25.24	12.17	2.60	4.95	16.51	69.03
261-280	20.96	8.18	2.32	5.31	13.23	68.55
281-300	15.23	3.61	2.08	5.69	9.94	70.09
301-320	9.35	-0.78	1.65	5.95	7.25	72.69
321-340	3.09	-5.90	1.18	6.12	5.62	75.37
341-366	-2.25	-10.98	0.86	6.14	5.14	76.95

2045						
Days	Maximum Temperature °C	Minimum Temperature °C	Precipitation mm	Wind Speed m/s	Solar Radiation MJ/m^2	Relative Humidity %
1-20	-3.20	-11.78	0.74	6.11	5.76	75.80
21-40	-2.68	-11.66	0.77	6.11	7.52	74.18
41-60	0.46	-8.96	0.98	6.20	9.92	71.92
61-80	5.35	-4.63	1.36	6.25	12.53	69.27
81-100	11.01	0.16	2.04	6.29	15.09	66.99
101-120	16.26	4.48	2.68	6.21	17.32	65.82
121-140	20.93	8.46	3.43	5.94	19.69	65.86
141-160	25.24	12.32	3.54	5.56	21.70	66.60
161-180	28.30	15.51	3.48	5.12	22.86	68.38
181-200	30.32	17.77	3.36	4.78	22.66	69.90
201-220	30.87	18.24	3.00	4.59	21.46	70.10
221-240	29.69	16.76	2.75	4.63	19.38	69.16
241-260	26.66	13.46	2.60	4.84	16.53	67.94
261-280	22.19	9.24	2.31	5.17	13.36	67.80
281-300	16.65	4.83	2.04	5.54	10.05	69.16
301-320	10.41	0.06	1.69	5.79	7.32	72.41
321-340	4.48	-4.58	1.22	5.97	5.63	74.69
341-366	-0.54	-9.08	0.91	6.05	5.05	76.26

2080						
Days	Maximum Temperature °C	Minimum Temperature °C	Precipitation mm	Wind Speed m/s	Solar Radiation MJ/m^2	Relative Humidity %
1-20	-2.43	-10.85	0.77	6.03	5.76	74.33
21-40	-1.69	-10.42	0.79	6.02	7.48	72.56
41-60	1.60	-7.69	1.00	6.11	9.93	70.26
61-80	6.51	-3.59	1.44	6.17	12.49	68.63
81-100	11.95	0.91	2.03	6.18	15.00	67.13
101-120	16.97	5.04	2.76	6.10	17.42	66.01
121-140	21.81	9.08	3.40	5.85	19.67	66.07
141-160	26.10	13.01	3.53	5.45	21.68	66.57
161-180	29.17	16.22	3.55	5.04	22.98	68.05
181-200	31.09	18.48	3.40	4.74	22.82	69.98
201-220	31.44	18.87	3.00	4.55	21.56	70.40
221-240	30.27	17.43	2.95	4.61	19.34	69.78
241-260	27.21	14.19	2.80	4.77	16.58	68.48
261-280	22.99	10.15	2.43	5.11	13.33	68.29
281-300	17.74	5.84	2.10	5.50	10.07	69.73
301-320	11.53	1.07	1.57	5.81	7.35	71.64
321-340	5.52	-3.64	1.18	5.98	5.59	73.99
341-366	0.10	-8.21	0.89	6.03	5.02	75.01

A1.1 - WINDS 20-Day Weather Outputs for RCP 8.5 (METDATA downscaling method). Results are averages of outputs for respective day ranges

Baseline						
Days	Maximum Temperature °C	Minimum Temperature °C	Precipitation mm	Wind Speed m/s	Solar Radiation MJ/m^2	Relative Humidity %
1-20	-5.77	-15.26	0.65	6.19	5.99	77.98
21-40	-5.34	-15.16	0.68	6.18	7.77	76.83
41-60	-2.18	-12.05	0.87	6.21	10.21	75.26
61-80	2.56	-7.60	1.27	6.29	12.72	73.36
81-100	8.16	-2.46	1.80	6.34	15.21	70.88
101-120	13.73	2.20	2.55	6.30	17.28	68.66
121-140	19.23	6.65	2.99	6.09	19.42	66.63
141-160	23.22	10.38	3.39	5.68	21.42	66.59
161-180	26.06	13.55	3.44	5.24	22.52	69.06
181-200	27.58	15.54	3.35	4.87	22.43	71.97
201-220	27.77	15.79	3.49	4.67	21.08	73.70
221-240	26.39	14.01	2.98	4.72	19.00	72.87
241-260	23.63	10.82	2.69	4.98	16.10	71.03
261-280	19.46	6.94	2.31	5.36	12.91	69.82
281-300	13.96	2.62	1.82	5.72	9.75	71.18
301-320	7.87	-2.12	1.46	5.97	7.19	74.03
321-340	1.98	-7.07	1.07	6.13	5.60	76.25
341-366	-3.13	-12.19	0.84	6.16	5.12	78.05

2015						
Days	Maximum Temperature °C	Minimum Temperature °C	Precipitation mm	Wind Speed m/s	Solar Radiation MJ/m^2	Relative Humidity %
1-20	-4.55	-13.50	0.67	6.20	5.95	77.43
21-40	-3.73	-13.13	0.67	6.22	7.71	75.94
41-60	-0.55	-10.21	0.90	6.26	10.08	73.50
61-80	4.32	-5.78	1.34	6.33	12.62	70.90
81-100	9.53	-1.19	2.01	6.36	15.02	68.87
101-120	15.00	3.24	2.65	6.30	17.50	67.19
121-140	20.26	7.46	3.16	6.06	19.86	66.19
141-160	24.68	11.51	3.51	5.68	21.79	66.22
161-180	27.69	14.80	3.36	5.20	22.95	67.86
181-200	29.31	16.99	3.31	4.84	22.73	69.66
201-220	29.22	17.06	3.13	4.67	21.45	70.76
221-240	27.86	15.36	2.95	4.75	19.23	70.55
241-260	25.24	12.30	2.58	4.97	16.41	69.33
261-280	21.15	8.49	2.26	5.33	13.09	68.64
281-300	15.60	4.07	1.90	5.67	9.83	69.98
301-320	9.37	-0.77	1.60	5.97	7.25	72.59
321-340	2.98	-5.89	1.23	6.14	5.65	75.31
341-366	-2.34	-10.96	0.89	6.20	5.15	77.18

2045						
Days	Maximum Temperature °C	Minimum Temperature °C	Precipitation mm	Wind Speed m/s	Solar Radiation MJ/m^2	Relative Humidity %
1-20	-2.71	-11.25	0.71	6.25	5.80	75.47
21-40	-2.09	-11.23	0.78	6.27	7.50	73.67
41-60	0.93	-8.76	1.03	6.28	9.93	71.26
61-80	5.42	-4.69	1.43	6.32	12.51	69.68
81-100	10.97	0.24	2.10	6.37	14.99	68.06
101-120	16.24	4.67	2.84	6.32	17.19	66.99
121-140	21.20	8.71	3.44	6.05	19.48	66.34
141-160	25.63	12.55	3.57	5.64	21.71	66.86
161-180	28.88	15.93	3.29	5.14	23.05	68.26
181-200	30.74	18.22	3.14	4.79	22.98	69.14
201-220	31.34	18.88	2.99	4.64	21.61	69.53
221-240	30.02	17.26	2.74	4.68	19.48	68.93
241-260	27.08	13.92	2.67	4.93	16.62	68.11
261-280	22.64	9.62	2.45	5.24	13.29	68.00
281-300	16.75	4.99	2.17	5.62	9.96	69.78
301-320	10.49	0.48	1.74	5.90	7.27	72.81
321-340	4.87	-3.67	1.29	6.11	5.53	74.83
341-366	-0.56	-8.62	0.94	6.20	5.03	76.23

2080						
Days	Maximum Temperature °C	Minimum Temperature °C	Precipitation mm	Wind Speed m/s	Solar Radiation MJ/m^2	Relative Humidity %
1-20	0.16	-7.84	0.76	6.19	5.61	71.77
21-40	0.83	-7.50	0.80	6.23	7.22	69.46
41-60	4.05	-4.99	1.09	6.27	9.55	67.83
61-80	8.57	-1.44	1.55	6.35	12.19	66.65
81-100	13.58	2.48	2.22	6.37	14.84	66.00
101-120	18.85	6.85	3.12	6.27	17.35	65.50
121-140	23.84	11.01	3.66	5.99	19.76	65.30
141-160	28.10	14.95	3.61	5.54	21.89	65.30
161-180	31.54	18.41	3.34	5.04	23.10	66.05
181-200	33.72	20.78	3.05	4.71	23.01	66.73
201-220	34.34	21.39	2.87	4.53	21.66	66.97
221-240	33.21	20.02	2.79	4.58	19.52	66.47
241-260	30.15	16.89	2.73	4.82	16.73	65.91
261-280	25.52	12.60	2.55	5.16	13.48	66.00
281-300	19.82	7.75	2.10	5.50	10.16	67.74
301-320	13.50	2.96	1.71	5.85	7.39	70.52
321-340	7.61	-1.55	1.20	6.05	5.60	72.67
341-366	2.45	-5.67	0.94	6.18	4.96	73.23

A1.1 - WINDS 20-Day Weather Outputs for RCP 4.5 (Livneh downscaling method). Results are averages of outputs for respective day ranges

Baseline						
Days	Maximum Temperature °C	Minimum Temperature °C	Precipitation mm	Wind Speed m/s	Solar Radiation MJ/m^2	Relative Humidity %
1-20	-5.77	-15.26	0.65	6.19	5.99	77.98
21-40	-5.34	-15.16	0.68	6.18	7.77	76.83
41-60	-2.18	-12.05	0.87	6.21	10.21	75.26
61-80	2.56	-7.60	1.27	6.29	12.72	73.36
81-100	8.16	-2.46	1.80	6.34	15.21	70.88
101-120	13.73	2.20	2.55	6.30	17.28	68.66
121-140	19.23	6.65	2.99	6.09	19.42	66.63
141-160	23.22	10.38	3.39	5.68	21.42	66.59
161-180	26.06	13.55	3.44	5.24	22.52	69.06
181-200	27.58	15.54	3.35	4.87	22.43	71.97
201-220	27.77	15.79	3.49	4.67	21.08	73.70
221-240	26.39	14.01	2.98	4.72	19.00	72.87
241-260	23.63	10.82	2.69	4.98	16.10	71.03
261-280	19.46	6.94	2.31	5.36	12.91	69.82
281-300	13.96	2.62	1.82	5.72	9.75	71.18
301-320	7.87	-2.12	1.46	5.97	7.19	74.03
321-340	1.98	-7.07	1.07	6.13	5.60	76.25
341-366	-3.13	-12.19	0.84	6.16	5.12	78.05

2015						
Days	Maximum Temperature °C	Minimum Temperature °C	Precipitation mm	Wind Speed m/s	Solar Radiation MJ/m^2	Relative Humidity %
1-20	-4.89	-13.79	0.70	6.15	5.92	76.53
21-40	-4.02	-13.29	0.71	6.16	7.72	75.09
41-60	-0.54	-10.09	0.91	6.18	10.12	72.80
61-80	4.64	-5.37	1.31	6.21	12.78	70.85
81-100	10.22	-0.61	1.92	6.27	15.11	68.55
101-120	15.40	3.74	2.62	6.23	17.34	66.97
121-140	20.18	7.58	3.19	5.98	19.73	66.44
141-160	24.24	11.27	3.50	5.57	21.73	66.67
161-180	27.22	14.42	3.57	5.08	23.01	68.39
181-200	29.08	16.65	3.34	4.73	22.87	70.11
201-220	29.40	17.01	3.14	4.56	21.57	70.14
221-240	28.22	15.39	2.80	4.63	19.39	69.15
241-260	25.23	12.16	2.69	4.90	16.44	68.31
261-280	20.82	8.09	2.35	5.28	13.20	68.04
281-300	15.44	3.84	1.96	5.62	9.91	70.00
301-320	9.39	-0.82	1.62	5.93	7.25	72.63
321-340	3.54	-5.55	1.19	6.04	5.61	75.38
341-366	-2.23	-10.99	0.82	6.12	5.12	76.73

2045						
Days	Maximum Temperature °C	Minimum Temperature °C	Precipitation mm	Wind Speed m/s	Solar Radiation MJ/m^2	Relative Humidity %
1-20	-3.42	-11.97	0.73	6.06	5.77	74.73
21-40	-2.61	-11.55	0.79	6.10	7.46	73.57
41-60	0.38	-9.10	1.00	6.12	9.84	71.91
61-80	5.77	-4.37	1.41	6.22	12.51	69.71
81-100	11.22	0.21	2.02	6.22	14.98	67.55
101-120	16.65	4.61	2.75	6.14	17.33	65.97
121-140	21.26	8.54	3.47	5.88	19.57	65.59
141-160	25.28	12.25	3.42	5.44	21.62	66.22
161-180	28.30	15.39	3.33	5.00	22.88	67.22
181-200	30.42	17.80	3.25	4.73	22.85	67.71
201-220	30.85	18.22	2.96	4.54	21.56	67.21
221-240	29.59	16.71	2.76	4.55	19.35	65.85
241-260	26.66	13.50	2.65	4.74	16.52	65.50
261-280	22.07	9.24	2.26	5.09	13.27	66.38
281-300	16.52	4.77	2.00	5.40	9.98	68.73
301-320	10.34	0.05	1.66	5.75	7.30	71.90
321-340	4.39	-4.75	1.32	5.93	5.56	74.15
341-366	-0.76	-9.29	0.97	6.05	5.01	74.98

2080						
Days	Maximum Temperature °C	Minimum Temperature °C	Precipitation mm	Wind Speed m/s	Solar Radiation MJ/m^2	Relative Humidity %
1-20	-2.34	-10.70	0.77	5.96	5.70	72.97
21-40	-1.85	-10.64	0.77	5.98	7.40	71.51
41-60	1.42	-8.00	0.96	6.03	9.87	69.73
61-80	6.24	-3.90	1.40	6.09	12.58	68.59
81-100	12.01	0.95	2.07	6.14	15.02	67.57
101-120	17.09	5.08	2.77	5.99	17.39	66.29
121-140	21.96	9.17	3.36	5.75	19.65	65.81
141-160	25.90	12.87	3.57	5.34	21.70	66.00
161-180	29.25	16.31	3.48	4.94	22.96	66.81
181-200	31.11	18.52	3.24	4.62	22.83	67.50
201-220	31.51	18.95	3.02	4.46	21.53	67.49
221-240	30.18	17.32	2.98	4.47	19.35	67.01
241-260	27.33	14.20	2.73	4.64	16.54	66.53
261-280	22.99	10.08	2.32	5.00	13.37	67.29
281-300	17.51	5.65	2.09	5.36	10.09	69.25
301-320	11.50	1.02	1.55	5.67	7.34	71.97
321-340	5.61	-3.45	1.24	5.87	5.60	74.03
341-366	0.21	-8.09	0.89	5.94	4.97	74.23

A1.1 - WINDS 20-Day Weather Outputs for RCP 8.5 (Livneh downscaling method). Results are averages of outputs for respective day ranges

Baseline						
Days	Maximum Temperature °C	Minimum Temperature °C	Precipitation mm	Wind Speed m/s	Solar Radiation MJ/m^2	Relative Humidity %
1-20	-5.77	-15.26	0.65	6.19	5.99	77.98
21-40	-5.34	-15.16	0.68	6.18	7.77	76.83
41-60	-2.18	-12.05	0.87	6.21	10.21	75.26
61-80	2.56	-7.60	1.27	6.29	12.72	73.36
81-100	8.16	-2.46	1.80	6.34	15.21	70.88
101-120	13.73	2.20	2.55	6.30	17.28	68.66
121-140	19.23	6.65	2.99	6.09	19.42	66.63
141-160	23.22	10.38	3.39	5.68	21.42	66.59
161-180	26.06	13.55	3.44	5.24	22.52	69.06
181-200	27.58	15.54	3.35	4.87	22.43	71.97
201-220	27.77	15.79	3.49	4.67	21.08	73.70
221-240	26.39	14.01	2.98	4.72	19.00	72.87
241-260	23.63	10.82	2.69	4.98	16.10	71.03
261-280	19.46	6.94	2.31	5.36	12.91	69.82
281-300	13.96	2.62	1.82	5.72	9.75	71.18
301-320	7.87	-2.12	1.46	5.97	7.19	74.03
321-340	1.98	-7.07	1.07	6.13	5.60	76.25
341-366	-3.13	-12.19	0.84	6.16	5.12	78.05

2015						
Days	Maximum Temperature °C	Minimum Temperature °C	Precipitation mm	Wind Speed m/s	Solar Radiation MJ/m^2	Relative Humidity %
1-20	-4.58	-13.49	0.67	6.19	5.95	77.38
21-40	-3.63	-12.91	0.72	6.21	7.68	75.91
41-60	-0.53	-10.09	0.89	6.22	10.10	73.68
61-80	4.06	-5.88	1.33	6.32	12.66	71.22
81-100	9.55	-1.14	1.93	6.34	15.09	69.00
101-120	15.17	3.39	2.69	6.29	17.44	67.53
121-140	20.43	7.72	3.09	5.98	19.89	66.24
141-160	24.77	11.76	3.42	5.60	21.86	65.89
161-180	27.81	15.07	3.38	5.23	23.07	66.87
181-200	29.27	17.08	3.25	4.88	22.89	68.42
201-220	29.25	17.11	3.21	4.70	21.55	69.45
221-240	28.12	15.48	2.83	4.70	19.34	69.45
241-260	25.46	12.38	2.66	4.92	16.51	68.81
261-280	21.44	8.56	2.34	5.27	13.11	68.63
281-300	15.84	4.08	1.87	5.59	9.91	69.99
301-320	9.31	-0.90	1.58	5.91	7.26	72.88
321-340	3.09	-5.90	1.18	6.10	5.65	75.99
341-366	-2.17	-10.82	0.87	6.19	5.16	77.42

2045						
Days	Maximum Temperature °C	Minimum Temperature °C	Precipitation mm	Wind Speed m/s	Solar Radiation MJ/m^2	Relative Humidity %
1-20	-2.77	-11.10	0.71	6.26	5.75	73.56
21-40	-2.15	-10.88	0.76	6.22	7.49	72.68
41-60	0.74	-8.60	1.00	6.27	9.92	71.69
61-80	5.56	-4.44	1.51	6.34	12.52	70.56
81-100	11.09	0.19	2.07	6.41	14.99	69.25
101-120	16.39	4.60	2.79	6.30	17.27	67.70
121-140	21.18	8.66	3.33	5.99	19.55	66.66
141-160	25.45	12.53	3.42	5.57	21.84	66.56
161-180	28.70	15.98	3.50	5.10	22.99	67.26
181-200	30.84	18.31	3.32	4.70	23.06	67.15
201-220	31.39	18.82	3.01	4.53	21.75	66.13
221-240	30.27	17.36	2.90	4.58	19.45	65.32
241-260	27.00	13.84	2.76	4.83	16.59	65.24
261-280	22.37	9.57	2.52	5.16	13.29	66.99
281-300	16.61	4.98	2.08	5.55	9.98	70.18
301-320	10.52	0.54	1.64	5.81	7.24	72.96
321-340	4.85	-3.94	1.26	6.03	5.54	74.49
341-366	-0.26	-8.47	0.89	6.19	4.99	74.49

2080						
Days	Maximum Temperature °C	Minimum Temperature °C	Precipitation mm	Wind Speed m/s	Solar Radiation MJ/m^2	Relative Humidity %
1-20	0.02	-7.90	0.78	6.25	5.50	70.26
21-40	0.76	-7.56	0.82	6.28	7.10	68.52
41-60	4.07	-5.05	1.11	6.32	9.42	67.21
61-80	8.70	-1.38	1.56	6.39	12.17	66.56
81-100	13.73	2.65	2.31	6.36	14.67	65.87
101-120	18.91	6.91	3.07	6.20	17.24	65.71
121-140	23.65	10.95	3.52	5.87	19.71	65.02
141-160	28.04	15.00	3.49	5.43	21.83	63.95
161-180	31.51	18.53	3.24	4.97	22.95	63.01
181-200	33.70	20.90	3.05	4.64	22.86	61.97
201-220	34.25	21.51	2.81	4.46	21.60	61.24
221-240	32.91	19.98	2.81	4.48	19.51	61.03
241-260	30.08	16.91	2.79	4.69	16.75	61.95
261-280	25.61	12.62	2.48	5.01	13.52	64.21
281-300	19.80	7.70	2.16	5.39	10.15	67.39
301-320	13.72	3.01	1.73	5.73	7.36	70.38
321-340	7.65	-1.55	1.17	5.98	5.59	72.12
341-366	2.35	-5.76	0.91	6.15	4.92	71.89

A1.2 - WINDS input files for the METDATA downscaled dataset, RCP 4.5. Values shown are increase or decrease factors predicted by the global climate models.

2015

Day Interval	1-20	21-40	41-60	61-80	81-100	101-120	121-140	141-160	161-180	181-200	201-220	221-240	241-260	261-280	281-300	301-320	321-340	341-366
Maximum Temperature*	0.003	0.004	0.006	0.007	0.008	0.005	0.004	0.003	0.004	0.005	0.004	0.005	0.007	0.004	0.005	0.005	0.005	0.006
Minimum Temperature*	0.005	0.005	0.007	0.007	0.007	0.005	0.004	0.003	0.003	0.004	0.004	0.004	0.006	0.004	0.004	0.004	0.006	0.007
Maximum rh*	-.009	-.004	-.010	-.014	-.017	-.017	-.009	0.000	-.005	-.024	-.032	-.032	-.033	-.017	-.004	-.015	-.007	-.009
Minimum rh*	-.026	-.018	-.041	-.056	-.068	-.048	-.003	0.006	-.007	-.014	-.021	-.033	-.043	-.020	-.013	-.042	-.016	-.024
Dew point*	0.000	0.000	0.000	0.000	0.000	0.000	0.000	0.000	0.000	0.000	0.000	0.000	0.000	0.000	0.000	0.000	0.000	0.000
Wind Speed*	-.004	-.012	-.010	-.004	0.011	-.007	0.006	-.019	-.013	-.010	-.002	-.004	-.004	-.001	-.016	0.017	-.023	0.012
Maximum Wind*	0.000	0.000	0.000	0.000	0.000	0.000	0.000	0.000	0.000	0.000	0.000	0.000	0.000	0.000	0.000	0.000	0.000	0.000
Wind Direction*	0.000	0.000	0.000	0.000	0.000	0.000	0.000	0.000	0.000	0.000	0.000	0.000	0.000	0.000	0.000	0.000	0.000	0.000
Atmospheric Press*	0.000	0.000	0.000	0.000	0.000	0.000	0.000	0.000	0.000	0.000	0.000	0.000	0.000	0.000	0.000	0.000	0.000	0.000
Radiation*	-.005	-.012	-.003	-.009	-.009	0.011	0.015	-.001	0.015	0.020	0.017	0.021	0.028	0.015	0.011	0.025	-.007	-.006
Daily Precipitation*	-.045	0.076	0.085	0.077	0.051	0.073	0.091	0.121	0.012	-.039	-.037	-.135	-.022	0.047	0.206	0.038	0.045	0.096

2045

Day Interval	1-20	21-40	41-60	61-80	81-100	101-120	121-140	141-160	161-180	181-200	201-220	221-240	241-260	261-280	281-300	301-320	321-340	341-366
Maximum Temperature*	0.010	0.009	0.010	0.010	0.010	0.008	0.006	0.006	0.008	0.009	0.009	0.011	0.011	0.009	0.009	0.009	0.010	0.010
Minimum Temperature*	0.014	0.012	0.013	0.011	0.009	0.008	0.007	0.006	0.007	0.008	0.008	0.009	0.010	0.009	0.008	0.007	0.010	0.013
Maximum rh*	-.020	-.019	-.035	-.030	-.019	-.033	-.008	-.008	-.015	-.032	-.047	-.051	-.045	-.019	-.016	-.007	-.007	-.018
Minimum rh*	-.039	-.036	-.087	-.101	-.079	-.069	0.005	0.002	-.012	-.033	-.055	-.071	-.068	-.032	-.038	-.040	-.042	-.048
Dew point*	0.000	0.000	0.000	0.000	0.000	0.000	0.000	0.000	0.000	0.000	0.000	0.000	0.000	0.000	0.000	0.000	0.000	0.000
Wind Speed*	-.007	-.016	-.005	-.012	-.004	-.003	-.021	-.031	-.011	-.019	-.014	-.017	-.034	-.032	-.027	-.021	-.039	-.015
Maximum Wind*	0.000	0.000	0.000	0.000	0.000	0.000	0.000	0.000	0.000	0.000	0.000	0.000	0.000	0.000	0.000	0.000	0.000	0.000
Wind Direction*	0.000	0.000	0.000	0.000	0.000	0.000	0.000	0.000	0.000	0.000	0.000	0.000	0.000	0.000	0.000	0.000	0.000	0.000
Atmospheric Press*	0.000	0.000	0.000	0.000	0.000	0.000	0.000	0.000	0.000	0.000	0.000	0.000	0.000	0.000	0.000	0.000	0.000	0.000
Radiation*	-.035	-.031	-.015	-.031	-.022	0.025	0.006	0.013	0.008	0.014	0.016	0.026	0.023	0.025	0.026	0.024	-.000	-.021
Daily Precipitation*	0.131	0.189	0.014	0.152	0.165	0.019	0.242	0.049	0.026	-.035	-.093	-.118	-.094	0.102	0.104	0.207	0.011	0.087

2080

Day Interval	1-20	21-40	41-60	61-80	81-100	101-120	121-140	141-160	161-180	181-200	201-220	221-240	241-260	261-280	281-300	301-320	321-340	341-366
Maximum Temperature*	0.013	0.013	0.013	0.013	0.014	0.010	0.009	0.010	0.010	0.012	0.012	0.012	0.013	0.012	0.013	0.012	0.013	0.014
Minimum Temperature*	0.018	0.017	0.017	0.013	0.012	0.010	0.009	0.009	0.009	0.011	0.011	0.011	0.012	0.012	0.012	0.010	0.013	0.018
Maximum rh*	-.037	-.048	-.040	-.042	-.020	-.021	-.009	-.010	-.015	-.036	-.042	-.050	-.037	-.015	-.013	-.010	-.010	-.031
Minimum rh*	-.052	-.079	-.088	-.128	-.094	-.045	0.011	-.006	-.015	-.027	-.041	-.064	-.045	-.012	-.040	-.050	-.048	-.071
Dew point*	0.000	0.000	0.000	0.000	0.000	0.000	0.000	0.000	0.000	0.000	0.000	0.000	0.000	0.000	0.000	0.000	0.000	0.000
Wind Speed*	-.024	-.031	-.015	-.036	-.023	-.014	-.041	-.042	-.046	-.015	-.031	-.024	-.040	-.049	-.034	-.017	-.044	-.014
Maximum Wind*	0.000	0.000	0.000	0.000	0.000	0.000	0.000	0.000	0.000	0.000	0.000	0.000	0.000	0.000	0.000	0.000	0.000	0.000
Wind Direction*	0.000	0.000	0.000	0.000	0.000	0.000	0.000	0.000	0.000	0.000	0.000	0.000	0.000	0.000	0.000	0.000	0.000	0.000
Atmospheric Press*	0.000	0.000	0.000	0.000	0.000	0.000	0.000	0.000	0.000	0.000	0.000	0.000	0.000	0.000	0.000	0.000	0.000	0.000
Radiation*	-.046	-.029	-.036	-.010	-.014	0.010	0.013	0.028	0.014	0.018	0.015	0.027	0.031	0.024	0.033	0.034	0.002	-.028
Daily Precipitation*	0.112	0.126	0.227	0.073	0.177	0.172	0.144	0.055	0.052	-.042	-.079	-.079	0.088	0.127	0.102	0.177	-.021	0.097

A1.2 - WINDS input files for the METDATA downscaled dataset, RCP 8.5. Values shown are increase or decrease factors predicted by the global climate models.

2015

Day Interval	1-20	21-40	41-60	61-80	81-100	101-120	121-140	141-160	161-180	181-200	201-220	221-240	241-260	261-280	281-300	301-320	321-340	341-366
Maximum Temperature*	0.004	0.005	0.008	0.004	0.005	0.004	0.004	0.005	0.006	0.005	0.006	0.004	0.006	0.005	0.007	0.004	0.004	0.005
Minimum Temperature*	0.006	0.007	0.010	0.004	0.004	0.004	0.004	0.004	0.004	0.005	0.006	0.004	0.005	0.006	0.005	0.004	0.005	0.007
Maximum rh*	0.003	-.001	-.006	-.023	-.011	-.008	0.002	-.011	-.020	-.036	-.050	-.041	-.033	-.012	-.014	-.001	-.011	-.008
Minimum rh*	-.016	-.016	-.037	-.075	-.057	-.036	0.010	-.024	-.035	-.031	-.046	-.007	-.045	-.018	-.044	-.016	-.020	-.030
Dew point*	0.000	0.000	0.000	0.000	0.000	0.000	0.000	0.000	0.000	0.000	0.000	0.000	0.000	0.000	0.000	0.000	0.000	0.000
Wind Speed*	-.006	0.032	0.002	-.006	0.002	0.025	-.005	-.007	-.011	0.007	0.005	-.003	-.006	-.004	0.002	0.000	-.001	0.008
Maximum Wind*	0.000	0.000	0.000	0.000	0.000	0.000	0.000	0.000	0.000	0.000	0.000	0.000	0.000	0.000	0.000	0.000	0.000	0.000
Wind Direction*	0.000	0.000	0.000	0.000	0.000	0.000	0.000	0.000	0.000	0.000	0.000	0.000	0.000	0.000	0.000	0.000	0.000	0.000
Atmospheric Press*	0.000	0.000	0.000	0.000	0.000	0.000	0.000	0.000	0.000	0.000	0.000	0.000	0.000	0.000	0.000	0.000	0.000	0.000
Radiation*	-.004	-.013	-.025	0.003	0.002	0.001	0.015	0.029	0.019	0.008	0.017	0.002	0.035	0.007	0.022	0.002	0.008	0.008
Daily Precipitation*	-.045	-.007	0.214	0.014	0.044	0.165	0.056	0.019	0.013	-.099	-.097	0.020	-.125	0.005	0.096	0.150	0.053	0.083

2045

Day Interval	1-20	21-40	41-60	61-80	81-100	101-120	121-140	141-160	161-180	181-200	201-220	221-240	241-260	261-280	281-300	301-320	321-340	341-366
Maximum Temperature*	0.012	0.011	0.011	0.011	0.010	0.009	0.007	0.007	0.009	0.011	0.012	0.012	0.013	0.009	0.010	0.009	0.011	0.012
Minimum Temperature*	0.017	0.015	0.013	0.011	0.009	0.009	0.008	0.007	0.008	0.010	0.011	0.011	0.011	0.009	0.010	0.009	0.012	0.016
Maximum rh*	-.023	-.024	-.028	-.034	-.013	-.014	-.003	-.002	-.019	-.038	-.056	-.053	-.051	-.017	-.009	0.000	-.008	-.022
Minimum rh*	-.048	-.045	-.084	-.101	-.067	-.022	0.031	-.003	-.035	-.045	-.062	-.059	-.077	-.032	-.025	-.013	-.040	-.050
Dew point*	0.000	0.000	0.000	0.000	0.000	0.000	0.000	0.000	0.000	0.000	0.000	0.000	0.000	0.000	0.000	0.000	0.000	0.000
Wind Speed*	0.011	0.010	0.005	0.013	0.002	0.004	0.008	-.021	-.018	-.011	-.008	-.003	-.015	-.020	-.017	-.010	-.012	0.011
Maximum Wind*	0.000	0.000	0.000	0.000	0.000	0.000	0.000	0.000	0.000	0.000	0.000	0.000	0.000	0.000	0.000	0.000	0.000	0.000
Wind Direction*	0.000	0.000	0.000	0.000	0.000	0.000	0.000	0.000	0.000	0.000	0.000	0.000	0.000	0.000	0.000	0.000	0.000	0.000
Atmospheric Press*	0.000	0.000	0.000	0.000	0.000	0.000	0.000	0.000	0.000	0.000	0.000	0.000	0.000	0.000	0.000	0.000	0.000	0.000
Radiation*	-.039	-.035	-.025	-.017	-.014	-.002	-.000	0.016	0.031	0.017	0.019	0.027	0.039	0.029	0.013	0.008	-.001	-.020
Daily Precipitation*	0.127	0.175	0.119	0.215	0.142	0.155	0.176	0.053	0.000	-.076	-.160	-.090	-.003	0.116	0.137	0.285	0.057	0.068

2080

Day Interval	1-20	21-40	41-60	61-80	81-100	101-120	121-140	141-160	161-180	181-200	201-220	221-240	241-260	261-280	281-300	301-320	321-340	341-366
Maximum Temperature*	0.022	0.022	0.024	0.022	0.019	0.017	0.016	0.016	0.018	0.021	0.022	0.022	0.023	0.021	0.021	0.019	0.020	0.023
Minimum Temperature*	0.030	0.029	0.029	0.022	0.018	0.017	0.016	0.015	0.016	0.019	0.021	0.020	0.021	0.021	0.020	0.017	0.020	0.027
Maximum rh*	-.062	-.075	-.070	-.057	-.034	-.033	-.020	-.018	-.046	-.067	-.089	-.080	-.068	-.041	-.035	-.021	-.015	-.041
Minimum rh*	-.113	-.121	-.153	-.161	-.109	-.042	-.004	-.029	-.073	-.082	-.115	-.117	-.108	-.067	-.069	-.078	-.075	-.105
Dew point*	0.000	0.000	0.000	0.000	0.000	0.000	0.000	0.000	0.000	0.000	0.000	0.000	0.000	0.000	0.000	0.000	0.000	0.000
Wind Speed*	0.009	0.012	0.015	-.006	0.015	0.001	-.005	-.041	-.033	-.020	-.021	-.040	-.028	-.042	-.031	-.007	-.028	0.005
Maximum Wind*	0.000	0.000	0.000	0.000	0.000	0.000	0.000	0.000	0.000	0.000	0.000	0.000	0.000	0.000	0.000	0.000	0.000	0.000
Wind Direction*	0.000	0.000	0.000	0.000	0.000	0.000	0.000	0.000	0.000	0.000	0.000	0.000	0.000	0.000	0.000	0.000	0.000	0.000
Atmospheric Press*	0.000	0.000	0.000	0.000	0.000	0.000	0.000	0.000	0.000	0.000	0.000	0.000	0.000	0.000	0.000	0.000	0.000	0.000
Radiation*	-.060	-.068	-.076	-.049	-.018	-.003	0.018	0.035	0.031	0.017	0.025	0.034	0.047	0.036	0.043	0.034	-.002	-.039
Daily Precipitation*	0.087	0.143	0.366	0.310	0.210	0.262	0.252	0.135	-.069	-.101	-.191	-.118	0.026	0.174	0.154	0.182	0.038	0.167

A1.2 - WINDS input files for the Livneh downscaled dataset, RCP 4.5. Values shown are increase or decrease factors predicted by the global climate models.

2015

Day Interval	1-20	21-40	41-60	61-80	81-100	101-120	121-140	141-160	161-180	181-200	201-220	221-240	241-260	261-280	281-300	301-320	321-340	341-366
Maximum Temperature*	0.002	0.003	0.006	0.007	0.008	0.005	0.004	0.003	0.004	0.005	0.005	0.005	0.007	0.004	0.005	0.005	0.005	0.006
Minimum Temperature*	0.004	0.006	0.007	0.008	0.007	0.005	0.004	0.003	0.003	0.004	0.004	0.004	0.006	0.004	0.004	0.004	0.006	0.007
Maximum rh*	-.027	-.021	-.034	-.042	-.033	-.018	-.011	0.000	-.010	-.033	-.047	-.053	-.058	-.019	-.005	-.035	-.011	-.016
Minimum rh*	-.027	-.021	-.034	-.042	-.033	-.018	-.011	0.000	-.010	-.033	-.047	-.053	-.058	-.019	-.005	-.035	-.011	-.016
Dew point*	0.000	0.000	0.000	0.000	0.000	0.000	0.000	0.000	0.000	0.000	0.000	0.000	0.000	0.000	0.000	0.000	0.000	0.000
Wind Speed*	-.009	-.011	-.008	-.007	0.000	-.019	-.003	-.022	-.037	-.013	-.020	-.030	-.015	-.007	-.030	0.015	-.036	0.010
Maximum Wind*	0.000	0.000	0.000	0.000	0.000	0.000	0.000	0.000	0.000	0.000	0.000	0.000	0.000	0.000	0.000	0.000	0.000	0.000
Wind Direction*	0.000	0.000	0.000	0.000	0.000	0.000	0.000	0.000	0.000	0.000	0.000	0.000	0.000	0.000	0.000	0.000	0.000	0.000
Atmospheric Press*	0.000	0.000	0.000	0.000	0.000	0.000	0.000	0.000	0.000	0.000	0.000	0.000	0.000	0.000	0.000	0.000	0.000	0.000
Radiation*	-.007	-.015	-.003	-.008	-.006	0.011	0.017	0.007	0.019	0.020	0.022	0.023	0.027	0.016	0.012	0.027	-.007	-.008
Daily Precipitation*	-.051	0.041	0.075	0.018	0.075	0.072	0.058	0.096	-.009	-.016	-.050	-.124	-.014	0.039	0.108	0.007	0.074	0.083

2045

Day Interval	1-20	21-40	41-60	61-80	81-100	101-120	121-140	141-160	161-180	181-200	201-220	221-240	241-260	261-280	281-300	301-320	321-340	341-366
Maximum Temperature*	0.010	0.009	0.010	0.010	0.011	0.009	0.007	0.006	0.008	0.010	0.009	0.011	0.011	0.009	0.009	0.009	0.010	0.010
Minimum Temperature*	0.014	0.012	0.013	0.011	0.009	0.008	0.007	0.006	0.007	0.008	0.008	0.009	0.010	0.009	0.008	0.007	0.010	0.013
Maximum rh*	-.035	-.040	-.060	-.058	-.041	-.049	-.013	-.011	-.031	-.066	-.089	-.104	-.094	-.036	-.028	-.021	-.022	-.046
Minimum rh*	-.035	-.040	-.060	-.058	-.041	-.049	-.013	-.011	-.031	-.066	-.089	-.104	-.094	-.036	-.028	-.021	-.022	-.046
Dew point*	0.000	0.000	0.000	0.000	0.000	0.000	0.000	0.000	0.000	0.000	0.000	0.000	0.000	0.000	0.000	0.000	0.000	0.000
Wind Speed*	-.007	-.016	-.015	-.009	-.013	-.024	-.030	-.059	-.030	-.031	-.024	-.044	-.049	-.046	-.053	-.031	-.051	-.019
Maximum Wind*	0.000	0.000	0.000	0.000	0.000	0.000	0.000	0.000	0.000	0.000	0.000	0.000	0.000	0.000	0.000	0.000	0.000	0.000
Wind Direction*	0.000	0.000	0.000	0.000	0.000	0.000	0.000	0.000	0.000	0.000	0.000	0.000	0.000	0.000	0.000	0.000	0.000	0.000
Atmospheric Press*	0.000	0.000	0.000	0.000	0.000	0.000	0.000	0.000	0.000	0.000	0.000	0.000	0.000	0.000	0.000	0.000	0.000	0.000
Radiation*	-.043	-.039	-.018	-.032	-.019	0.018	0.007	0.010	0.012	0.017	0.022	0.026	0.023	0.022	0.027	0.024	-.003	-.026
Daily Precipitation*	0.105	0.154	0.061	0.136	0.133	0.046	0.181	0.064	0.010	-.061	-.077	-.138	-.082	0.119	0.060	0.184	0.082	0.091

2080

Day Interval	1-20	21-40	41-60	61-80	81-100	101-120	121-140	141-160	161-180	181-200	201-220	221-240	241-260	261-280	281-300	301-320	321-340	341-366
Maximum Temperature*	0.013	0.013	0.013	0.013	0.014	0.010	0.009	0.010	0.010	0.012	0.012	0.012	0.013	0.012	0.013	0.012	0.013	0.014
Minimum Temperature*	0.018	0.017	0.017	0.013	0.012	0.010	0.009	0.009	0.009	0.011	0.011	0.011	0.012	0.012	0.012	0.010	0.013	0.018
Maximum rh*	-.070	-.072	-.064	-.082	-.043	-.023	-.002	-.022	-.039	-.069	-.078	-.097	-.076	-.023	-.028	-.025	-.025	-.055
Minimum rh*	-.070	-.072	-.064	-.082	-.043	-.023	-.002	-.022	-.039	-.069	-.078	-.097	-.076	-.023	-.028	-.025	-.025	-.055
Dew point*	0.000	0.000	0.000	0.000	0.000	0.000	0.000	0.000	0.000	0.000	0.000	0.000	0.000	0.000	0.000	0.000	0.000	0.000
Wind Speed*	-.036	-.037	-.025	-.031	-.040	-.027	-.057	-.068	-.059	-.037	-.050	-.050	-.069	-.073	-.062	-.031	-.066	-.024
Maximum Wind*	0.000	0.000	0.000	0.000	0.000	0.000	0.000	0.000	0.000	0.000	0.000	0.000	0.000	0.000	0.000	0.000	0.000	0.000
Wind Direction*	0.000	0.000	0.000	0.000	0.000	0.000	0.000	0.000	0.000	0.000	0.000	0.000	0.000	0.000	0.000	0.000	0.000	0.000
Atmospheric Press*	0.000	0.000	0.000	0.000	0.000	0.000	0.000	0.000	0.000	0.000	0.000	0.000	0.000	0.000	0.000	0.000	0.000	0.000
Radiation*	-.056	-.033	-.041	-.010	-.013	0.008	0.013	0.023	0.017	0.017	0.015	0.025	0.029	0.021	0.033	0.035	0.001	-.036
Daily Precipitation*	0.080	0.146	0.240	0.064	0.174	0.167	0.138	0.049	0.032	-.049	-.067	-.098	0.059	0.142	0.085	0.192	-.020	0.074

A1.2 - WINDS input files for the Livneh downscaled dataset, RCP 8.5. Values shown are increase or decrease factors predicted by the global climate models.

2015

Day Interval	1-20	21-40	41-60	61-80	81-100	101-120	121-140	141-160	161-180	181-200	201-220	221-240	241-260	261-280	281-300	301-320	321-340	341-366
Maximum Temperature*	0.004	0.005	0.008	0.004	0.005	0.004	0.004	0.005	0.005	0.005	0.007	0.004	0.006	0.006	0.007	0.005	0.004	0.005
Minimum Temperature*	0.006	0.007	0.010	0.005	0.004	0.004	0.004	0.004	0.005	0.005	0.006	0.004	0.005	0.006	0.005	0.004	0.005	0.007
Maximum rh*	-.003	-.012	-.015	-.047	-.020	-.013	0.002	-.021	-.040	-.047	-.074	-.034	-.055	-.008	-.018	0.000	-.011	-.014
Minimum rh*	-.003	-.012	-.015	-.047	-.020	-.013	0.002	-.021	-.040	-.047	-.074	-.034	-.055	-.008	-.018	0.000	-.011	-.014
Dew point*	0.000	0.000	0.000	0.000	0.000	0.000	0.000	0.000	0.000	0.000	0.000	0.000	0.000	0.000	0.000	0.000	0.000	0.000
Wind Speed*	-.015	0.020	-.004	0.009	-.019	0.018	-.010	-.016	-.008	0.007	0.013	-.007	-.016	-.021	-.011	-.005	-.002	0.006
Maximum Wind*	0.000	0.000	0.000	0.000	0.000	0.000	0.000	0.000	0.000	0.000	0.000	0.000	0.000	0.000	0.000	0.000	0.000	0.000
Wind Direction*	0.000	0.000	0.000	0.000	0.000	0.000	0.000	0.000	0.000	0.000	0.000	0.000	0.000	0.000	0.000	0.000	0.000	0.000
Atmospheric Press*	0.000	0.000	0.000	0.000	0.000	0.000	0.000	0.000	0.000	0.000	0.000	0.000	0.000	0.000	0.000	0.000	0.000	0.000
Radiation*	-.004	-.015	-.028	0.004	0.004	0.003	0.018	0.030	0.027	0.024	0.022	0.005	0.040	0.007	0.024	0.002	0.010	0.011
Daily Precipitation*	-.058	0.062	0.183	0.019	0.041	0.141	0.037	0.012	0.016	-.101	-.073	-.031	-.131	0.050	0.021	0.156	0.040	0.050

2045

Day Interval	1-20	21-40	41-60	61-80	81-100	101-120	121-140	141-160	161-180	181-200	201-220	221-240	241-260	261-280	281-300	301-320	321-340	341-366
Maximum Temperature*	0.012	0.010	0.010	0.011	0.010	0.009	0.007	0.007	0.009	0.011	0.012	0.012	0.013	0.009	0.010	0.009	0.011	0.012
Minimum Temperature*	0.017	0.015	0.013	0.011	0.009	0.009	0.008	0.007	0.008	0.010	0.011	0.011	0.011	0.009	0.010	0.009	0.012	0.016
Maximum rh*	-.065	-.053	-.051	-.055	-.022	-.014	0.009	-.007	-.036	-.067	-.111	-.097	-.100	-.024	-.011	-.001	-.019	-.048
Minimum rh*	-.065	-.053	-.051	-.055	-.022	-.014	0.009	-.007	-.036	-.067	-.111	-.097	-.100	-.024	-.011	-.001	-.019	-.048
Dew point*	0.000	0.000	0.000	0.000	0.000	0.000	0.000	0.000	0.000	0.000	0.000	0.000	0.000	0.000	0.000	0.000	0.000	0.000
Wind Speed*	0.006	0.011	0.006	0.019	-.002	-.000	0.012	-.034	-.030	-.029	-.027	-.025	-.034	-.031	-.032	-.017	-.023	0.016
Maximum Wind*	0.000	0.000	0.000	0.000	0.000	0.000	0.000	0.000	0.000	0.000	0.000	0.000	0.000	0.000	0.000	0.000	0.000	0.000
Wind Direction*	0.000	0.000	0.000	0.000	0.000	0.000	0.000	0.000	0.000	0.000	0.000	0.000	0.000	0.000	0.000	0.000	0.000	0.000
Atmospheric Press*	0.000	0.000	0.000	0.000	0.000	0.000	0.000	0.000	0.000	0.000	0.000	0.000	0.000	0.000	0.000	0.000	0.000	0.000
Radiation*	-.050	-.040	-.029	-.016	-.014	-.002	0.005	0.020	0.034	0.026	0.024	0.029	0.043	0.026	0.016	0.008	-.003	-.024
Daily Precipitation*	0.065	0.154	0.158	0.220	0.129	0.184	0.152	0.041	-.003	-.073	-.126	-.090	-.012	0.112	0.083	0.285	0.029	0.063

2080

Day Interval	1-20	21-40	41-60	61-80	81-100	101-120	121-140	141-160	161-180	181-200	201-220	221-240	241-260	261-280	281-300	301-320	321-340	341-366
Maximum Temperature*	0.022	0.022	0.024	0.022	0.019	0.016	0.016	0.016	0.018	0.020	0.022	0.021	0.022	0.021	0.021	0.020	0.020	0.023
Minimum Temperature*	0.030	0.029	0.029	0.021	0.018	0.017	0.016	0.015	0.017	0.019	0.021	0.020	0.021	0.021	0.020	0.017	0.020	0.027
Maximum rh*	-.111	-.106	-.112	-.100	-.055	-.037	-.024	-.043	-.094	-.136	-.184	-.164	-.142	-.068	-.056	-.045	-.048	-.083
Minimum rh*	-.111	-.106	-.112	-.100	-.055	-.037	-.024	-.043	-.094	-.136	-.184	-.164	-.142	-.068	-.056	-.045	-.048	-.083
Dew point*	0.000	0.000	0.000	0.000	0.000	0.000	0.000	0.000	0.000	0.000	0.000	0.000	0.000	0.000	0.000	0.000	0.000	0.000
Wind Speed*	0.011	0.019	0.017	0.007	0.007	-.005	-.023	-.071	-.053	-.025	-.039	-.065	-.051	-.063	-.056	-.025	-.044	0.006
Maximum Wind*	0.000	0.000	0.000	0.000	0.000	0.000	0.000	0.000	0.000	0.000	0.000	0.000	0.000	0.000	0.000	0.000	0.000	0.000
Wind Direction*	0.000	0.000	0.000	0.000	0.000	0.000	0.000	0.000	0.000	0.000	0.000	0.000	0.000	0.000	0.000	0.000	0.000	0.000
Atmospheric Press*	0.000	0.000	0.000	0.000	0.000	0.000	0.000	0.000	0.000	0.000	0.000	0.000	0.000	0.000	0.000	0.000	0.000	0.000
Radiation*	-.076	-.081	-.085	-.050	-.020	-.004	0.017	0.027	0.026	0.014	0.021	0.029	0.044	0.031	0.043	0.035	-.004	-.051
Daily Precipitation*	0.099	0.151	0.346	0.307	0.238	0.270	0.202	0.133	-.070	-.112	-.186	-.129	0.030	0.158	0.129	0.167	0.060	0.151

A2.1 - Mean surface flow (mm) for different scenario lengths (1 Run, 2 Runs, 3 Runs, 4 Runs, 5 Runs, and 10 Runs) and 95% (left column) and 99% (right column)confidence intervals.

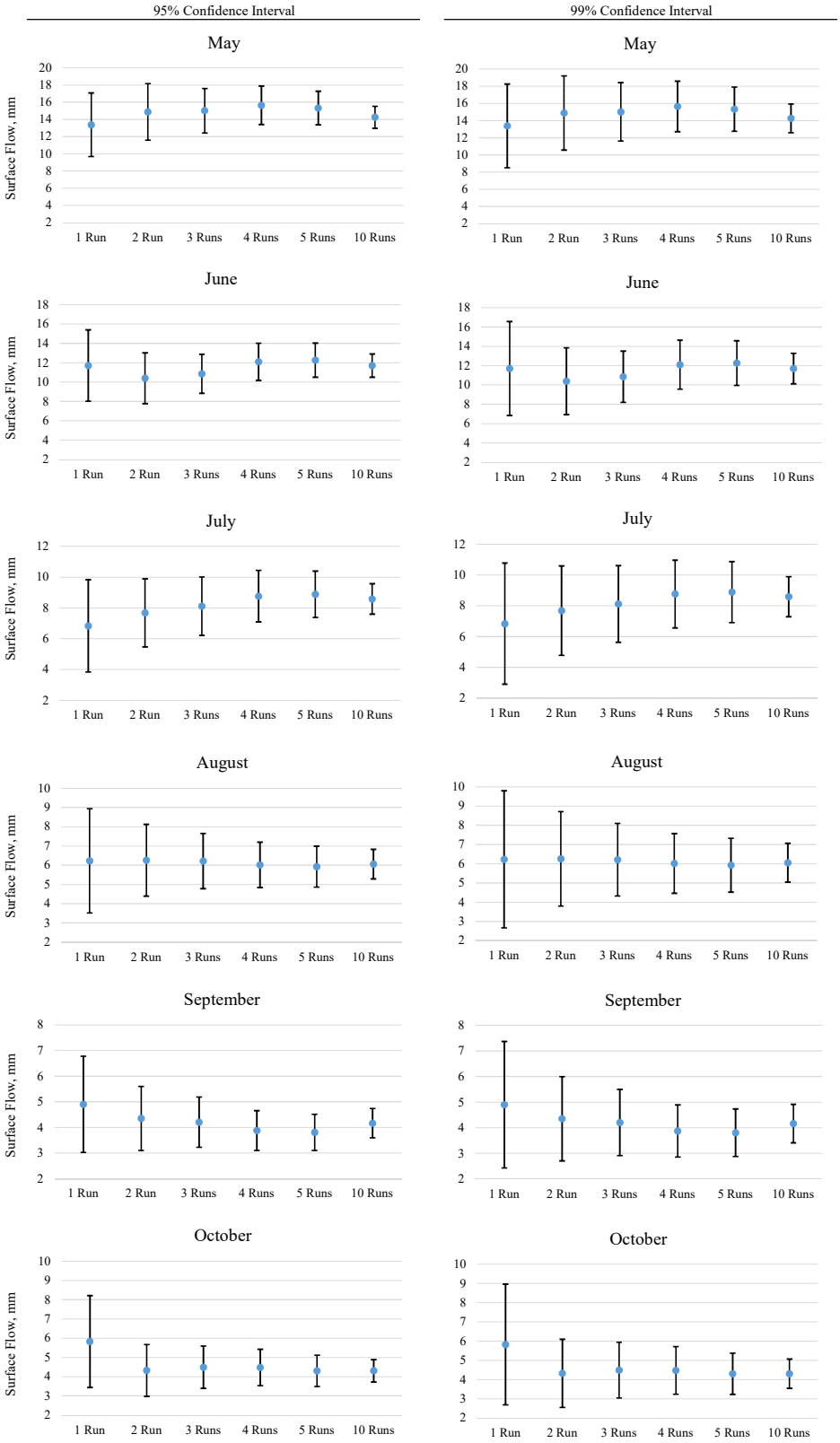

A2.2 - Monthly mean nitrate export (line chart, left horizontal axis) and monthly mean watershed outflow (bar chart, right horizontal axis). Data show for RCP 4.5.

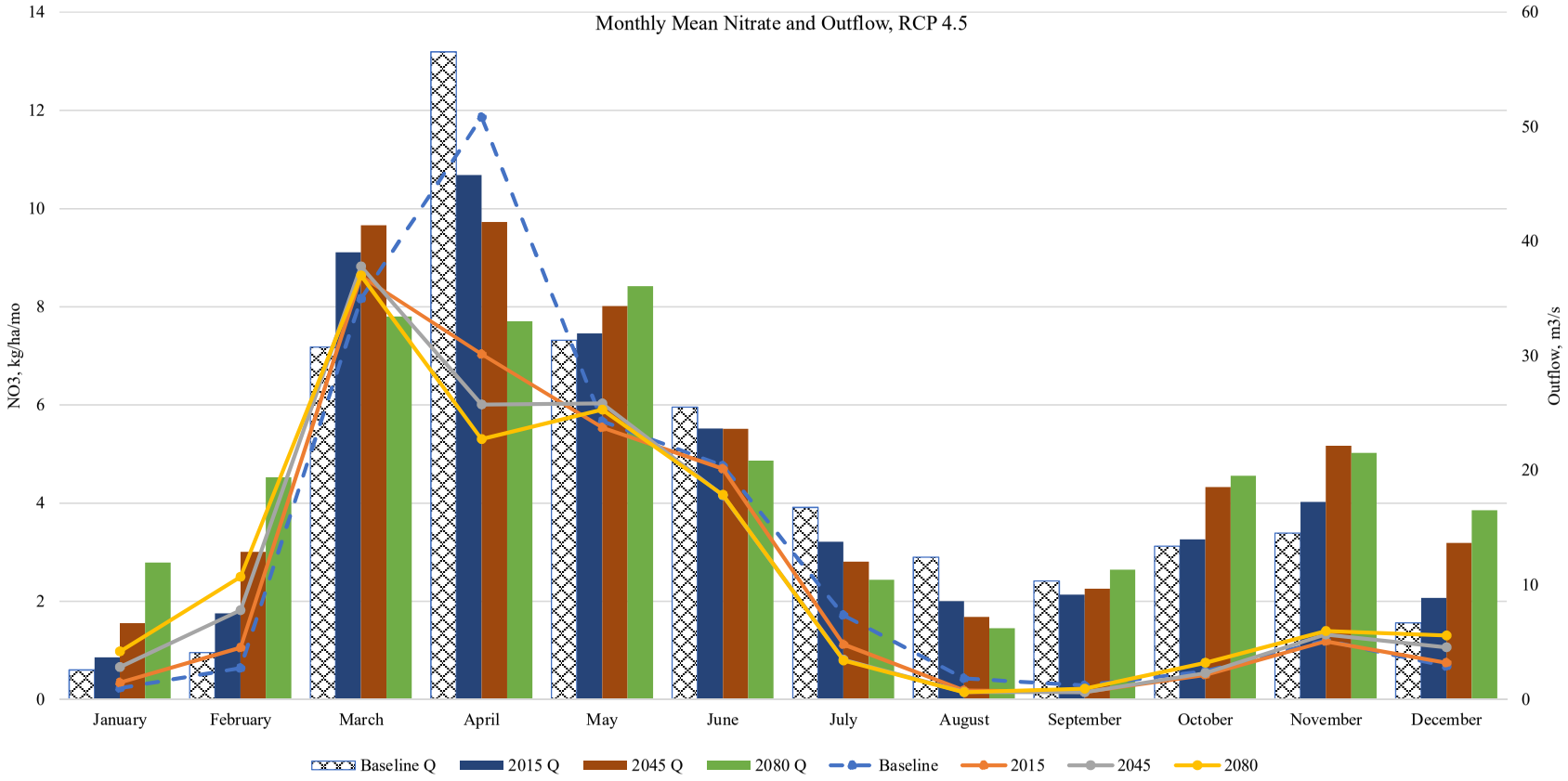

A2.2 - Monthly mean nitrate export (line chart, left horizontal axis) and monthly mean watershed outflow (bar chart, right horizontal axis). Data show for RCP 8.5.

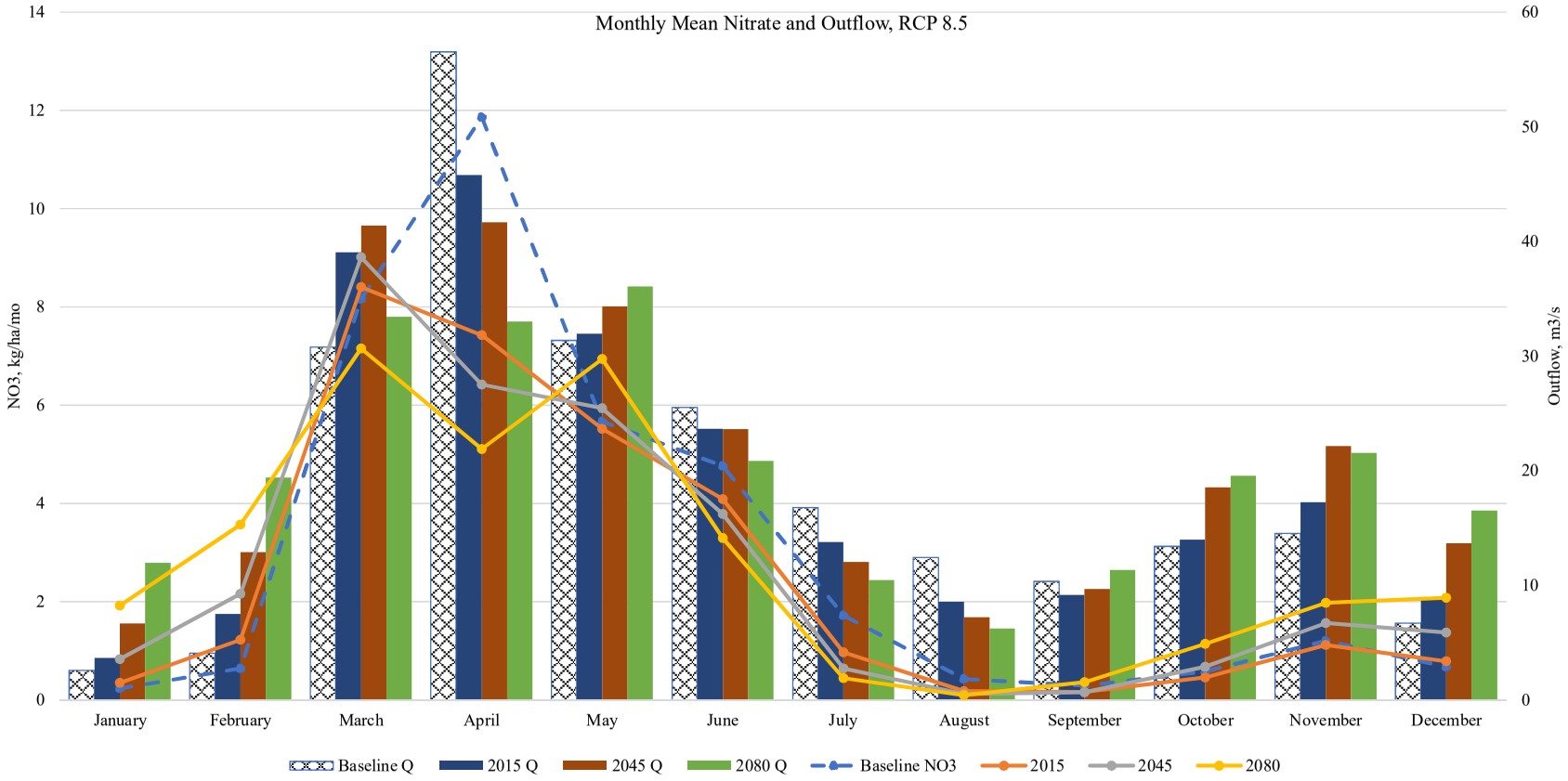

A2.3 - Monthly mean nitrogen export (kg/ha) for RCP 4.5 and RCP 8.5 for Fields 1108, 1109, 1111, and 1112.

RCP 4.5

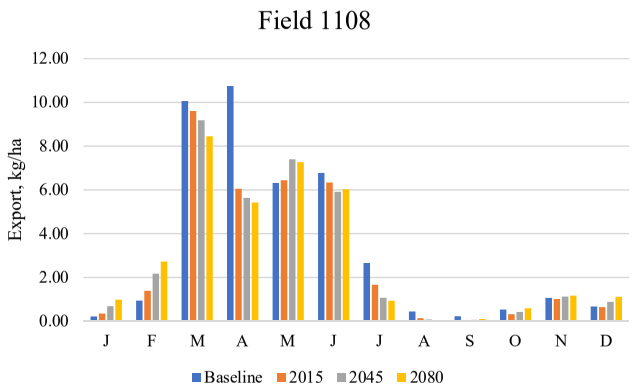

RCP 8.5

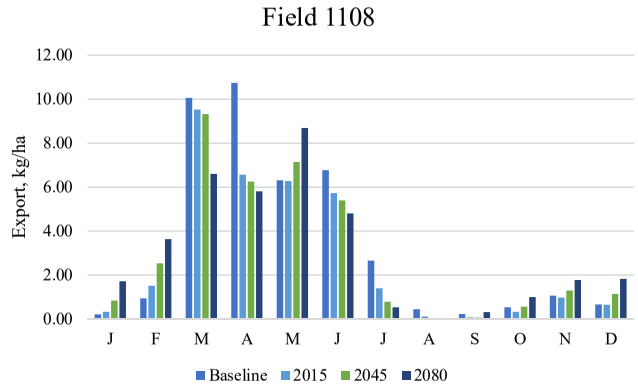

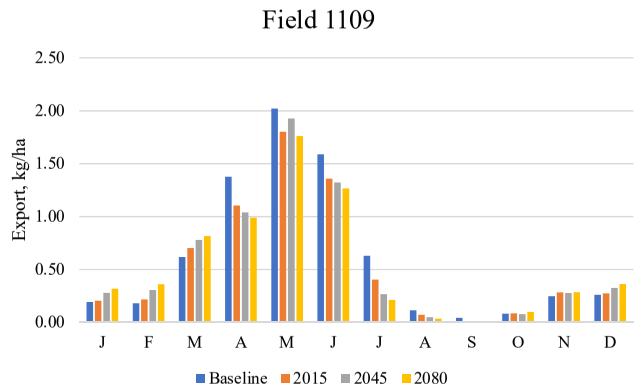

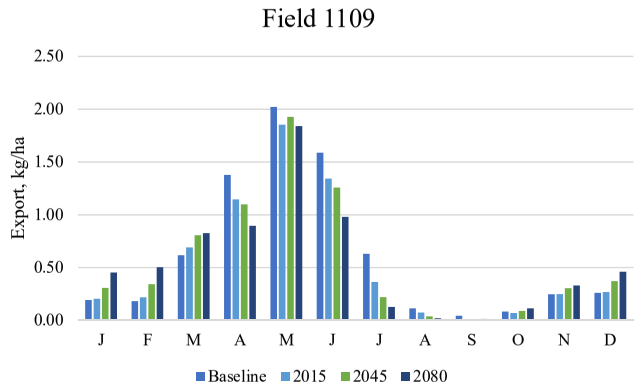

A2.3- Monthly mean nitrogen export (kg/ha) for RCP 4.5 and RCP 8.5 for Fields 1108, 1109, 1111, and 1112, continued.

RCP 4.5

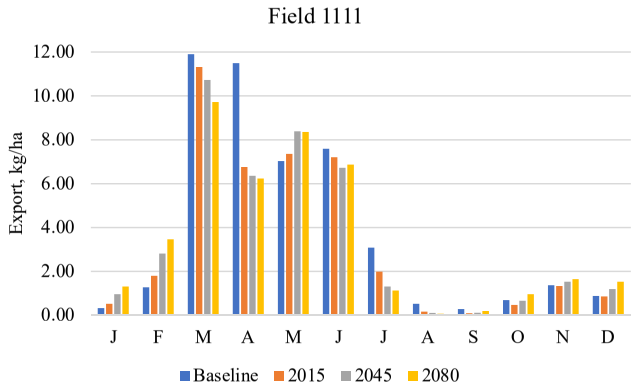

RCP 8.5

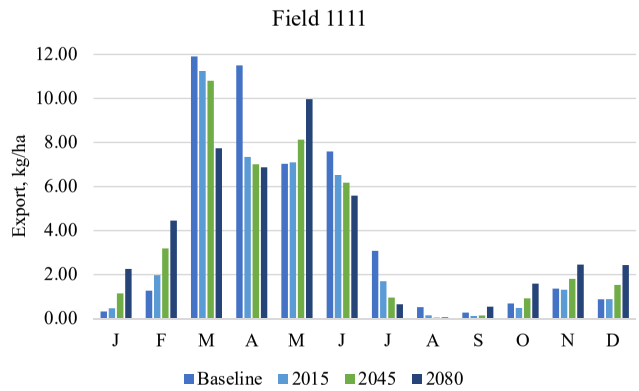

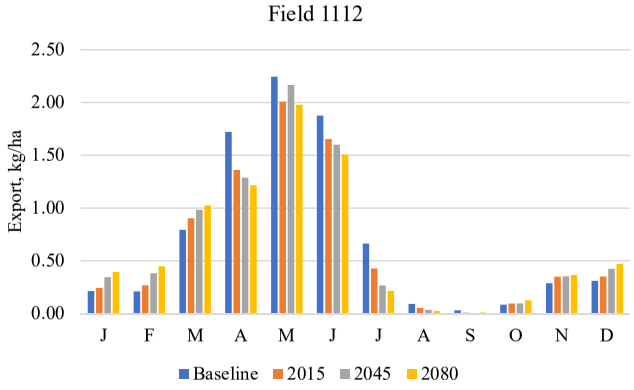

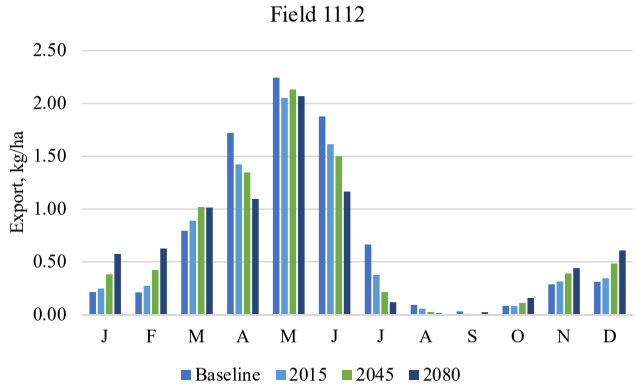

A2.4- Box and whisker plots of 1000-years of SWAT output for annual nitrogen export (kg/ha) for RCP 4.5 and RCP 8.5 for Fields 1108, 1109, 1111, and 1112.

RCP 4.5

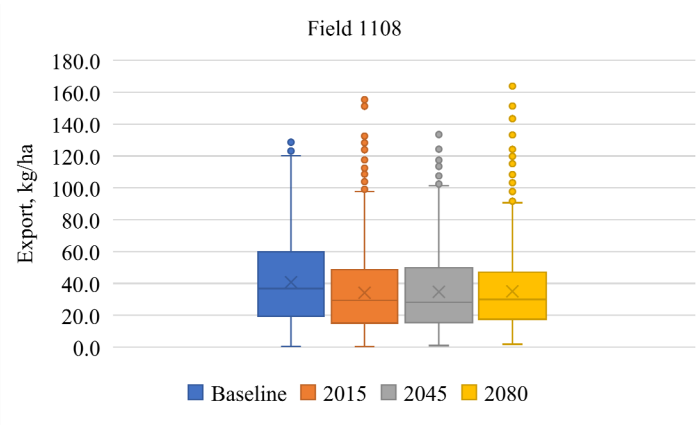

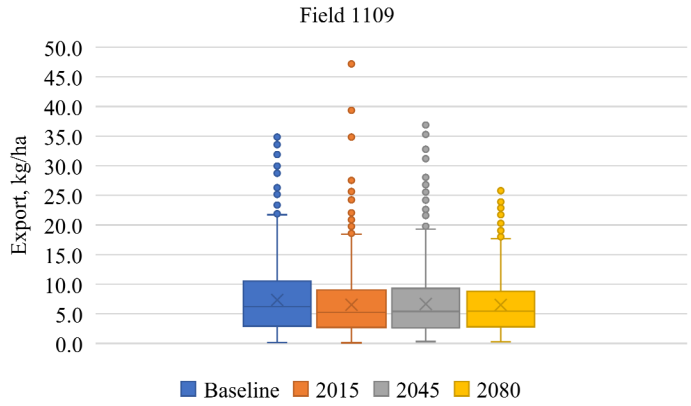

RCP 8.5

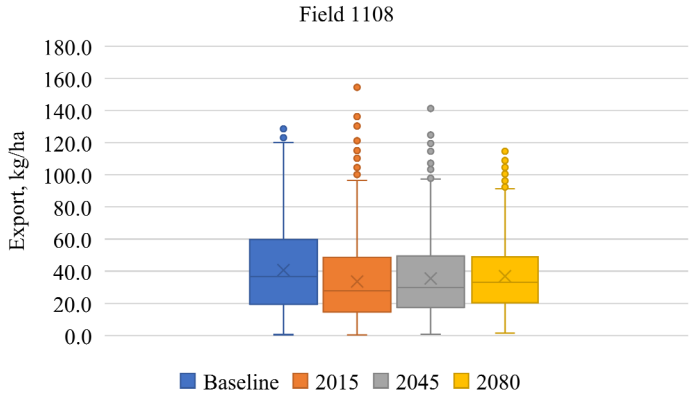

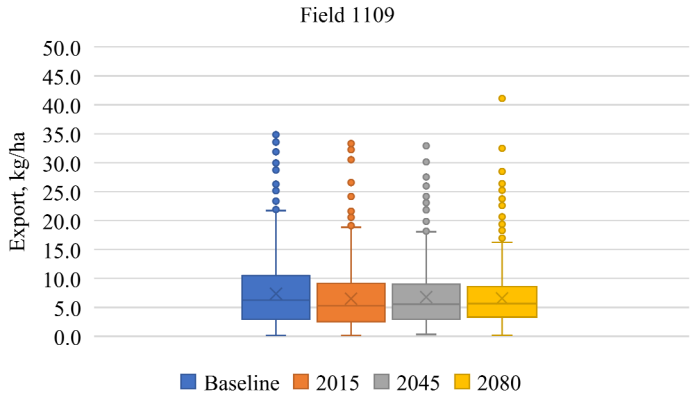

A2.4 - Box and whisker plots of 1000-years of SWAT output for annual nitrogen export (kg/ha) for RCP 4.5 and RCP 8.5 for Fields 1108, 1109, 1111, and 1112.

RCP 4.5

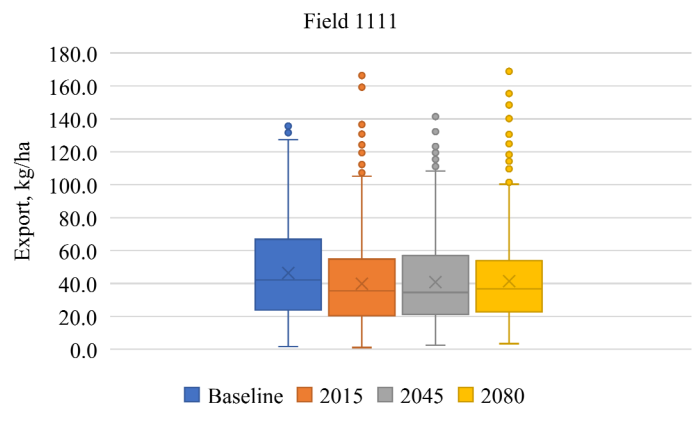

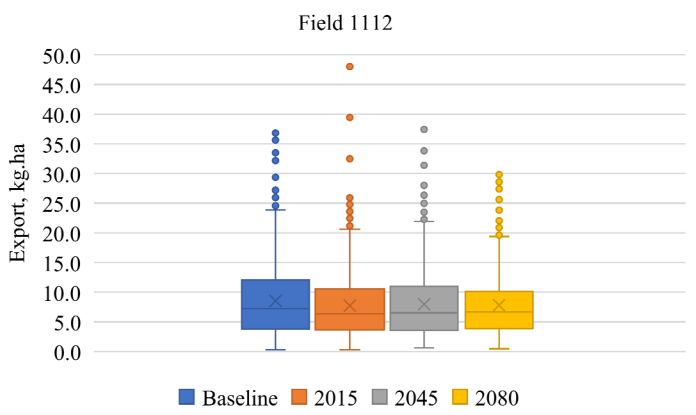

RCP 8.5

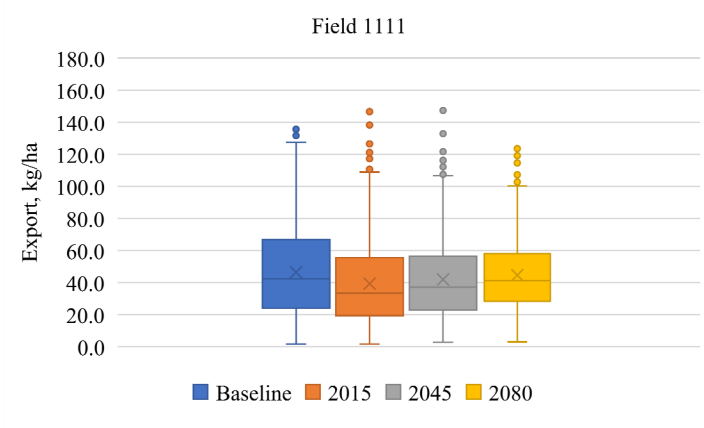

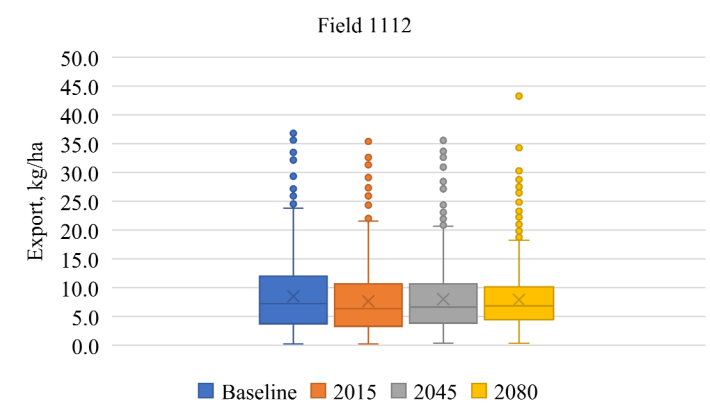

A2.5 - Monthly mean tile flow (left axis, mm) and nitrate export (right axis, kg/ha) for RCP 4.5 (left column) and RCP 8.5 (right column) for Fields 1108 and 1111.

RCP 4.5

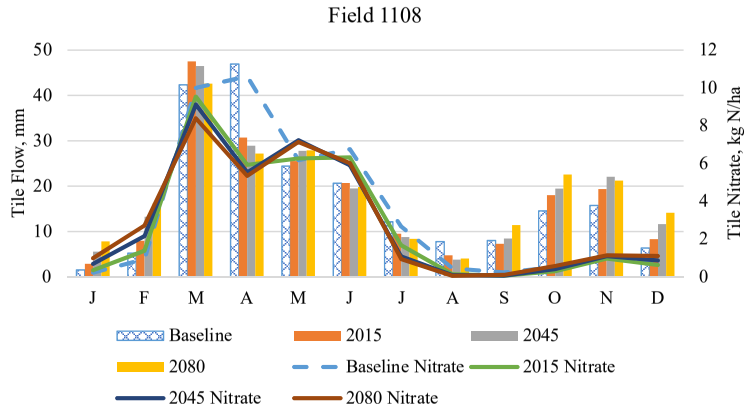

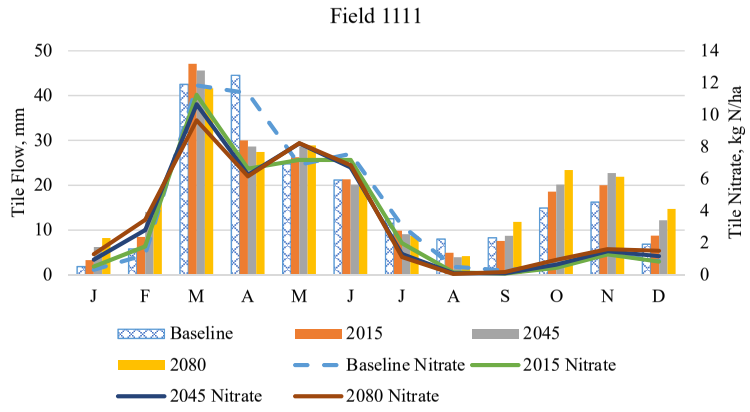

RCP 8.5

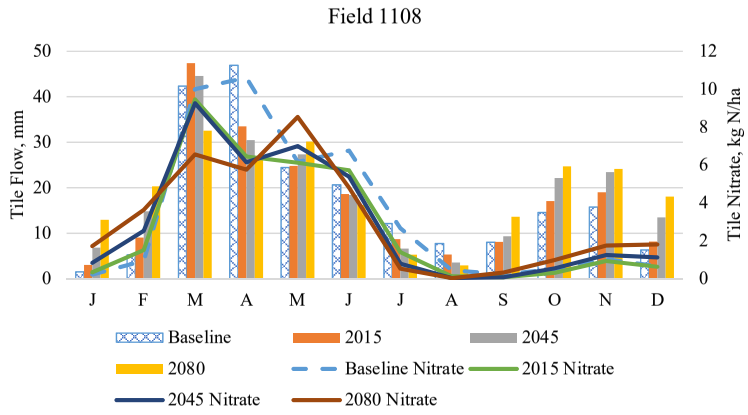

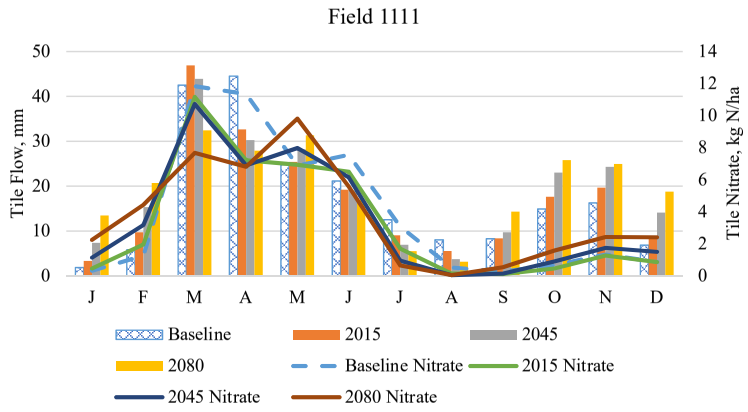

A2.6 - Monthly mean phosphorus export (kg/ha) for RCP 4.5 and RCP 8.5 for Fields 1108, 1109, 1111, and 1112.

RCP 4.5

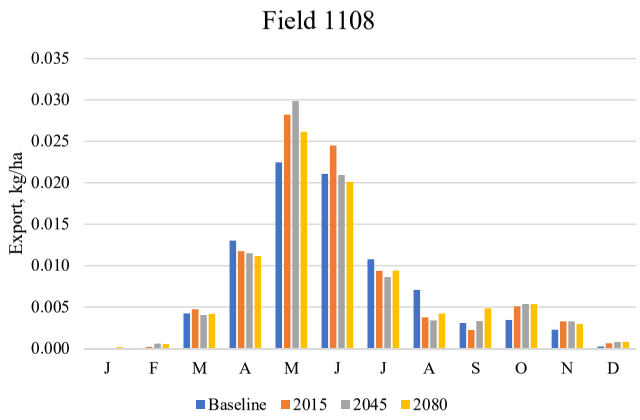

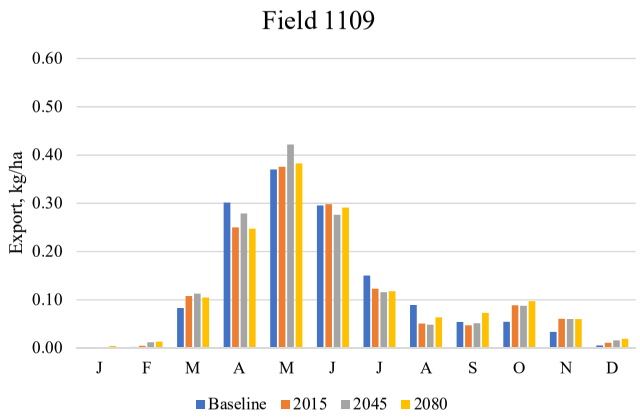

RCP 8.5

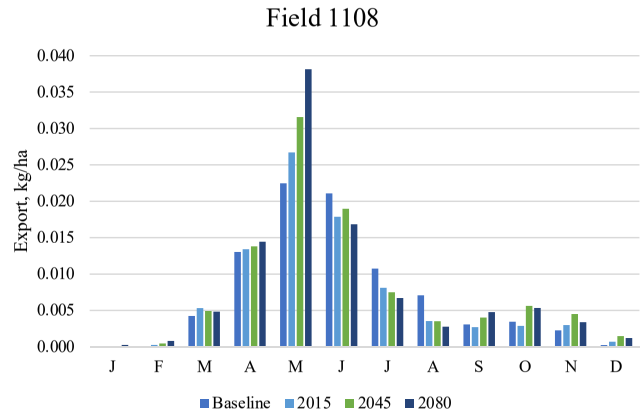

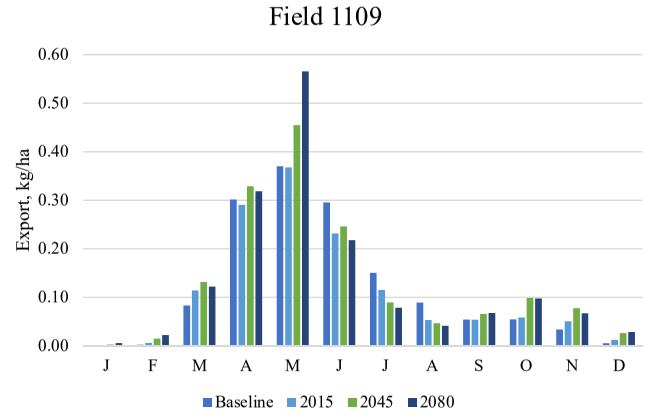

A2.6 - Monthly mean phosphorus export (kg/ha) for RCP 4.5 and RCP 8.5 for Fields 1108, 1109, 1111, and 1112, continued.

RCP 4.5

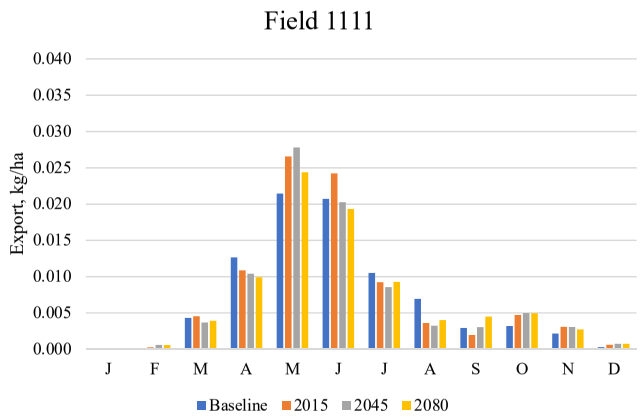

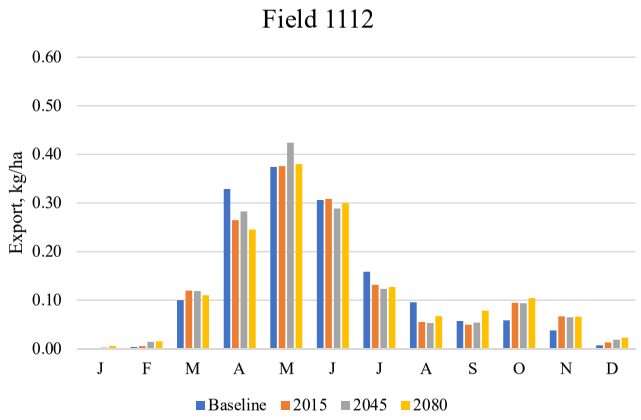

RCP 8.5

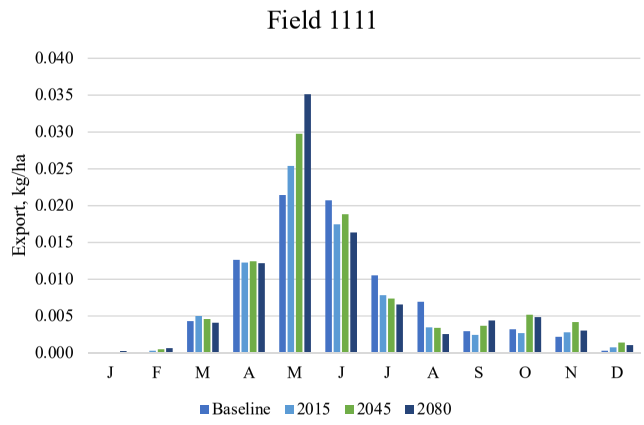

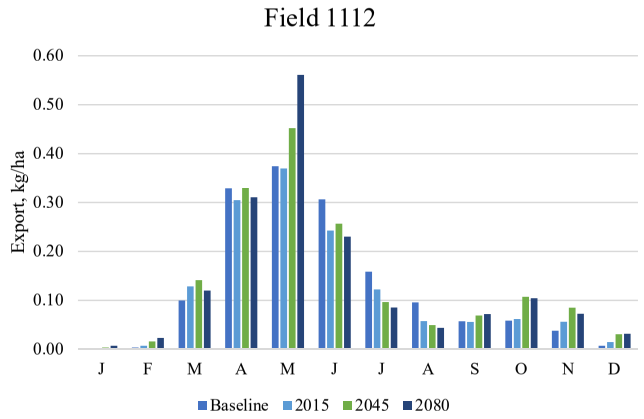

A2.7 - Box and whisker plots of 1000-years of SWAT output for annual phosphorus export (kg/ha) for RCP 4.5 and RCP 8.5 for Fields 1108, 1109, 1111, and 1112.

RCP 4.5

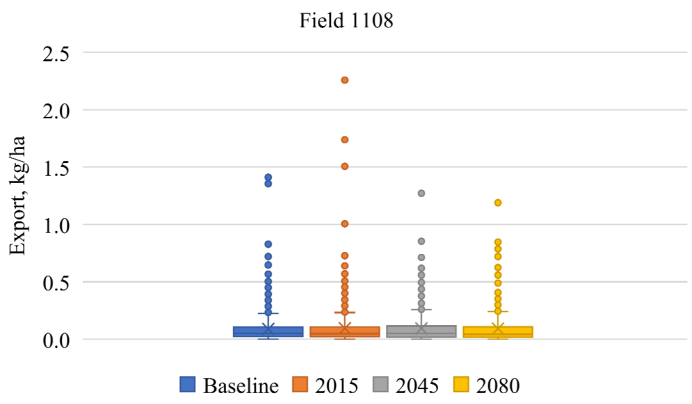

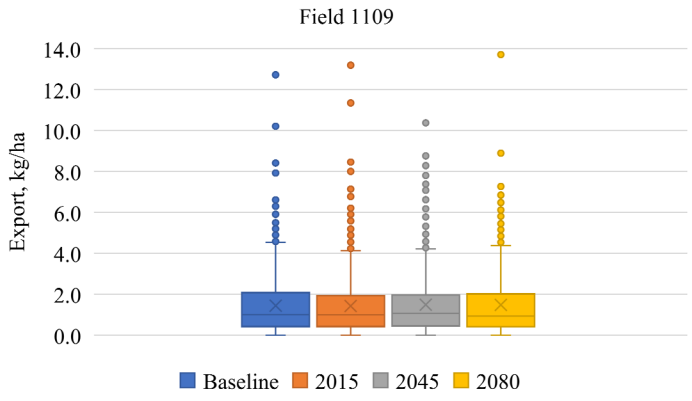

RCP 8.5

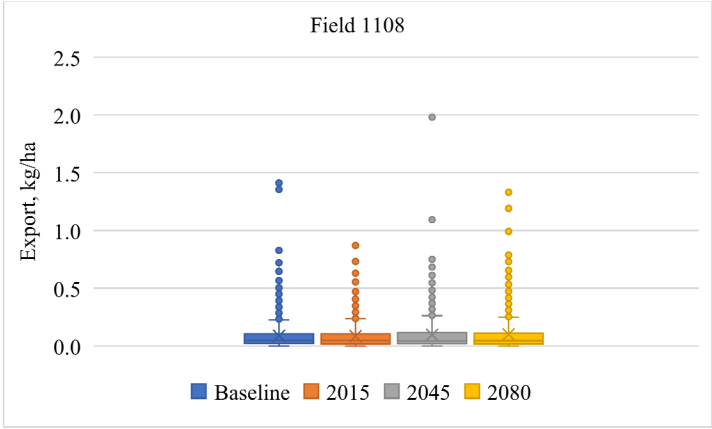

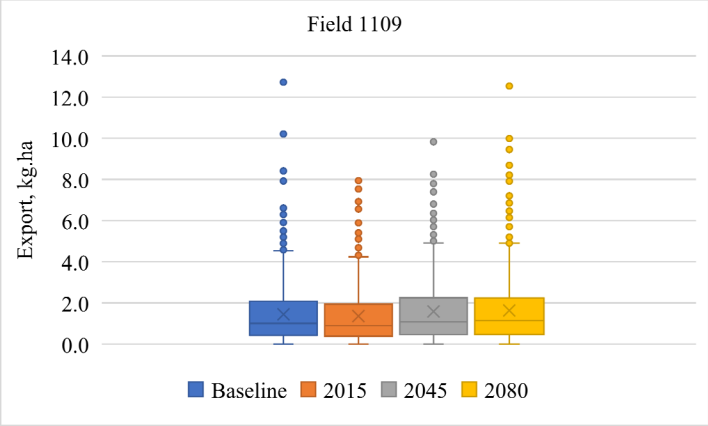

A2.7 - Box and whisker plots of 1000-years of SWAT output for annual phosphorus export (kg/ha) for RCP 4.5 and RCP 8.5 for Fields 1108, 1109, 1111, and 1112.

RCP 4.5

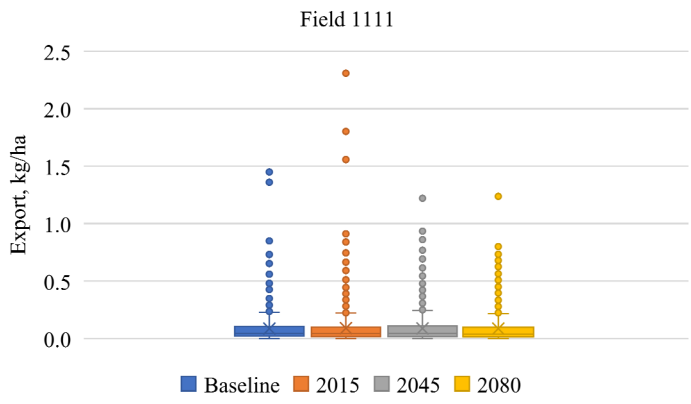

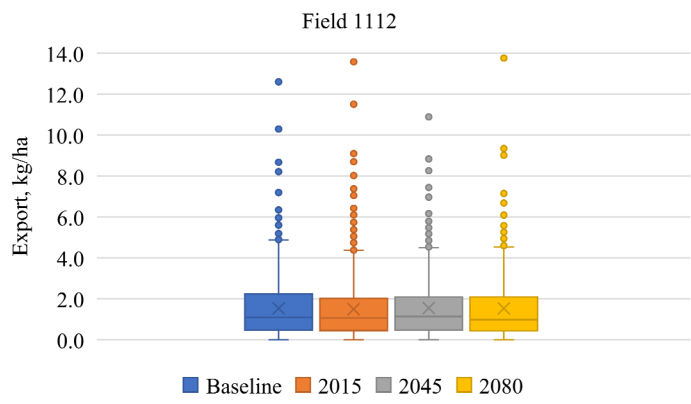

RCP 8.5

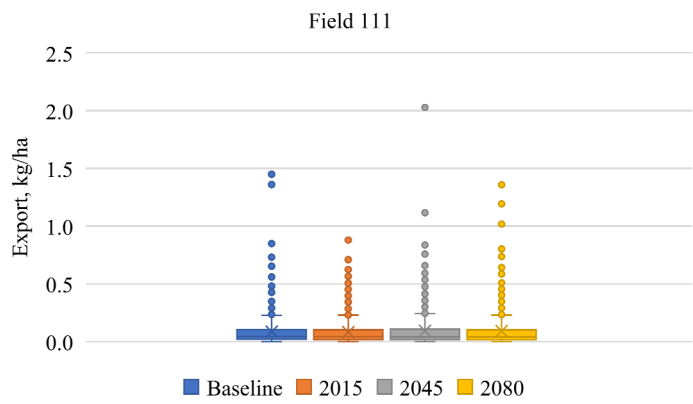

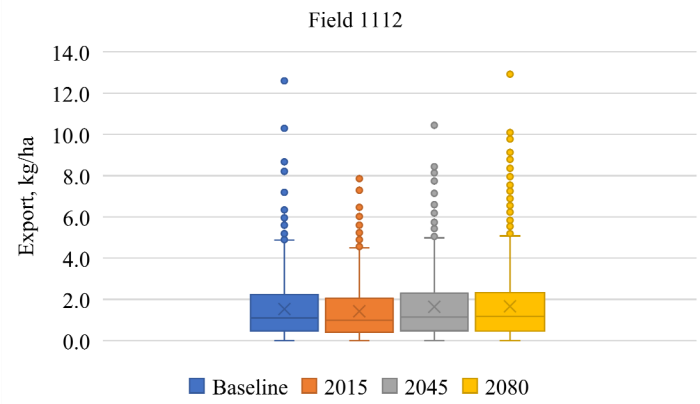

A2.8 - Monthly mean sediment export (tons/ha) for RCP 4.5 and RCP 8.5 for Fields 1108, 1109, 1111, and 1112.

RCP 4.5

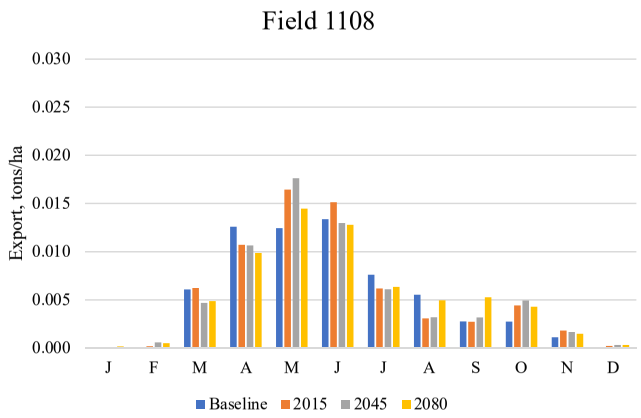

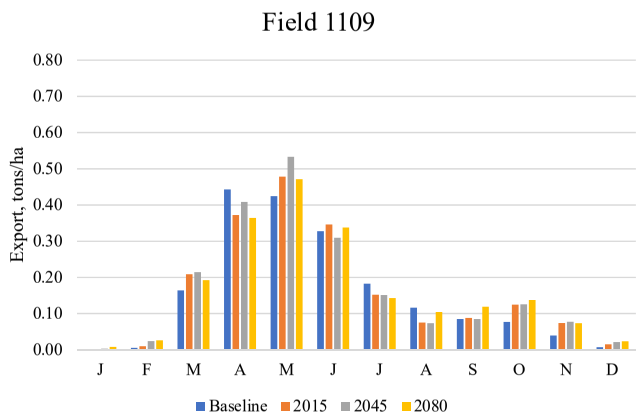

RCP 8.5

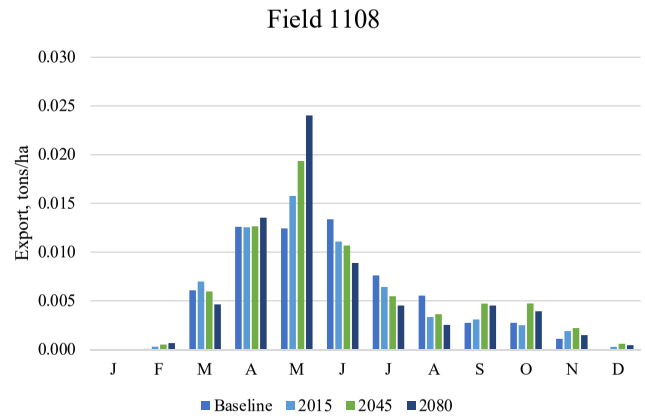

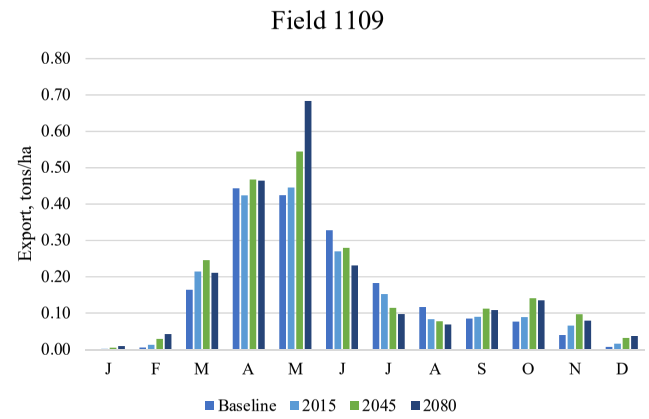

A2.8 - Monthly mean sediment export (tons/ha) for RCP 4.5 and RCP 8.5 for Fields 1108, 1109, 1111, and 1112, continued.

RCP 4.5

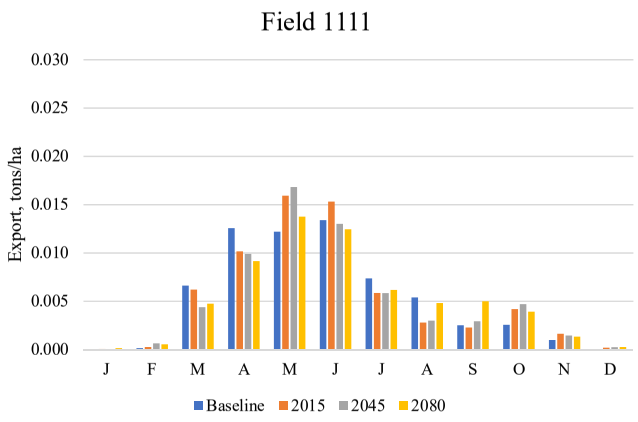

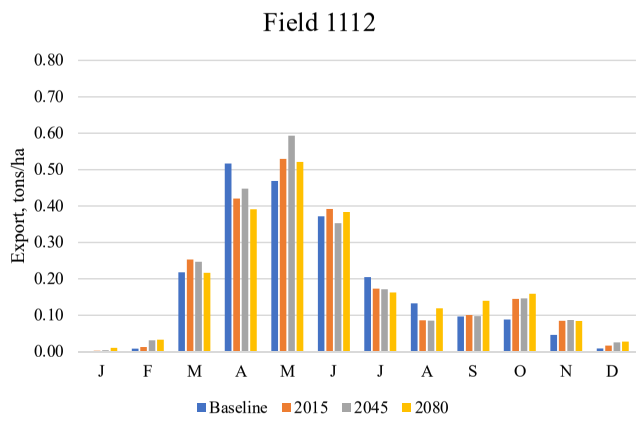

RCP 8.5

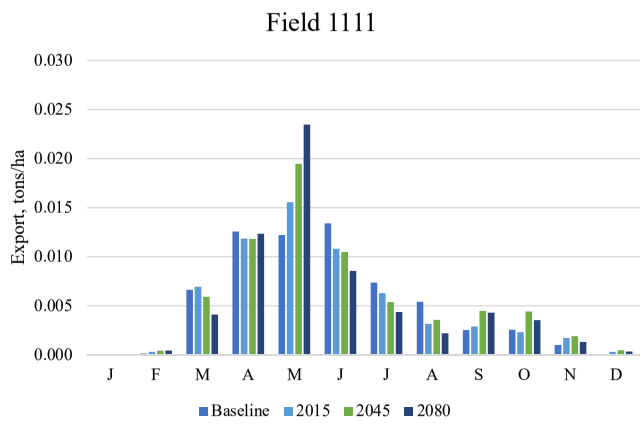

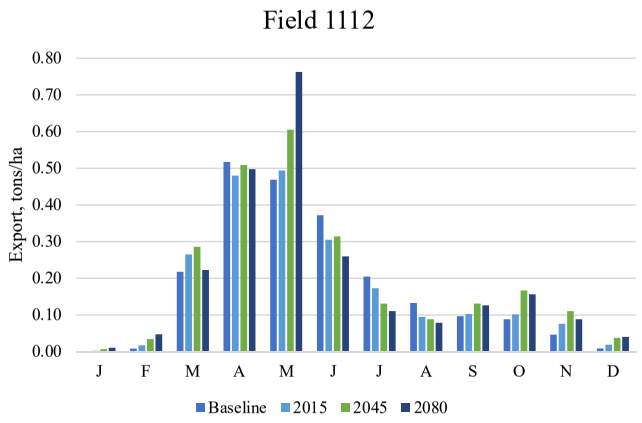

A2.9 - Box and whisker plots of 1000-years of SWAT output for annual sediment export (ton/ha) for RCP 4.5 and RCP 8.5 for Fields 1108, 1109, 1111, and 1112.

RCP 4.5

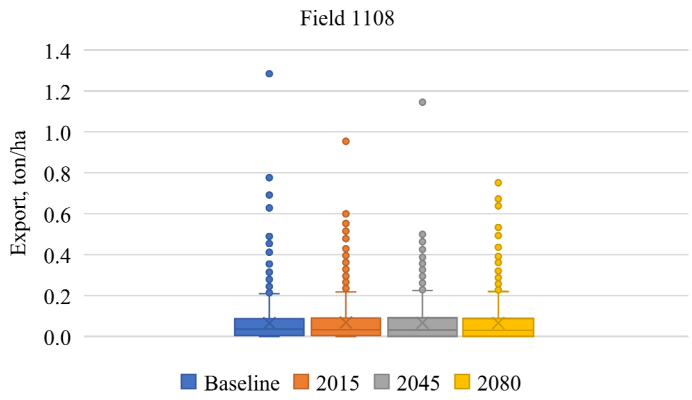

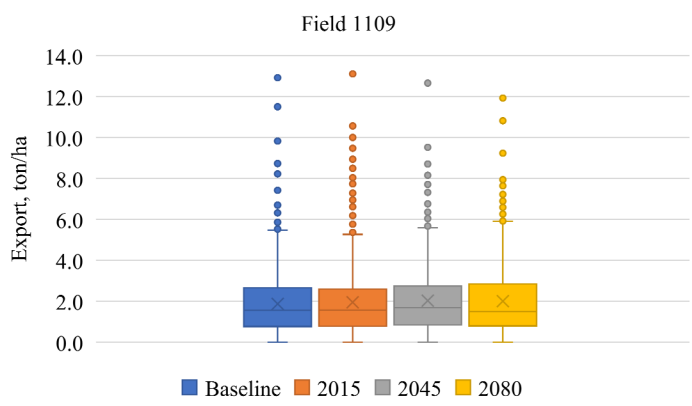

RCP 8.5

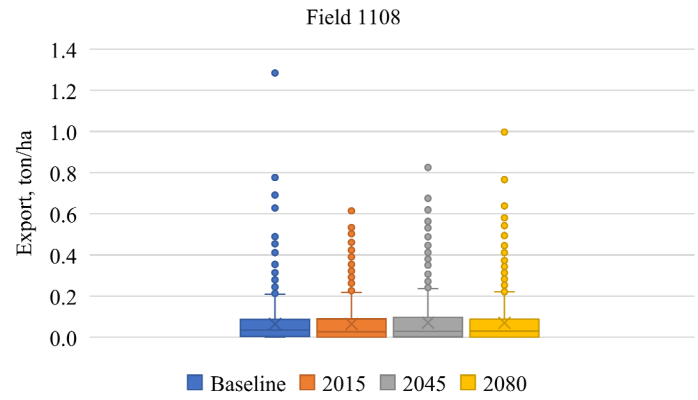

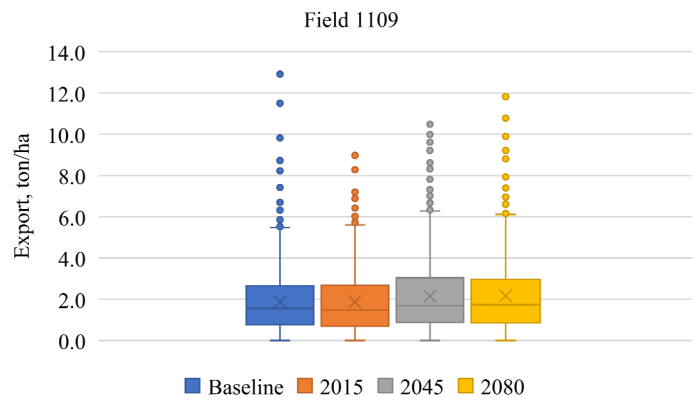

A2.9 - Box and whisker plots of 1000-years of SWAT output for annual sediment export (ton/ha) for RCP 4.5 and RCP 8.5 for Fields 1108, 1109, 1111, and 1112.

RCP 4.5

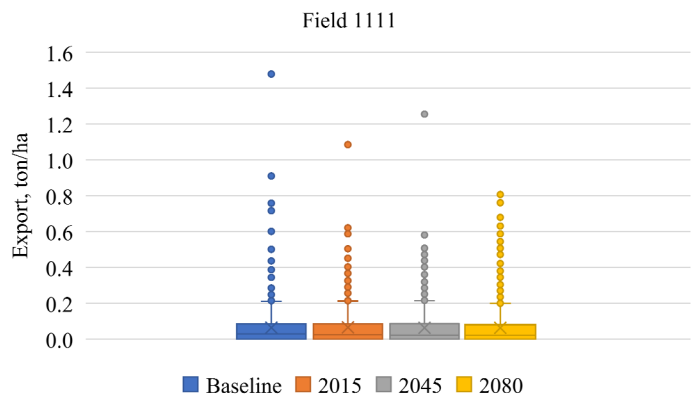

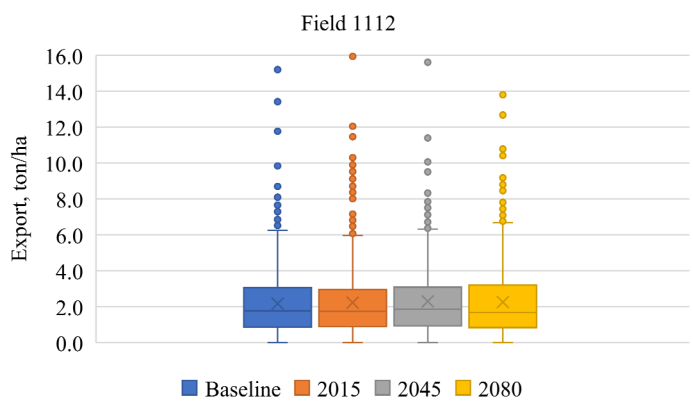

RCP 8.5